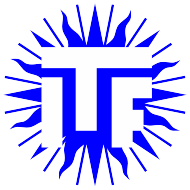

Institute for Theoretical Physics

Quantum dissipative systems coupled fractionally to a bath

Master Thesis

Audrique Vertessen

Supervisors:

Prof. Dr. C. de Morais Smith
Institute for Theoretical Physics at Utrecht University

R.C. Verstraten, Msc.
Institute for Theoretical Physics at Utrecht University

July 7, 2023

Abstract

Quantum diffusion is a major topic in condensed-matter physics, and the Caldeira-Leggett model has been one of the most successful approaches to study this phenomenon. Here, we generalize this model by coupling the bath to the system through a Weyl fractional derivative. The Weyl fractional Langevin equation is then derived without imposing a non-Ohmic macroscopic spectral function for the bath. By investigating the short- and long-time behavior of the mean squared displacement (MSD), we show that this model is able to describe a large variety of anomalous diffusion. Indeed, we find ballistic, sub-ballistic, and super-ballistic behavior for short times, whereas for long times we find saturation, and sub- and super-diffusion.

Acknowledgments

I would like to thank my supervisors, Prof. Dr. Cristiane de Morais Smith and Robin Verstraten. They provided me with guidance, ideas and a lot of feedback while still giving me the freedom to explore fascinating ideas on my own. Working with them was of great pleasure and has taught me how to do quality research.

Working in the master room and seeing all the other students working hard on their theses kept me motivated and inspired me to do the same. That is why I want to thank those hard working students as well. I also want to thank my friends Mithuss Tharmalingam, Giovanni Mistretta and Prajit Baruah, who provided me with plenty of feedback on my presentations and thesis. Especially, Mithuss, who helped me more than once to correct mistakes in my thesis.

Finally, I want to thank my mom and dad, Els and Dominique, who provided me with the love and support throughout these two years of studying abroad. In particular, they gave me the confidence that I could do quality research when I second guessed myself. I love you!

Contents

Chapter 1

Introduction

Quantum diffusion [**1, 2, 3, 4, 5, 6**] has been at the attention of researchers for many years, posing the fundamental questions on the description of dissipation in open quantum systems. A more complete understanding of these mechanisms could lead to important breakthroughs in engineering devices that have a better energy efficiency. Despite the existence of several models, numerous unanswered questions remain. For instance, experimental evidence [**7, 8, 9, 10**] indicates that diffusion does not always conform to the linear behavior described by Einstein [**11**], but instead exhibits a power-law scaling in the mean squared displacement (MSD), commonly known as *anomalous diffusion* [**12, 13**]. One such example is quantum diffusion on a fractal [**14**], where the exponent scales with the fractal dimension. For readers not familiar with fractals, we provide a short introduction to the topic in App. A. Typically, models that describe anomalous diffusion assume a different environment compared to regular diffusion. Our aim here is to achieve a description of anomalous diffusion within the usual environment using instead a fractional interaction.

In order to build a dissipative model, the environment of a system should be included in the Hamiltonian, since energy is conserved in quantum mechanics. In the *Caldeira-Leggett* model [**15, 16, 17, 18, 19, 20, 21**], the system of interest, which we will take to be a single quantum particle, is coupled linearly with a thermal bath that consists of harmonic oscillators. Although this might seem arbitrary at first, it is a very good approximation for coupling a system to an in-equilibrium environment, since each degree of freedom of such an environment must oscillate around a local minimum. The benefit of this approximation is that the harmonic oscillators can be integrated out exactly, thus leading to an effective description of the particle. In doing so, one needs to know the spectral function of the bath, which is given by the imaginary part of the Fourier transform of the retarded dynamical susceptibility. This spectral function is, however, often difficult to measure experimentally, and is therefore often assumed to be linear (*Ohmic*) for simplicity. This assumption on the reservoir leads to a Langevin equation, which shows linear diffusion. However, more recent

works [**22, 23, 24, 25**] have shown that a power-law (*non-Ohmic*) bath leads to a *fractional Langevin equation*, which will typically have colored noise due to the fluctuation-dissipation theorem, but can also have white noise [**23**].

In the fractional Langevin equation, the first derivative friction term is replaced by a fractional derivative [**26, 27**]. These are operators which generalize the order of derivatives to be not just an integer number, like a first or second derivative, but any real (or even complex) number. There are, however, many different fractional derivatives, which are not all equivalent [**25, 28, 29**], and this can often lead to different results. The first main question then is: which fractional derivative should one use? For this, we have to realize that fractional derivatives are non-local operators, which means that it is important to specify the time domain. Refs. [**22, 23**] both use a Caputo derivative, which is only possible if we have a clear initialization time. Since we are interested in dynamics, the boundaries of the action are taken from $-\infty$ to $+\infty$, which is an issue if we want to use Caputo derivatives inside the action. Therefore, we must take the domain of the fractional derivative to be the same as of the action. Furthermore, one would like to preserve the Fourier transform, since this has proven to be a powerful mathematical tool in physics. Hence, we would like a fractional derivative that is compatible with it. Because of these two reasons, we thus select the *Weyl fractional derivative* [**30, 31, 32**].

In spin-boson models [**33, 34, 35**], a spin half particle is coupled to a bosonic harmonic oscillator bath. Although reminiscent of the Caldeira-Leggett model, the spin-boson models are accessible to study in the fully quantum domain. In Ref. [**34**], they show that the effect of a sub-Ohmic bath can be fully characterized by a single effective interaction term. This term consists of two parts from the interaction and one from the Greens function of the bath. One of the conclusions from this was that any complexity in interactions can be described solely by the spectral function of the bath, since that controls this Greens function. Hence, the interaction term is almost always considered in its most elementary form: direct linear interaction. Physically, however, this might not be the most appropriate description of the system of interest. In many systems, the spectral function is known to be Ohmic. Therefore, we will study the other end of the line: What if the bath is kept to its most simple form, Ohmic, and the interaction term is complex? Through fractional partial integration we find that the non-linear power from the spectral function can be transferred to a fractional derivative in the interaction.

Hence, here we generalize the Caldeira-Leggett model by introducing a Weyl fractional derivative coupling term and show that it can describe a whole family of anomalous diffusion. Unlike previous works [**22, 23, 25**], we derive a fractional Langevin equation *without imposing a non-Ohmic macroscopic spectral function.* Motivated by the general velocity depended coupling in Ref. [**36**], we consider a fractional Weyl derivative to couple the system to the bath. In order to study the Lagrangian, which will now contain a Weyl fractional

derivative, we first derive the *Weyl fractional Euler-Lagrange equation* in analogy with Ref. [**37**], but adapted to Weyl fractional derivatives. Then, we are able to derive the *Weyl fractional Langevin equation* for an Ohmic bath, which we solve analytically using Fox H-functions. We calculate the asymptotic behavior of the MSD and show that it is comparable to previous results of a non-Ohmic Caldeira-Leggett model [**22, 38, 39, 40, 41, 42**].

The outline of this thesis is the following: In Ch. 2 we introduce classical and quantum Brownian motion. To do this we discuss the Langevin equation and the Caldeira-Leggett model. Moving on the Ch. 3, which is novel work, we start by introducing the Weyl fractional derivative. Then, we derive the Weyl fractional Langevin equation. Its solution for the free case is also presented. Next, we investigate the asymptotic behavior of the MSD by making use of less-known mathematics that is introduced in the various sections of App. B. In App. C we numerical investigate some properties of fractals. These will be used in App. D, in which we give a first attempt to derive the fractional Caldeira-Leggett model. However, this derivation has at least one crucial link missing such that this has to be investigated further. Finally, we provide a conclusion and outlook.

Chapter 2

Classical and quantum Brownian motion

In 1827, the Scottish Botanist Robert Brown observed the random movement of pollen grains suspended in water [**43**]. This phenomena is therefore called *Brownian motion*. It took almost 80 years for the first microscopic explanation of Brownian motion to be given. In 1905, Albert Einstein [**11**] used statistical physics to explain that the random movement of the pollen particle was due to collisions with the water molecules. In Sec. 2.1.1, we will describe classical motion by studying the *Langevin equation* [**15, 25, 44**]. With the rise of quantum mechanics in the 20^{th} century, the race to find a quantum version of Brownian motion was on. The main problem that emerged was to quantize a process that is dissipative, meaning that energy is not conserved. Quantizing a theory that violates energy conservation results in many problems, such as non-unitarity. After Einstein's initial classical description of Brownian motion, it took another 80 years for a suitable quantum version of Brownian motion to be developed. This was done by Caldeira and Leggett in 1983 [**17**], and is therefore named the *Caldeira-Leggett model*. They proposed a solution to the violation of energy conservation by embedding the system in a bath of harmonic oscillators, resulting in energy conservation for the total system. The Caldeira-Leggett model [**15, 16, 17, 18, 19, 20, 21, 25**] will be discussed in Sec. 2.2.

2.1 Classical Brownian motion: The Langevin equation

2.1.1 The Langevin equation

To derive an equation that describes classical Brownian motion, we start with Newton's second law, which is given by

$$F = M\frac{d^2}{dt^2}Q(t), \tag{2.1}$$

where F is the collection of all forces acting on the particle with position $Q(t)$ and mass M. The force consists of three components, the friction force, $-\eta\frac{d}{dt}Q(t)$, a force coming from an external potential, $-V'(Q)$, and a random force, $f(t)$, resulting from the bombardment of the particles in the bath.

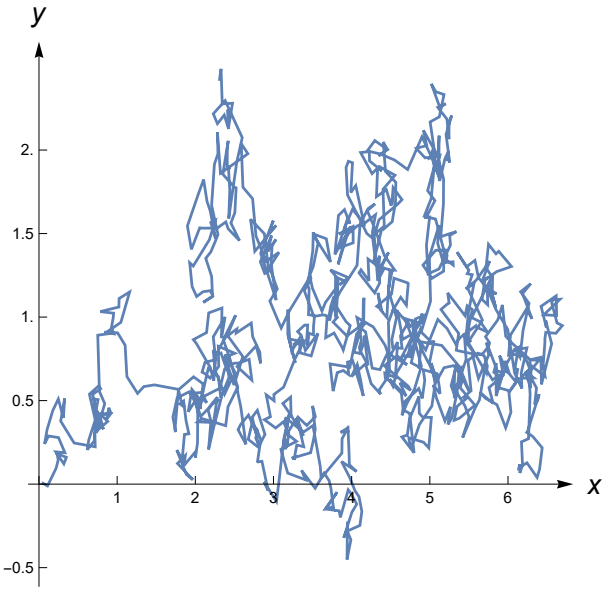

Figure 2.1: The trajectory in the xy-plane of a particle undergoing a Brownian motion in two dimensions. The initial position and velocity are set to zero.

Combining these terms Eq. (2.1) yields

$$M\frac{d^2}{dt^2}Q(t) + \eta\frac{d}{dt}Q(t) + V'(Q) = f(t). \tag{2.2}$$

One remaining question is: what is the statistics of the random force, $f(t)$? To be consistent with the diffusion equation, which is known to describe the time evolution of the probability density function associated to a Brownian particle, $\langle f(t)\rangle = 0$ and $\langle f(t)f(t')\rangle = 2\eta k_B T\delta(t-t')$, where $\langle\cdot\rangle$ denotes the ensemble average and the prefactor $2\eta k_B T$ was chosen such that equipartition of the bath holds (since we assume the bath to be in thermal equilibrium). Here, T is the temperature and k_B is the Boltzmann constant. When the time correlation is proportional to a delta function, the noise is named "white noise". Eq. (2.2) is called the *Langevin equation*. It will be important throughout this thesis that the Langevin equation describes classical Brownian motion. Hence, this equation should be recovered in certain approximations and/or limits.

2.1.2 Solving the Langevin equation for the free case by Laplace transformation

In the free case, for which $V(Q) = 0$, we can calculate $Q(t)$ by taking the Laplace transform on both sides. Using Lem. B.2.2 (see App. B), we obtain

$$Ms^2Q(s) - MsQ(0) - M\dot{Q}(0) + \eta sQ(s) - \eta Q(0) = F(s), \tag{2.3}$$

where $F(s) = \mathscr{L}[f(t); s]$. Since we have a translation invariant system, we chose $Q(0) = 0$, which gives

$$Q(s) = \frac{F(s) + M\dot{Q}(0)}{s(Ms + \eta)}. \tag{2.4}$$

Next, we use partial fraction to write $1/[s(Ms + \eta)] = [1/s - 1/(s + \eta/M)]/\eta$, thus obtaining

$$Q(s) = \frac{F(s) + M\dot{Q}(0)}{\eta}\left(\frac{1}{s} - \frac{1}{s + \frac{\eta}{M}}\right). \tag{2.5}$$

Taking the inverse Laplace transform of the above equation yields

$$\begin{aligned} Q(t) =& \mathscr{L}^{-1}\left[\frac{F(s) + M\dot{Q}(0)}{\eta}\left(\frac{1}{s} - \frac{1}{s + \frac{\eta}{M}}\right)\right] \\ =& \frac{1}{\eta}f(t) * \mathscr{L}^{-1}\left[\left(\frac{1}{s} - \frac{1}{s + \frac{\eta}{M}}\right)\right] + \frac{M\dot{Q}(0)}{\eta}\mathscr{L}^{-1}\left[\left(\frac{1}{s} - \frac{1}{s + \frac{\eta}{M}}\right)\right] \\ =& \frac{1}{\eta}f(t) * \left(1 - e^{-\frac{\eta}{M}t}\right) + \frac{M\dot{Q}(0)}{\eta}\left(1 - e^{-\frac{\eta}{M}t}\right), \end{aligned} \tag{2.6}$$

where in the second line we used Eq. (B.13) and in the last line we used Eqs. (B.16) and (B.18). We can now calculate some observables, e.g. $\langle Q(t)\rangle$ and $\langle Q(t)^2\rangle$. We will assume that the bath initially is in equilibrium such that the equipartition theorem holds for it. The equiparition theorem states that for particles $q_j, q_{j'}$ that are in thermal equilibrium,

$$\begin{cases} \langle q_j(0)\rangle = \langle \dot{q}_j(0)\rangle = \langle \dot{q}_j(0)q_{j'}(0)\rangle = 0, \\ \langle \dot{q}_j(0)\dot{q}_{j'}(0)\rangle = \frac{k_BT}{m_j}\delta_{jj'}, \\ \langle q_j(0)q_{j'}(0)\rangle = \frac{k_BT}{m_j\omega_j^2}\delta_{jj'}, \end{cases} \tag{2.7}$$

the averages are taken over the ensemble. Using the equipartition theorem and $\langle f(t)\rangle = 0$, we directly get $\langle Q(t)\rangle = 0$. This is what we would expect, since we chose $Q(0) = 0$ and

the system is symmetric. For the mean squared displacement, we get

$$\begin{aligned}\langle Q(t)^2\rangle &= \left\langle \left[\frac{1}{\eta}f(t) * \left(1-e^{-\frac{\eta}{M}t}\right) + \frac{M\dot{Q}(0)}{\eta}\left(1-e^{-\frac{\eta}{M}t}\right)\right]^2 \right\rangle \\ &= \frac{1}{\eta^2}\int_0^t d\tau \int_0^t d\tau' \langle f(\tau)f(\tau')\rangle \left(1-e^{-\frac{\eta}{M}\tau}\right)\left(1-e^{-\frac{\eta}{M}\tau'}\right) + \frac{M^2\langle\dot{Q}(0)^2\rangle}{\eta^2}\left(1-e^{-\frac{\eta}{M}t}\right)^2 \\ &= \frac{2k_BT}{\eta}\int_0^t d\tau \left(1-e^{-\frac{\eta}{M}\tau}\right)^2 + \frac{Mk_BT}{\eta^2}\left(1-e^{-\frac{\eta}{M}t}\right)^2, \end{aligned} \tag{2.8}$$

where in the second line we started looking at Brownian motion, which means that the system is essentially just one of the particles of the bath, meaning that it is in thermal equilibrium with the bath. Therefore, we have $\langle f(t)\dot{Q}(0)\rangle = 0$ since $f(t)$ is generated by the bath. In the last line, we used $\langle f(\tau)f(\tau')\rangle = 2\eta k_BT\delta(\tau-\tau')$ and the equipartition theorem for the system. Finally, we calculate the integral in Eq. (2.8) to end up with

$$\begin{aligned}\langle Q(t)^2\rangle &= \frac{2k_BT}{\eta}t + \frac{4k_BTM}{\eta^2}e^{-\frac{\eta}{M}t} - \frac{k_BTM}{\eta^2}e^{-2\frac{\eta}{M}t} - \frac{3k_BTM}{\eta^2} \\ &\quad + \frac{Mk_BT}{\eta^2} - \frac{2Mk_BT}{\eta^2}e^{-\frac{\eta}{M}t} + \frac{Mk_BT}{\eta^2}e^{-2\frac{\eta}{M}t} \\ &= -\frac{2k_BTM}{\eta^2} + \frac{2k_BT}{\eta}t + \frac{2k_BTM}{\eta^2}e^{-\frac{\eta}{M}t}. \end{aligned} \tag{2.9}$$

For short times ($t \ll \eta/M$), we can Taylor expand the exponential in Eq. (2.9) up to second order, to get

$$\langle Q(t)^2\rangle \approx \frac{k_BT}{M}t^2, \text{ for } t \ll \frac{\eta}{M}. \tag{2.10}$$

The long-time behavior ($t \gg \eta/M$) can be calculated by neglecting the exponential in Eq. (2.9) since it decays rapidly, thus giving us

$$\langle Q(t)^2\rangle \approx -\frac{2k_BTM}{\eta^2} + \frac{2k_BT}{\eta}t, \text{ for } t \gg \frac{\eta}{M}. \tag{2.11}$$

We can thus conclude that the mean squared displacement in the free case resulting from the Brownian motion described by Eq. (2.2) yields ballistic behavior (quadratic) for short times and diffusive behavior (linear) for long times, which we can visually verify in Fig. 2.2.

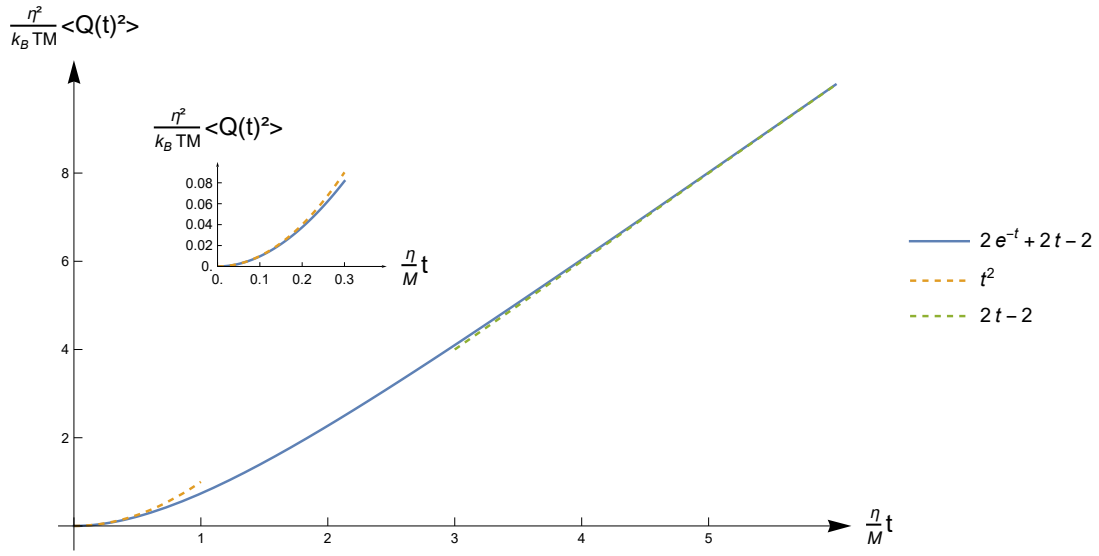

Figure 2.2: The mean squared displacement of a Brownian particle is shown in blue. The short-and long-time behavior are represented by orange and green dashed lines, respectively. Here, $\langle Q(t)^2 \rangle$ is measured in units of $\eta^2/k_b TM$ and the time is measured in units of η/M.

2.1.3 Solving the Langevin equation for the free case by Fourier transformation

In this section, we take a non-traditional approach to solve the Langevin equation for the free particle case, namely, we use Fourier transforms. This is done because the next chapter we use Fourier transforms to solve more difficult equations. Let us begin by finding the particular solution, $Q^p(t)$, of the Langevin equation. This is done by taking the Fourier transform (2.2) for the case $V = 0$. We then obtain

$$Q^p(\omega) = \frac{f(\omega)}{-M\omega^2 + i\eta\omega}. \tag{2.12}$$

Next, we take the inverse Fourier transform of the above equation,

$$\begin{aligned} Q^p(t) &= \mathcal{F}^{-1}\left[\frac{f(\omega)}{-M\omega^2 + i\eta\omega}; t\right] \\ &= \frac{1}{2\pi} f(t) * \mathcal{F}^{-1}\left[\frac{1}{\omega(-M\omega + i\eta)}; t\right] \\ &= \left(\frac{1}{2\pi}\right)^2 f(t) * \left\{\mathcal{F}^{-1}\left[\frac{1}{\omega}; t\right] * \mathcal{F}^{-1}\left[\frac{1}{-M\omega + i\eta}; t\right]\right\}, \end{aligned} \tag{2.13}$$

where in the second and third lines we used Lem. B.1.4 (see App. B). Now, we interpret $\mathcal{F}^{-1}[1/\omega; t]$ in the positive $i\epsilon$-interpretation. The mathematical reason for this is because we want to get the same result as was obtained using Laplace transforms in the previous section. A physical interpretation would be that we couple the particle to the bath after $t = 0$, such that this part is zero beforehand. This is insured by the Heaviside function, which arises in the positive $i\epsilon$-interpretation. Using Eq. (B.31), we get

$$\mathcal{F}^{-1}\left[\frac{1}{\omega}; t\right] = 2\pi i\Theta(t) \tag{2.14}$$

The inverse Fourier transform of $1/(-M\omega + i\eta) = 1/[M(-\omega + i\eta/M)]$ can be directly calculated by applying the residue theorem (Thm. B.4.1) and Jordan's lemma (Lem. B.4.1), where the closing of the contour is done in the same way as in Ex. B.4.1 (noting that $\eta/M > 0$). This gives

$$\mathcal{F}^{-1}\left[\frac{1}{-M\omega + i\eta}; t\right] = -\frac{2\pi i}{M} e^{-\frac{\eta}{M}t}\Theta(t). \tag{2.15}$$

Substituting Eqs. (2.14) and (2.15) into Eq. (2.13), gives

$$Q^p(t) = f(t) * \left\{\frac{1}{M}\left[\Theta(t) * e^{-\frac{\eta}{M}t}\Theta(t)\right]\right\}. \tag{2.16}$$

Finally, we apply Eq. (B.5) to calculate the inner convolution, which yields

$$\begin{aligned} Q^p(t) &= f(t) * \left(\frac{1}{M}\int_0^t d\tau e^{-\frac{\eta}{M}\tau}\right) \\ &= \frac{1}{\eta} f(t) * \left(1 - e^{-\frac{\eta}{M}t}\right), \end{aligned} \tag{2.17}$$

where we implicitly assume that $t > 0$.
The homogeneous part of the solution, $Q^h(t)$, is found by solving the homogeneous equation in Fourier space, namely

$$\left(-M\omega^2 + i\eta\omega\right) Q(\omega) = 0, \tag{2.18}$$

which has non-trivial solutions if

$$\omega = 0 \text{ or } \omega = \frac{\eta}{M} i. \tag{2.19}$$

This means that the homogeneous solution is given by

$$\begin{aligned} Q^h(t) &= \mathcal{F}^{-1}\left[A\delta(\omega) + B\delta\left(\omega - \frac{\eta}{M}i\right); t\right] \\ &= A + Be^{-\frac{\eta}{M}t}, \end{aligned} \tag{2.20}$$

where A and B are determined by initial conditions. Since, $Q^p(t \leq 0) = 0$, and $Q(t) = Q^p(t) + Q^h(t)$, we find

$$A = Q(0) - B \text{ and } \dot{Q}(0) = -\frac{\eta}{M}B, \tag{2.21}$$

which, if we take $Q(0) = 0$, yields

$$\begin{cases} B = -\frac{M}{\eta}\dot{Q}(0), \\ A = \frac{M}{\eta}\dot{Q}(0). \end{cases} \tag{2.22}$$

The full solution to the Langevin equation is the sum of the particular solution and the homogeneous solution, which is thus given by

$$Q(t) = \frac{1}{\eta}f(t) * \left(1 - e^{-\frac{\eta}{M}t}\right) + \frac{M}{\eta}\dot{Q}(0)\left(1 - e^{-\frac{\eta}{M}t}\right), \tag{2.23}$$

which is exactly the solution, see Eq. (2.6), that we obtained by using the Laplace transform. This justifies the positive $i\epsilon$-interpretation used in Eq. (2.14).

2.2 Quantum Brownian motion: the Caldeira-Leggett model

In the Caldeira-Leggett model, we consider a particle with mass M and coordinate Q coupled linearly to a bath of harmonic oscillators, each with mass m_k, frequency ω_k and coordinates q_k. A schematic overview of this model can be seen in Fig. 2.3. The Caldeira-Leggett model is thus described by the Lagrangian

$$\mathcal{L}_{CL} = \mathcal{L}_p + \mathcal{L}_{bath} + \mathcal{L}_{int} + \mathcal{L}_{CT}, \tag{2.24}$$

where $\mathcal{L}_p$ describes the particle, $\mathcal{L}_{bath}$ accounts for the harmonic oscillators, $\mathcal{L}_{int}$ describes the linear coupling between the particle and the harmonic oscillators, and $\mathcal{L}_{CT}$ is a counter-term, needed to renormalize the potential to which the particle is subject. Here,

$$\mathcal{L}_p = \frac{1}{2}M\dot{Q}^2 - V(Q), \tag{2.25}$$

$$\mathcal{L}_{bath} = \frac{1}{2}\sum_{k=1}^{N} m_k(\dot{q}_k^2 - \omega_k^2 q_k^2), \tag{2.26}$$

$$\mathcal{L}_{int} = Q\sum_{k=1}^{N} C_k q_k, \tag{2.27}$$

$$\mathcal{L}_{CT} = -\frac{1}{2}\sum_{k=1}^{N}\frac{C_k^2}{m_k\omega_k^2}Q^2. \tag{2.28}$$

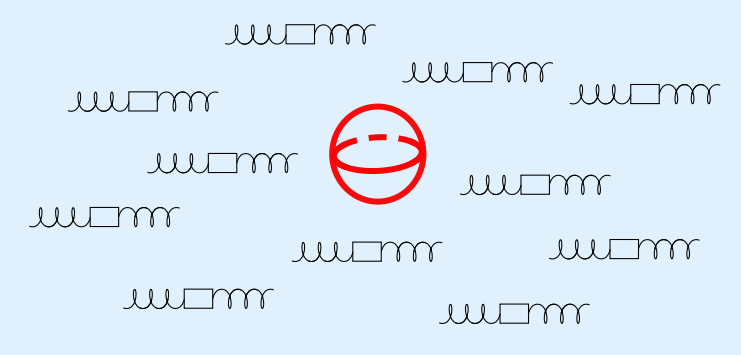

Figure 2.3: A schematic representation of the Caldeira-Leggett model in which a particle is coupled to a bath of harmonic oscillators.

It is not immediately clear that this Lagrangian is able to describe Brownian motion. The justification of this model is given a posteriori, meaning that the Langevin equation will come out of the equations of motions of this particular Lagrangian. The classical equations of motions can be found through the Euler-Lagrange equations and are given by

$$M\ddot{Q} = -V'(Q) + \sum_{k=1}^{N} C_k q_k - \sum_{k=1}^{N} \frac{C_k^2}{m_k \omega_k^2} Q, \tag{2.29}$$

$$m_j \ddot{q}_j = -m_j \omega_j^2 q_j + C_j Q. \tag{2.30}$$

The goal is to end up with an equation that describes Brownian motion of the particle, Q, namely the Langevin equation, see Eq. (2.2). Thus, we want to eliminate the bath out of Eq. (2.29). To achieve this, we first solve Eq. (2.30). Taking the Laplace transform of Eq. (2.30), which is defined in Sec. B.2 of App. B, gives

$$\begin{aligned} q_j(s) &= \frac{\dot{q}_j(0)}{s^2+\omega_j^2} + \frac{s q_j(0)}{s^2+\omega_j^2} + \frac{C_j Q(s)}{m_j\left(s^2+\omega_j^2\right)} \\ &= \frac{\dot{q}_j(0)}{s^2+\omega_j^2} + \frac{s q_j(0)}{s^2+\omega_j^2} + \frac{C_j Q(s)}{m_j}\left(\frac{1}{\omega_j^2} - \frac{1}{\omega_j^2}\frac{s^2}{s^2+\omega_j^2}\right), \end{aligned} \tag{2.31}$$

where we used Lem. B.2.2 in the first line and in the last line we separated a term that will cancel the term coming from $\mathcal{L}_{CT}$. Th solution in the time domain is obtained by taking the inverse Laplace transform of Eq. (2.31), which results in

$$q_j(t) = \frac{\dot{q}_j(0)}{\omega_j}\sin(\omega_j t) + q_j(0)\cos(\omega_j t) + \frac{C_j Q(t)}{m_j \omega_j^2} - \mathscr{L}^{-1}\left[\frac{C_j Q(s)}{m_j \omega_j^2}\frac{s^2}{s^2+\omega_j^2}; t\right], \tag{2.32}$$

where we used Eqs. (B.20) and (B.21). Next, we use two properties of the inverse Laplace transform given by Eqs. (B.13) and (B.15), noting that we chose $Q(0) = 0$ since our system is translation invariant. This yields

$$\begin{aligned} q_j(t) &= \frac{\dot{q}_j(0)}{\omega_j}\sin(\omega_j t) + q_j(0)\cos(\omega_j t) + \frac{C_j Q(t)}{m_j\omega_j^2} - \frac{d}{dt}\mathscr{L}^{-1}\left[\frac{C_j Q(s)}{m_j\omega_j^2}\frac{s}{s^2+\omega_j^2}; t\right] \\ &= \frac{\dot{q}_j(0)}{\omega_j}\sin(\omega_j t) + q_j(0)\cos(\omega_j t) + \frac{C_j Q(t)}{m_j\omega_j^2} - \frac{d}{dt}\left[\frac{C_j Q(t)}{m_j\omega_j^2} * \cos(\omega_j t)\right]. \end{aligned} \tag{2.33}$$

Inserting the above solution into Eq. (2.29), gives

$$M\ddot{Q} + V'(Q) + \sum_{k=1}^{N}\frac{d}{dt}\left[\frac{C_k^2 Q(t)}{m_k\omega_k^2} * \cos(\omega_k t)\right] = \sum_{k=1}^{N} C_k\left[\frac{\dot{q}_k(0)}{\omega_k}\sin(\omega_k t) + q_k(0)\cos(\omega_k t)\right]. \tag{2.34}$$

To simplify the above equation, we calculate the spectral function of the bath, which is defined by

$$J(\omega) \equiv \mathrm{Im}\mathcal{F}\left\{-i\theta(t-t')\langle\left[F(t), F(t')\right]\rangle\right\} \tag{2.35}$$

where $F(t)$ is the force exerted by the particle on the harmonic oscillators of the bath. The spectral function can be more easily calculated as the imaginary part of the dynamical susceptibility of $F(\omega) = \sum_{k=1}^{N} C_k q_k(\omega)$. Taking the Fourier transform of equation (2.30) yields

$$q_j(\omega) = -\frac{C_j}{m_j(\omega^2 - \omega_j^2)}Q(\omega). \tag{2.36}$$

The above equation tells us that $q_j(\omega)$ is a function of $Q(\omega)$. The dynamical susceptibility is thus given by

$$\begin{aligned} \chi_B(\omega) &\equiv \frac{\partial F(\omega)}{\partial Q(\omega)} \\ &= -\sum_{k=1}^{N}\frac{C_k^2}{m_k(\omega^2 - \omega_k^2)}. \end{aligned} \tag{2.37}$$

The Caldeira-Leggett spectral function is thus given by

$$\begin{aligned} J_{CL}(\omega) &= \mathrm{Im}\left[\chi_B(\omega)\right] \\ &= \frac{\pi}{2}\sum_{k=1}^{N}\frac{C_k^2}{m_k\omega_k}\left[\delta(\omega-\omega_k) - \delta(\omega+\omega_k)\right] \\ &= \frac{\pi}{2}\sum_{k=1}^{N}\frac{C_k^2}{m_k\omega_k}\delta(\omega-\omega_k), \end{aligned} \tag{2.38}$$

where in the second line we used Eq. (B.43) and in the third line we imposed that physical frequencies are positive, $\omega > 0$, and $\omega_k > 0$ such that $\delta(\omega + \omega_k)$ can be dropped. Now, we can turn our focus back to Eq. (2.34), where we define the friction force as

$$F_{fr} \equiv \sum_{k=1}^{N} \frac{d}{dt}\left[\frac{C_k^2 Q(t)}{m_k \omega_k^2} * \cos(\omega_k t)\right]. \tag{2.39}$$

To see why this is a friction force, we insert the Caldeira-Leggett spectral function that is given by Eq. (2.38) into the above equation, finding

$$\begin{aligned} F_{fr} &= \frac{d}{dt}\left\{\int_0^t d\tau \int_0^\infty d\omega \sum_{k=1}^{N} \frac{C_k^2}{m_k \omega_k^2}\delta(\omega - \omega_k)\cos[\omega(t-\tau)]Q(\tau)\right\} \\ &= \frac{2}{\pi}\frac{d}{dt}\left\{\int_0^t d\tau \int_0^\infty d\omega \frac{J_{CL}(\omega)}{\omega}\cos[\omega(t-\tau)]Q(\tau)\right\}. \end{aligned} \tag{2.40}$$

To simplify the above expression, we assume an Ohmic bath, which means that the spectral function can effectively be described by

$$J_{CL}(\omega) = \begin{cases} \eta\omega & \text{for } \omega < \Omega, \\ 0 & \text{for } \omega > \Omega, \end{cases} \tag{2.41}$$

where Ω is a high-frequency cut-off ($\Omega \to \infty$) and η the macroscopic friction coefficient. The above function can also be seen in Fig. 2.4. Substituting Eq. (2.41) into Eq. (2.40) gives

$$\begin{aligned} F_{fr} &= \frac{2\eta}{\pi}\frac{d}{dt}\left\{\int_0^t d\tau \int_0^\infty d\omega \cos[\omega(t-\tau)]Q(\tau)\right\} \\ &= 2\eta\frac{d}{dt}\left\{\int_0^t d\tau \delta(t-\tau)Q(\tau)\right\} \\ &= \eta\dot{Q}(t), \end{aligned} \tag{2.42}$$

where in the first line we used the cosine representation of the delta function and in the third line we obtain a factor of $1/2$ because the the evaluation of the delta function sits exactly on the boundary[1]. This justifies our definition of F_{fr} since this reproduces the classical form of a friction force under the Ohmic bath assumption. Turning our focus to the RHS of Eq. (2.34), which we define to be a random white noise force,

$$f(t) \equiv \sum_{k=1}^{N} C_k\left[\frac{\dot{q}_k(0)}{\omega_k}\sin(\omega_k t) + q_k(0)\cos(\omega_k t)\right]. \tag{2.43}$$

[1] An intuitive way to see why this gives a factor of $1/2$ is by considering the following: $\int_{-\infty}^{\infty} dx\delta(x-x_0)g(x) = \int_{-\infty}^{x_0}\delta(x-x_0)g(x) + \int_{x_0}^{\infty} dx\delta(x-x_0)g(x)$. Next, using the delta functions in the usual way, gives us $g(x_0) = 2g(x_0)$, such that you get an extra factor of $1/2$ when using a delta function on the boundary.

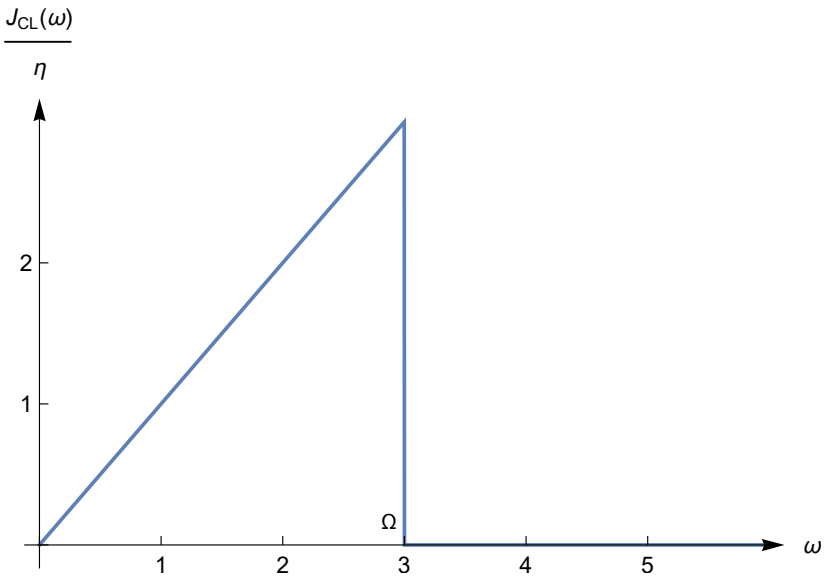

Figure 2.4: The spectral function of an Ohmic bath, which means that for frequencies lower than a high frequency cut-off, Ω, the spectral function is given by $J_{CL}(\omega) = \eta\omega$ and is zero for frequencies higher than the cut-off. $J_{CL}(\omega)$ is measured in units of $1/\eta$ and we chose for $\Omega = 3$.

We will show that this is indeed a white noise force by calculating its statistics. To do this, we assume that the bath is in thermal equilibrium, such that in the classical limit the equipartition theorem must hold (see Eqs. (2.7)). This implies that $\langle f(t)\rangle = 0$. Focusing our attention to the autocorrelator, we get

$$\begin{aligned}
\langle f(t)f(t')\rangle &= \left\langle \sum_{kk'} C_k C_{k'} \left[\frac{\dot{q}_k(0)}{\omega_k}\sin(\omega_k t) + q_k(0)\cos(\omega_k t)\right]\left[\frac{\dot{q}_{k'}(0)}{\omega_{k'}}\sin(\omega_{k'} t') + q_{k'}(0)\cos(\omega_{k'} t')\right]\right\rangle \\
&= \sum_{kk'} C_k C_{k'}\left[\frac{1}{\omega_k\omega_{k'}}\langle \dot{q}_k(0)\dot{q}_{k'}(0)\rangle \sin(\omega_k t)\sin(\omega_{k'} t') + \langle q_k(0)q_{k'}(0)\rangle \cos(\omega_k t)\cos(\omega_{k'} t')\right. \\
&\quad \left. + \frac{1}{\omega_k}\langle \dot{q}_k(0)q_{k'}(0)\rangle \sin(\omega_k t)\cos(\omega_{k'} t') + \frac{1}{\omega_{k'}}\langle q_k(0)\dot{q}_{k'}(0)\rangle \cos(\omega_k t)\sin(\omega_{k'} t')\right] \\
&= k_B T \sum_k \frac{C_k^2}{m_k\omega_k^2}\left[\sin(\omega_k t)\sin(\omega_k t') + \cos(\omega_k t)\cos(\omega_k t')\right], \qquad (2.44)
\end{aligned}$$

where in third line we used Eqs. (2.7). Now, we can use the formula for the cosine of a difference to get

$$\begin{aligned}\langle f(t)f(t')\rangle &= k_BT\sum_k \frac{C_k^2}{m_k\omega_k^2}\cos[\omega_k(t-t')] \\ &= k_BT\int_0^\infty d\omega \sum_k \frac{C_k^2}{m_k\omega_k^2}\cos[\omega(t-t')] \\ &= \frac{2k_BT}{\pi}\int_0^\infty d\omega \frac{J_{CL}(\omega)}{\omega}\cos[\omega(t-t')],\end{aligned} \tag{2.45}$$

where, in the last line, we identified the form of the spectral function, given by Eq. (2.38). Substituting the macroscopic form of this spectral function in the above equation, just as for the friction force, yields

$$\langle f(t)f(t')\rangle = \frac{2\eta k_BT}{\pi}\int_0^\infty d\omega\cos[\omega(t-t')] = 2\eta k_BT\delta(t-t'). \tag{2.46}$$

Finally, substituting Eqs. (2.42) and (2.43) into Eq. (2.34) gives

$$M\ddot{Q} + V'(Q) + \eta\dot{Q} = f(t), \tag{2.47}$$

with $\langle f(t)\rangle = 0$ and $\langle f(t)f(t')\rangle = 2\eta k_BT\delta(t-t')$. Thus, we see that Lagrangian (2.24) is able to describe Brownian motion since in the semi-classical limit the Euler-Lagrange equations yield the Langevin equation, see Eq. (2.2).

Chapter 3

The Caldeira-Leggett model with Weyl fractional coupling

This chapter consists of original work, developed by us. Here, we generalize the Caldeira-Leggett model to be able to describe a whole family of anomalous diffusion, in particular anomalous diffusion in fractals [**14, 45**]. Unlike previous works [**22, 23, 25**], we do this *without imposing a non-Ohmic macroscopic spectral function*. Motivated by the general velocity depended coupling in Ref. [**36**], we consider a fractional derivative coupling to the bath. However, there are many different fractional derivatives and they are not all equivalent to each other [**25, 28, 29**]. Therefore, they often lead to different results. The main question then is: which fractional derivative should we chose? There are two motivations that resolve this issue. The first is that we are interested in the dynamics of the particle instead of equilibrium physics of the particle. The boundaries of the action are therefore taken to be from negative infinity to positive infinity. It is then logical to take the boundaries of the fractional derivative to be the same. Another important argument that will lead to one specific fractional derivative is that we would like to keep the Fourier transform as a mathematical tool, since in physics this is extremely powerful. Therefore, we would like a fractional derivative that is compatible with it. Because of these two reasons, we chose for the *Weyl fractional derivative*. The definition and some of its properties are introduced in Sec. 3.1. It turns out that every fractional derivative that is Fourier compatible can be shown to be equivalent to the Weyl fractional derivative (for example the Liouville fractional derivative in Ref. [**25**]). To study Lagrangians with Weyl fractional derivatives in it, we derive the equations of motion for these types of Lagrangians in Sec. 3.2. These will be called the *Weyl fractional Euler-Lagrange equations*. This is done in analogy with Ref. [**37**], but then for Weyl fractional derivatives instead of the Riemann–Liouville ones. Finally, in Sec. 3.3, we use the tools developed in the preceding sections to generalize the Caldeira-Leggett model to a model with Weyl fractional coupling. With this model, we are able to derive the *Weyl fractional Langevin equation*, which is solved in Sec. 3.4. The

asymptotic behavior of the mean square displacement, which is a very important characteristic of (anomalous) diffusion, is discussed in Sec. 3.5.

3.1 The Weyl fractional derivative

Although the Weyl fractional derivative has been mentioned briefly in the literature (see Refs. [**12, 23, 25, 46, 47, 48**]), its mathematical exploration has been very limited, as far as we are aware. In this section, we explore various novel properties and examples, one of them being a partial integration formula for the Weyl fractional derivative, which turns out to be of significant importance.

Definition 3.1.1. *Let $\alpha \in \mathbb{R}$, $f \in L^2(\mathbb{R})$[1], then*

$$ {}^{W}_{+}\boldsymbol{D}^{\alpha}_{t} f(t) = \mathcal{F}^{-1}\left\{(i\omega)^{\alpha}\mathcal{F}\left[f(t);\omega\right];t\right\} \tag{3.1} $$

is defined to be the Weyl fractional derivative of order α, where $(i\omega)^{\alpha}$ is the complex power function[2]*.*

Example 3.1.1. *Let us calculate the Weyl fractional derivative of an exponential function. Let $a \in \mathbb{C}$, then*

$$ \begin{aligned} {}^{W}_{+}\boldsymbol{D}^{\alpha}_{t} e^{at} &= \mathcal{F}^{-1}\left\{(i\omega)^{\alpha}\mathcal{F}\left[e^{at};\omega\right];t\right\} \\ &= \mathcal{F}^{-1}\left\{(i\omega)^{\alpha}\delta(\omega+ia);t\right\} \\ &= a^{\alpha}e^{at} \end{aligned} \tag{3.2} $$

Definition 3.1.2. *Let $\alpha \in \mathbb{R}$, $f \in L^2(\mathbb{R})$, then*

$$ {}^{W}_{-}\boldsymbol{D}^{\alpha}_{t} f(t) = \mathcal{F}^{-1}\left\{(-i\omega)^{\alpha}\mathcal{F}\left[f(t);\omega\right];t\right\} \tag{3.3} $$

is called the pseudo Weyl fractional derivative of order α.

Example 3.1.2. *Let us calculate the pseudo Weyl fractional derivative of an exponential function. Let $a \in \mathbb{C}$, then*

$$ \begin{aligned} {}^{W}_{-}\boldsymbol{D}^{\alpha}_{t} e^{at} &= \mathcal{F}^{-1}\left\{(-i\omega)^{\alpha}\mathcal{F}\left[e^{at};\omega\right];t\right\} \\ &= \mathcal{F}^{-1}\left\{(-i\omega)^{\alpha}\delta(\omega+ia);t\right\} \\ &= (-a)^{\alpha}e^{at} \end{aligned} \tag{3.4} $$

[1] Readers familiar with pseudo-differential operators will notice that the Weyl fractional derivative is a pseudo-differential operator with symbol $(i\omega)^{\alpha}$. These operators can be defined on more general spaces than $L^2(\mathbb{R})$ [**46**]. We will often not be too strict on which functions we apply these operators, as long as they can make sense in terms of a function or distribution.

[2] See Sec. B.3 for its definition and some properties.

Remark 3.1.1. *Note that the combination* ${}^{W}_{-}\boldsymbol{D}^{\alpha}_{t}\,{}^{W}_{+}\boldsymbol{D}^{\alpha}_{t} f(t) = \mathcal{F}^{-1}\left\{|\omega|^{2\alpha}\mathcal{F}\left[f(t);\omega\right];t\right\}$, *which is known as the fractional Laplacian* [**49, 50**]*, denoted by* $(-\Box_t)^{2\alpha} f(t)$*. Fractional Laplacians were shown to be relevant to describe the quantum valley Hall effect in graphene* [**51**]*, as well as excitations in transition metal dichalcogenides* [**52, 53**]*. In particular,* $\alpha = 1/4$*, yields*

$$ {}^{W}_{-}\boldsymbol{D}^{\frac{1}{4}}_{t}\,{}^{W}_{+}\boldsymbol{D}^{\frac{1}{4}}_{t} f(t) = \sqrt{-\Box_t} f(t), \tag{3.5} $$

which is encountered among others in the context of Pseudo QED [**54, 55**]*. This theory emerges from a projected QED* [**54**] *because in 2D systems like graphene, the dynamics of the electrons is restricted to a 2D plane, whereas the photons intermediate their interactions in 3D.*

Example 3.1.3. *The combination presented in Rem. 3.1.1 will often appear when working with these operators. We thus also calculate this combination acting on an exponential function. Let* $a \in \mathbb{C}$*, then*

$$ \begin{aligned} {}^{W}_{-}\boldsymbol{D}^{\frac{\alpha}{2}}_{t}\,{}^{W}_{+}\boldsymbol{D}^{\frac{\alpha}{2}}_{t} e^{at} &= \mathcal{F}^{-1}\left\{|\omega|^{\alpha}\mathcal{F}\left[e^{at};\omega\right];t\right\} \\ &= \mathcal{F}^{-1}\left\{|\omega|^{\alpha}\delta(\omega + ia);t\right\} \\ &= |a|^{\alpha} e^{at} \end{aligned} \tag{3.6} $$

Lemma 3.1.1. *The (pseudo) Weyl fractional derivative is a linear operator. Let* $f, g \in L^2(\mathbb{R})$*,* $a, b \in \mathbb{C}$ *and* $\alpha \in \mathbb{R}$*, then*

$$ {}^{W}_{\pm}\boldsymbol{D}^{\alpha}_{t}\left[af(t) + bg(t)\right] = a\,{}^{W}_{\pm}\boldsymbol{D}^{\alpha}_{t} f(t) + b\,{}^{W}_{\pm}\boldsymbol{D}^{\alpha}_{t} g(t). \tag{3.7} $$

Proof.

The proof follows immediately from the definition of the (pseudo) Weyl fractional derivative and linearity of integrals.

□

Lemma 3.1.2. *The (pseudo) Weyl fractional derivative is a real operator, meaning that for any* $f \in L^2(\mathbb{R})$ *and* $\alpha \in \mathbb{R}$ *we have*

$$ \left[{}^{W}_{\pm}\boldsymbol{D}^{\alpha}_{t} f(t)\right]^{*} = {}^{W}_{\pm}\boldsymbol{D}^{\alpha}_{t} f(t). \tag{3.8} $$

Proof.

We have

$$\begin{aligned}\left[{}^{W}_{\pm}\boldsymbol{D}^{\alpha}_{t} f(t)\right]^{*} &= \left[\int_{-\infty}^{\infty} d\omega e^{i\omega t}(\pm i\omega)^{\alpha}\int_{-\infty}^{\infty}\frac{d\tau}{2\pi}e^{-i\omega\tau}f(\tau)\right]^{*}\\ &= \int_{-\infty}^{\infty} d\omega e^{-i\omega t}(\mp i\omega)^{\alpha}\int_{-\infty}^{\infty}\frac{d\tau}{2\pi}e^{i\omega\tau}f(\tau)\\ &= \int_{-\infty}^{\infty} d\omega e^{i\omega t}(\pm i\omega)^{\alpha}\int_{-\infty}^{\infty}\frac{d\tau}{2\pi}e^{-i\omega\tau}f(\tau)\\ &= {}^{W}_{\pm}\boldsymbol{D}^{\alpha}_{t} f(t),\end{aligned}$$

where in the second line we used that $\omega \in \mathbb{R}$, such that $[(i\omega)^{\alpha}]^{*} = (-i\omega)^{\alpha}$ and in the third line we did the substitution $\omega \to -\omega$.

□

Lemma 3.1.3. *The Weyl fractional derivative and the pseudo Weyl fractional derivative commute. That is, for $f \in L^2(\mathbb{R})$ and $\alpha, \beta \in \mathbb{R}$, we have*

$${}^{W}_{-}\boldsymbol{D}^{\alpha}_{t}\,{}^{W}_{+}\boldsymbol{D}^{\beta}_{t} f(t) = {}^{W}_{+}\boldsymbol{D}^{\beta}_{t}\,{}^{W}_{-}\boldsymbol{D}^{\alpha}_{t} f(t). \tag{3.9}$$

Proof.

By definition, we have

$$\begin{aligned}{}^{W}_{-}\boldsymbol{D}^{\alpha}_{t}\,{}^{W}_{+}\boldsymbol{D}^{\beta}_{t} f(t) &= \mathcal{F}^{-1}\left\{(-i\omega)^{\alpha}\mathcal{F}\left[{}^{W}_{+}\boldsymbol{D}^{\alpha}_{t} f(t);\omega\right];t\right\}\\ &= \mathcal{F}^{-1}\left\{(-i\omega)^{\alpha}(i\omega)^{\beta}\mathcal{F}\left[f(t);\omega\right];t\right\}\\ &= \mathcal{F}^{-1}\left\{(i\omega)^{\beta}\mathcal{F}\left[{}^{W}_{-}\boldsymbol{D}^{\alpha}_{t} f(t);\omega\right];t\right\}\\ &= {}^{W}_{+}\boldsymbol{D}^{\beta}_{t}\,{}^{W}_{-}\boldsymbol{D}^{\alpha}_{t} f(t).\end{aligned}$$

□

Lemma 3.1.4. *The (pseudo) Weyl fractional derivative satisfies the semigroup property, meaning that its orders add up. That is, let $f \in L^2(\mathbb{R})$ and $\alpha, \beta \in \mathbb{R}$, then*

$${}^{W}_{\pm}\boldsymbol{D}^{\beta}_{t}\,{}^{W}_{\pm}\boldsymbol{D}^{\alpha}_{t} f(t) = {}^{W}_{\pm}\boldsymbol{D}^{\alpha+\beta}_{t} f(t). \tag{3.10}$$

Proof.

We directly see that

$$\begin{aligned}
{}^{W}_{\pm}\boldsymbol{D}^{\beta}_{t}\,{}^{W}_{\pm}\boldsymbol{D}^{\alpha}_{t} f(t) &= \mathcal{F}^{-1}\left\{(\pm i\omega)^{\alpha}(\pm i\omega)^{\beta}\mathcal{F}\left[f(t);\omega\right];t\right\} \\
&= \mathcal{F}^{-1}\left\{(\pm i\omega)^{\alpha+\beta}\mathcal{F}\left[f(t);\omega\right];t\right\} \\
&= {}^{W}_{\pm}\boldsymbol{D}^{\alpha+\beta}_{t} f(t).
\end{aligned}$$

□

Lemma 3.1.5. *Let $f, g \in L^2(\mathbb{R})$ and $\alpha \in \mathbb{R}$. Then, the (pseudo) Weyl fractional derivative of a convolution satisfies*

$$g(t) * {}^{W}_{\pm}\boldsymbol{D}^{\alpha}_{t} f(t) = {}^{W}_{\pm}\boldsymbol{D}^{\alpha}_{t} g(t) * f(t) = {}^{W}_{\pm}\boldsymbol{D}^{\alpha}_{t}\left[g(t) * f(t)\right]. \tag{3.11}$$

Proof.

We have

$$\begin{aligned}
\mathcal{F}\left[g(t) * {}^{W}_{\pm}\boldsymbol{D}^{\alpha}_{t} f(t);\omega\right] &= \mathcal{F}\left[g(t);\omega\right]\mathcal{F}\left[{}^{W}_{\pm}\boldsymbol{D}^{\alpha}_{t} f(t);\omega\right] \\
&= \mathcal{F}\left[g(t);\omega\right](\pm i\omega)^{\alpha}\mathcal{F}\left[f(t);\omega\right] \\
&= \mathcal{F}\left[{}^{W}_{\pm}\boldsymbol{D}^{\alpha}_{t} g(t);\omega\right]\mathcal{F}\left[f(t);\omega\right] \\
&= \mathcal{F}\left[{}^{W}_{\pm}\boldsymbol{D}^{\alpha}_{t} g(t) * f(t);\omega\right].
\end{aligned}$$

Furthermore, we know that

$$\mathcal{F}\left\{{}^{W}_{\pm}\boldsymbol{D}^{\alpha}_{t}\left[g(t) * f(t)\right];\omega\right\} = \mathcal{F}\left[g(t);\omega\right](\pm i\omega)^{\alpha}\mathcal{F}\left[f(t);\omega\right].$$

Hence we conclude, by uniqueness of the Fourier transform, that

$$g(t) * {}^{W}_{\pm}\boldsymbol{D}^{\alpha}_{t} f(t) = {}^{W}_{\pm}\boldsymbol{D}^{\alpha}_{t} g(t) * f(t) = {}^{W}_{\pm}\boldsymbol{D}^{\alpha}_{t}\left[g(t) * f(t)\right].$$

□

Theorem 3.1.1. (Weyl partial integration) *Let $f, g \in L^2(\mathbb{R})$ and $\alpha \in \mathbb{R}$, then the partial integration formula for the Weyl fractional derivative is given by*

$$\int_{-\infty}^{\infty} dt\, g(t)\,{}^{W}_{+}\boldsymbol{D}^{\alpha}_{t} f(t) = \int_{-\infty}^{\infty} dt\, f(t)\,{}^{W}_{-}\boldsymbol{D}^{\alpha}_{t} g(t). \tag{3.12}$$

Proof.

We have

$$\begin{aligned}\int_{-\infty}^{\infty} dt g(t)\, {}^{W}_{+}\boldsymbol{D}^{\alpha}_{t} f(t) &= \int_{-\infty}^{\infty} dt g(t) \int_{-\infty}^{\infty} d\omega e^{i\omega t} (i\omega)^{\alpha} \frac{1}{2\pi} \int_{-\infty}^{\infty} d\tau e^{-i\omega\tau} f(\tau) \\ &= \int_{-\infty}^{\infty} d\tau f(\tau) \int_{-\infty}^{\infty} d\omega e^{i\omega\tau} (-i\omega)^{\alpha} \frac{1}{2\pi} \int_{-\infty}^{\infty} dt e^{-i\omega t} g(t) \\ &= \int_{-\infty}^{\infty} dt f(t)\, {}^{W}_{-}\boldsymbol{D}^{\alpha}_{t} g(t),\end{aligned}$$

where, in the second line, we made the substitution $\omega \to -\omega$ and in the last line we renamed $t \longleftrightarrow \tau$.

□

Remark 3.1.2. *Notice that we needed the pseudo Weyl fractional derivative for this partial integration formula. Since $(i\omega)^{\alpha}$ is the complex power function, its impossible to get a partial integration formula with only the Weyl fractional derivative in it. This arises because, using Thm. B.3.1, we have*

$$(-i\omega)^{\alpha} = (-1)^{\alpha}(i\omega)^{\alpha} e^{2\pi i \alpha N_{+}} \text{ with } N_{+} = \begin{cases} -1 & \text{if } \operatorname{sign}(\omega) = 1, \\ 0 & \text{if } \operatorname{sign}(\omega) = -1. \end{cases}$$

This means that we would have to split the integral based on the sign of ω, thus not obtaining the Weyl fractional derivative again.

3.2 The Weyl fractional Euler-Lagrange equation

In the previous section, we were able to derive a partial integration formula for the (pseudo) Weyl fractional derivatives (see Thm. 3.1.1). This means that now we have the tools needed to derive the equations of motions of Lagrangians that are dependent on (pseudo) Weyl fractional derivatives, which will be done in this section. We will call them the Weyl fractional Euler-Lagrange equations, which are, to the best of our knowledge, not yet known in the literature.

Theorem 3.2.1. (The Weyl fractional Euler-Lagrange equation)
Consider the following action

$$S[y] = \int_{-\infty}^{\infty} dt \mathcal{L}\left(t, y(t), {}^{W}_{+}\boldsymbol{D}^{\alpha_1}_{t} y(t), ..., {}^{W}_{+}\boldsymbol{D}^{\alpha_n}_{t} y(t), ..., {}^{W}_{-}\boldsymbol{D}^{\beta_1}_{t} y(t), ..., {}^{W}_{-}\boldsymbol{D}^{\beta_m}_{t} y(t)\right), \quad (3.13)$$

where $y \in L^2(\mathbb{R})$, ${\alpha_k}'s, {\beta_j}'s \in \mathbb{R}_0$ and all ${\alpha_k}'s, {\beta_j}'s$ are different. Minimizing $S[y]$ with respect to y leads to the Weyl fractional Euler-Lagrange equation, which is given by

$$\frac{\partial \mathcal{L}}{\partial y} + \sum_{k=1}^{n} {}^{W}_{-}\boldsymbol{D}_t^{\alpha_k} \frac{\partial \mathcal{L}}{\partial\, {}^{W}_{+}\boldsymbol{D}_t^{\alpha_k} y} + \sum_{j=1}^{m} {}^{W}_{+}\boldsymbol{D}_t^{\beta_j} \frac{\partial \mathcal{L}}{\partial\, {}^{W}_{-}\boldsymbol{D}_t^{\beta_j} y} = 0. \tag{3.14}$$

Proof.

Taking a variation of this action gives

$$\delta S[y] = \int_{-\infty}^{\infty} dt \left(\frac{\partial \mathcal{L}}{\partial y}\delta y + \sum_{k=1}^{n} \frac{\partial \mathcal{L}}{\partial\, {}^{W}_{+}\boldsymbol{D}_t^{\alpha_k} y} \delta\, {}^{W}_{+}\boldsymbol{D}_t^{\alpha_k} y + \sum_{j=1}^{m} \frac{\partial \mathcal{L}}{\partial\, {}^{W}_{-}\boldsymbol{D}_t^{\beta_j} y} \delta\, {}^{W}_{-}\boldsymbol{D}_t^{\beta_j} y \right).$$

Swapping the order of the variation and the fractional derivatives and applying Thm. 3.1.1, yields

$$\delta S[y] = \int_{-\infty}^{\infty} dt \left(\frac{\partial \mathcal{L}}{\partial y} + \sum_{k=1}^{n} {}^{W}_{-}\boldsymbol{D}_t^{\alpha_k} \frac{\partial \mathcal{L}}{\partial\, {}^{W}_{+}\boldsymbol{D}_t^{\alpha_k} y} + \sum_{j=1}^{m} {}^{W}_{+}\boldsymbol{D}_t^{\beta_j} \frac{\partial \mathcal{L}}{\partial\, {}^{W}_{-}\boldsymbol{D}_t^{\beta_j} y} \right) \delta y, \ \forall \delta y.$$

Setting the above equation equal to zero implies

$$\frac{\partial \mathcal{L}}{\partial y} + \sum_{k=1}^{n} {}^{W}_{-}\boldsymbol{D}_t^{\alpha_k} \frac{\partial \mathcal{L}}{\partial\, {}^{W}_{+}\boldsymbol{D}_t^{\alpha_k} y} + \sum_{j=1}^{m} {}^{W}_{+}\boldsymbol{D}_t^{\beta_j} \frac{\partial \mathcal{L}}{\partial\, {}^{W}_{-}\boldsymbol{D}_t^{\beta_j} y} = 0.$$

□

Remark 3.2.1. *Usually, Lagrangians of the form $\mathcal{L}\left(y(t), \dot{y}(t), {}^{W}_{+}\boldsymbol{D}_t^{\alpha} y(t)\right)$ will be considered. This implies that the fractional Euler-Lagrange equation reduces to*

$$\frac{\partial \mathcal{L}}{\partial y} - \frac{d}{dt}\frac{\partial \mathcal{L}}{\partial \dot{y}} + {}^{W}_{-}\boldsymbol{D}_t^{\alpha} \frac{\partial \mathcal{L}}{\partial\, {}^{W}_{+}\boldsymbol{D}_t^{\alpha} y} = 0. \tag{3.15}$$

One must be careful with taking the limits $\alpha \to 0$ and $\alpha \to 1$ because overcounting will happen. It is therefore important to fully understand the proof of Thm. (3.14). This means that in the limits $\alpha \to 0, 1$, the last term in Eq. (3.15) should be ignored since it is already included in the first two terms of Eq. (3.15). In this way, the usual Euler-Lagrange equations are recovered in the limits $\alpha \to 0, 1$. Note that overcounting is not a problem as soon as one specifies a Lagrangian explicitly.

Remark 3.2.2. *If we have a Lagrangian of the form $\mathcal{L}\left(t, y(t), {}^{W}_{+}\boldsymbol{D}_t^{\alpha} y(t)\right)$ and we take $\alpha = 1$, implying that ${}^{W}_{+}\boldsymbol{D}_t^{\alpha} = d/dt$ and ${}^{W}_{-}\boldsymbol{D}_t^{\alpha} = -d/dt$, the standard Euler-Lagrange equation is recovered.*

3.3 Derivation of the Weyl fractional Langevin equation

3.3.1 The fractional Caldeira-Leggett model: fractional system-bath coupling

In our nomenclature the fractional Caldeira-Leggett model, denoted by $\mathcal{L}_{FCL}$, is an extension of the Caldeira-Leggett model described by the Lagrangian in Eq. (2.24) in which a modified interaction term is introduced in the Lagrangian. This modification allows the model to be interpreted as the Caldeira-Leggett model, with the exception that the interaction between the particle and the bath is altered by a 'fraction'. The rational behind this modification is that the particle and the bath remain exactly the same, however the interaction between them changes. This could be attributed to several external factors, such as the geometry in which the particle or bath resides. We thus consider

$$\mathcal{L}_{FCL} = \mathcal{L}_p + \mathcal{L}_{bath} + \mathcal{L}_{int} + \mathcal{L}_{CT} \tag{3.16}$$

where

$$\mathcal{L}_p = \frac{1}{2}M\dot{Q}^2 - V(Q), \tag{3.17}$$

$$\mathcal{L}_{bath} = \frac{1}{2}\sum_{k=1}^{N} m_k(\dot{q}_k^2 - \omega_k^2 q_k^2), \tag{3.18}$$

$$\mathcal{L}_{int} = {}^{W}_{+}\boldsymbol{D}_t^{\alpha} Q \sum_{k=1}^{N} C_k q_k. \tag{3.19}$$

Here, Q is the coordinate of the system, M is the mass of the system, $V(Q)$ is the potential that the system undergoes, q_k are the bath coordinates (which are subject to a harmonic potential), each having mass m_k, $\alpha \in \mathbb{R}$ is the order of the fractional derivative and $\mathcal{L}_{CT}$ is the counter-term Lagrangian, which renormalizes the potential and is independent of the bath coordinates.
$\mathcal{L}_{CT}$ is obtained by making sure that the system Q is subject to the potential V and not some shifted potential. Therefore, we need to impose that $\partial\mathcal{L}/\partial Q \overset{!}{=} -\partial V/\partial Q$. To do this, we first set

$$0 = \frac{\partial \mathcal{L}}{\partial q_j} = -m_j\omega_j^2 q_j + C_j\, {}^{W}_{+}\boldsymbol{D}_t^{\alpha} Q, \tag{3.20}$$

because we want the bath to be non-interacting, meaning that no particle of the bath should feel any potential. This then implies that

$$q_j = \frac{C_j}{m_j\omega_j^2}\, {}^{W}_{+}\boldsymbol{D}_t^{\alpha} Q. \tag{3.21}$$

Now, we can find the minimum of $\mathcal{L}$ with respect to Q, which we want to be at the minimum of the potential, such that

$$\frac{\partial \mathcal{L}}{\partial Q} = -\frac{\partial V}{\partial Q} + \frac{\partial}{\partial Q}\left({}^{W}_{+}\boldsymbol{D}^{\alpha}_{t}Q\right)\sum_{k=1}^{N} C_k q_k + \frac{\partial \mathcal{L}_{CT}}{\partial Q} \overset{!}{=} -\frac{\partial V}{\partial Q}. \tag{3.22}$$

Upon substituting Eq. (3.21) into Eq. (3.22), we obtain

$$\begin{aligned}\frac{\partial \mathcal{L}_{CT}}{\partial Q} &= -\frac{\partial}{\partial Q}\left({}^{W}_{+}\boldsymbol{D}^{\alpha}_{t}Q\right){}^{W}_{+}\boldsymbol{D}^{\alpha}_{t}Q\sum_{k=1}^{N}\frac{C_k^2}{m_k\omega_k^2} \\ &= -\frac{1}{2}\frac{\partial}{\partial Q}\left({}^{W}_{+}\boldsymbol{D}^{\alpha}_{t}Q\right)^2\sum_{k=1}^{N}\frac{C_k^2}{m_k\omega_k^2}.\end{aligned} \tag{3.23}$$

Therefore, we choose

$$\mathcal{L}_{CT} = -\frac{1}{2}\sum_{k=1}^{N}\frac{C_k^2}{m_k\omega_k^2}\left({}^{W}_{+}\boldsymbol{D}^{\alpha}_{t}Q\right)^2. \tag{3.24}$$

Now, we can begin studying the equations of motion, starting with the Euler-Lagrange equations for the bath, which are given by

$$m_j\ddot{q}_j = -m_j\omega_j^2 q_j + C_j\,{}^{W}_{+}\boldsymbol{D}^{\alpha}_{t}Q. \tag{3.25}$$

Taking the Fourier transform of this equation yields the particular solution, $q_j^p(t)$,

$$q_j^p(\omega) = -\frac{C_j}{m_j(\omega^2-\omega_j^2)}(i\omega)^{\alpha}Q(\omega). \tag{3.26}$$

In real space, this can be written as

$$\begin{aligned}q_j^p(t) &= -\mathcal{F}^{-1}\left[\frac{C_j}{m_j(\omega^2-\omega_j^2)}(i\omega)^{\alpha}Q(\omega);t\right] \\ &= \mathcal{F}^{-1}\left\{\frac{(i\omega)^{\alpha}C_j}{m_j\omega_j^2}\left[1-\frac{\omega^2}{\omega^2-\omega_j^2}\right]Q(\omega);t\right\} \\ &= \frac{C_j}{m_j\omega_j^2}\left\{{}^{W}_{+}\boldsymbol{D}^{\alpha}_{t}Q(t) - \mathcal{F}^{-1}\left[(i\omega)^{\alpha}\frac{\omega^2}{\omega^2-\omega_j^2}Q(\omega);t\right]\right\} \\ &= \frac{C_j}{m_j\omega_j^2}\left\{{}^{W}_{+}\boldsymbol{D}^{\alpha}_{t}Q(t) + \frac{d^2}{dt^2}\mathcal{F}^{-1}\left[(i\omega)^{\alpha}\frac{1}{\omega^2-\omega_j^2}Q(\omega);t\right]\right\} \\ &= \frac{C_j}{m_j\omega_j^2}\left\{{}^{W}_{+}\boldsymbol{D}^{\alpha}_{t}Q(t) + \frac{1}{2\pi}\frac{d^2}{dt^2}\mathcal{F}^{-1}\left[\frac{1}{\omega^2-\omega_j^2};t\right] * \mathcal{F}^{-1}\left[(i\omega)^{\alpha}Q(\omega);t\right]\right\},\end{aligned} \tag{3.27}$$

where in the second line we separated a term that will cancel the term coming from $\mathcal{L}_{CT}$ and in the last line we used Lem. B.1.4. We can further simplify the above expression by making use of

$$\begin{aligned}\mathcal{F}^{-1}\left[\frac{1}{\omega^2-\omega_j^2};t\right] &= -\frac{1}{2\omega_j}\left\{\mathcal{F}^{-1}\left[\frac{1}{\omega+\omega_j};t\right]-\mathcal{F}^{-1}\left[\frac{1}{\omega-\omega_j};t\right]\right\}\\ &= -\frac{2\pi}{\omega_j}\sin(\omega_j t)\Theta(t),\end{aligned} \tag{3.28}$$

where in the last line we interpreted the inverse Fourier integrals in the positive $i\epsilon$-interpretation, which allowed us to use Eq. (B.32). The positive $i\epsilon$-interpretation is justified, since in the limit of $\alpha \to 0$ we would like to recover the usual Caldeira-Leggett model. The physical justification is the same as in Sec. 2.1.3, namely that the particle is only put in the bath after time $t = 0$. Therefore, the interaction term should not have an impact before $t = 0$. A Heaviside function, which automatically comes out of the positive $i\epsilon$-interpretation, ensures that the coupling between the bath and the particle occurs after $t = 0$[3]. Substituting the above equation into Eq. (3.27) yields

$$\begin{aligned}q_j^p(t) &= \frac{C_j}{m_j\omega_j^2}\left\{{}^{W}_{+}\boldsymbol{D}_t^{\alpha}Q(t)-\frac{1}{\omega_j}\frac{d^2}{dt^2}\sin(\omega_j t)\Theta(t)*{}^{W}_{+}\boldsymbol{D}_t^{\alpha}Q(t)\right\}\\ &= \frac{C_j}{m_j\omega_j^2}\left\{{}^{W}_{+}\boldsymbol{D}_t^{\alpha}Q(t)-\frac{d}{dt}\left[\cos(\omega_j t)\Theta(t)+\frac{1}{\omega_j}\sin(\omega_j t)\delta(t)\right]*{}^{W}_{+}\boldsymbol{D}_t^{\alpha}Q(t)\right\}\\ &= \frac{C_j}{m_j\omega_j^2}\left\{{}^{W}_{+}\boldsymbol{D}_t^{\alpha}Q(t)-\frac{d}{dt}\cos(\omega_j t)\Theta(t)*{}^{W}_{+}\boldsymbol{D}_t^{\alpha}Q(t)\right\}\\ &= \frac{C_j}{m_j\omega_j^2}\left\{{}^{W}_{+}\boldsymbol{D}_t^{\alpha}Q(t)-\frac{d}{dt}\,{}^{W}_{+}\boldsymbol{D}_t^{\alpha}\left[\cos(\omega_j t)\Theta(t)*Q(t)\right]\right\},\end{aligned} \tag{3.29}$$

where in the second line we acted with a derivative on $\sin(\omega_j t)\Theta(t)$ and used the fact that $d/dt[\Theta(t)] = \delta(t)$ which results in a term of the form $\delta(t)\sin(\omega_k t) * Q(t) \sim \sin(0) = 0$, and in the last line we used Lem. 3.1.5. The homogeneous part of the solution is given by

$$q_j^h(t) = A\cos(\omega_j t) + B\sin(\omega_j t), \tag{3.30}$$

where A and B are constants determined by initial conditions. Thus, we have

$$\begin{aligned}q_j(t) = q_j^p(t) + q_j^h(t) =& \frac{C_j}{m_j\omega_j^2}\left\{{}^{W}_{+}\boldsymbol{D}_t^{\alpha}Q(t)-\frac{d}{dt}\,{}^{W}_{+}\boldsymbol{D}_t^{\alpha}\left[\cos(\omega_j t)\Theta(t)*Q(t)\right]\right\}\\ &+ A\cos(\omega_j t) + B\sin(\omega_j t),\end{aligned} \tag{3.31}$$

[3]The first term in Eq. (3.27) still shows a coupling between the bath and the particle, even for $t < 0$. However, this term will exactly cancel the term coming from $\mathcal{L}_{CT}$ such that it has no contribution in the equation of motion of the particle.

with A and B determined by initial conditions. After this analysis of the equations of motion for the bath, we can write the Weyl fractional Euler-Lagrange equation for the system. By applying Eq. (3.15) to Eq. (3.16), with $\mathcal{L}_{CT}$ given by Eq. (3.24), we get

$$M\ddot{Q}(t) = -\frac{\partial V(Q)}{\partial Q} + \sum_{k=1}^{N}\left[C_k\, {}^{W}_{-}\boldsymbol{D}^{\alpha}_{t}\, q_k(t) - \frac{C_k^2}{m_k\omega_k^2}\, {}^{W}_{-}\boldsymbol{D}^{\alpha}_{t}\, {}^{W}_{+}\boldsymbol{D}^{\alpha}_{t}\, Q(t)\right]. \tag{3.32}$$

Eliminating now the bath coordinates by inserting Eq. (3.31) into (3.32), we obtain

$$\begin{aligned} M\ddot{Q}(t) + \frac{\partial V(Q)}{\partial Q} = &-\sum_{k=1}^{N}\frac{C_k^2}{m_k\omega_k^2}\frac{d}{dt}\, {}^{W}_{-}\boldsymbol{D}^{\alpha}_{t}\, {}^{W}_{+}\boldsymbol{D}^{\alpha}_{t}\left[\cos(\omega_k t)\Theta(t) * Q(t)\right] \\ &+ C_k A\, {}^{W}_{-}\boldsymbol{D}^{\alpha}_{t}\cos(\omega_k t) + C_k B\, {}^{W}_{-}\boldsymbol{D}^{\alpha}_{t}\sin(\omega_k t). \end{aligned} \tag{3.33}$$

Next, we continue in the same way as we did for the Caldeira-Leggett model. We calculate the spectral function associated with Lagrangian (3.16). The force coming from the interaction term in Fourier space is this time given by $F(\omega) = (i\omega)^{\alpha}\sum_{k=1}^{N} C_k q_k(\omega)$. Eq. (3.31) tells us that $q_k(\omega)$ is a function of $Q(\omega)$. On closer inspection, one sees that only the particular solution is depended on $Q(t)$, meaning that Eq. (3.26) can be used. The dynamical susceptibility is thus given by

$$\begin{aligned} \chi_B(\omega) &\equiv \frac{\partial F(\omega)}{\partial Q(\omega)} \\ &= -\sum_{k=1}^{N}\frac{C_k^2(i\omega)^{2\alpha}}{m_k(\omega^2-\omega_j^2)}, \end{aligned} \tag{3.34}$$

where we also used the addition property of the complex power function, see Thm. B.3.1. Writing $(i\omega)^{2\alpha} = |\omega|^{2\alpha}e^{2\alpha i\arg(i\omega)} = |\omega|^{2\alpha}e^{\alpha i\pi\,\mathrm{sign}(\omega)} = |\omega|^{2\alpha}\left[\cos(\alpha\pi) + i\ \mathrm{sign}(\omega)\sin(\alpha\pi)\right]$ yields

$$\chi_B(\omega) = -\sum_{k=1}^{N}|\omega|^{2\alpha}\left[\cos(\alpha\pi) + i\ \mathrm{sign}(\omega)\sin(\alpha\pi)\right]\frac{C_k^2}{m_k(\omega^2-\omega_j^2)}. \tag{3.35}$$

Using Eq. (B.43) and (B.44), the spectral function becomes

$$\begin{aligned} J(\omega) = \mathrm{Im}\left[\chi_B(\omega)\right] &= \frac{\pi}{2}|\omega|^{2\alpha}\cos(\pi\alpha)\sum_{k=1}^{N}\frac{C_k^2}{m_k\omega_k}\left[\delta(\omega-\omega_k) - \delta(\omega+\omega_k)\right] \\ &= \frac{\pi}{2}\omega^{2\alpha}\cos(\pi\alpha)\sum_{k=1}^{N}\frac{C_k^2}{m_k\omega_k}\delta(\omega-\omega_k) \\ &= \omega^{2\alpha}\cos(\pi\alpha)J_{CL}(\omega), \end{aligned} \tag{3.36}$$

where in the second line we imposed that physical frequencies are positive, $\omega > 0$, and $\omega_k > 0$. In the last line we identified the usual Caldeira-Leggett spectral function given by Eq. (2.38).

Remark 3.3.1. *This already gives a hint that Lagrangian (3.16) will be able to describe anomalous diffusion without imposing a non-Ohmic macroscopic spectral function, since the microscopic spectral function has a non-Ohmic prefactor $\omega^{2\alpha}$.*

Remark 3.3.2. *In the limit of $\alpha \to 0$, which is the limit for the usual Caldeira-Leggett model, we get the Caldeira-Leggett spectral function.*

Returning back to Eq. (3.33), we define the friction force $F_{fr}(t)$ and the fluctuating force $f(t)$ by

$$F_{fr}(t) \equiv \sum_{k=1}^{N} \frac{C_k^2}{m_k \omega_k^2} \frac{d}{dt} {}_{-}^{W}\boldsymbol{D}_t^{\alpha} {}_{+}^{W}\boldsymbol{D}_t^{\alpha} \left[\cos(\omega_k t)\Theta(t) * Q(t)\right], \tag{3.37}$$

$$f(t) \equiv \sum_{k=1}^{N} C_k {}_{-}^{W}\boldsymbol{D}_t^{\alpha} \left[A\cos(\omega_k t) + B\sin(\omega_k t)\right]. \tag{3.38}$$

Remark 3.3.3. *Note that in the limit of $\alpha \to 0$, we get exactly the same friction and fluctuating forces as in the usual Caldeira-Leggett model, which are given by Eq. (2.39) and (2.43), respectively.*

3.3.2 The friction force

Starting with the friction force, we can insert Eq. (2.38) into Eq. (3.37) to get

$$\begin{aligned} F_{fr} =& \sum_{k=1}^{N} \frac{C_k^2}{m_k \omega_k^2} \frac{d}{dt} {}_{-}^{W}\boldsymbol{D}_t^{\alpha} {}_{+}^{W}\boldsymbol{D}_t^{\alpha} \left[\cos(\omega_k t)\Theta(t) * Q(t)\right] \\ =& \frac{d}{dt} {}_{-}^{W}\boldsymbol{D}_t^{\alpha} {}_{+}^{W}\boldsymbol{D}_t^{\alpha} \int_0^t d\tau \int_0^{\infty} d\omega \left\{ \frac{1}{\omega} \sum_{k=1}^{N} \frac{C_k^2}{m_k \omega_k} \delta(\omega - \omega_k) \cos[\omega(t-\tau)] Q(\tau) \right\} \\ =& \frac{2}{\pi} \frac{d}{dt} {}_{-}^{W}\boldsymbol{D}_t^{\alpha} {}_{+}^{W}\boldsymbol{D}_t^{\alpha} \int_0^t d\tau \int_0^{\infty} d\omega \frac{J_{CL}(\omega)}{\omega} \cos[\omega(t-\tau)] Q(\tau). \end{aligned} \tag{3.39}$$

To convince ourselves that the above actually is a friction term, we need to gain more knowledge of $J_{CL}(\omega)$. The spectral function tells us how the system reacts to a given frequency. It is thus logical that $J_{CL}(0) = 0$. Therefore, we can do a linear taylor approximation of $J_{CL}(\omega)$ to get linear behavior. We can thus take the Caldeira-Leggett spectral function to be Ohmic, which means that this spectral function can effectively be described as

$$J_{CL}(\omega) = \begin{cases} \eta\omega & \text{for } \omega < \Omega, \\ 0 & \text{for } \omega > \Omega, \end{cases} \tag{3.40}$$

where Ω is a high-frequency cut-off ($\Omega \to \infty$) and η the macroscopic friction coefficient. We then get

$$\begin{aligned} F_{fr} &= \frac{2\eta}{\pi}\frac{d}{dt}\,{}_{-}^{W}\boldsymbol{D}_t^{\alpha}\,{}_{+}^{W}\boldsymbol{D}_t^{\alpha}\left\{\int_0^t d\tau \int_0^{\infty} d\omega \cos[\omega(t-\tau)]Q(\tau)\right\} \\ &= 2\eta\frac{d}{dt}\,{}_{-}^{W}\boldsymbol{D}_t^{\alpha}\,{}_{+}^{W}\boldsymbol{D}_t^{\alpha}\left[\int_0^t d\tau\delta(t-\tau)Q(\tau)\right] \\ &= \eta\,{}_{-}^{W}\boldsymbol{D}_t^{\alpha}\,{}_{+}^{W}\boldsymbol{D}_t^{\alpha}\dot{Q}(t), \end{aligned} \tag{3.41}$$

where, like in the calculation for the Caldeira-Leggett friction term, the delta function is evaluated at the boundary. This gives an extra factor of 1/2. Eq. (3.41) reduces to a normal friction term in the limit of $\alpha \to 0$, which is indeed when our model should reduce to the normal Caldeira-Leggett model.

3.3.3 The fluctuating force

The first step is to determine the constants A and B in Eq. (3.31). This is done by only coupling the particle coordinate $Q(t)$ to the bath after $t = 0$, such that A and B can simply be found by inserting $t = 0$ in Eq. (3.30). We thus find

$$\begin{cases} A = q_j(0), \\ B = \frac{\dot{q}_j(0)}{\omega_j}. \end{cases} \tag{3.42}$$

Inserting this into Eq. (3.38), we get

$$f(t) = \sum_{k=1}^{N} C_k\,{}_{-}^{W}\boldsymbol{D}_t^{\alpha}\left[q_k(0)\cos(\omega_k t) + \frac{\dot{q}_k(0)}{\omega_k}\sin(\omega_k t)\right]. \tag{3.43}$$

Proceeding analogously to the calculation done in Sec. 2.2, we find that

$$\langle f(t)\rangle = 0, \tag{3.44}$$

$$\langle f(t)f(t')\rangle = 2\eta k_B T\,{}_{-}^{W}\boldsymbol{D}_t^{\alpha}\,{}_{-}^{W}\boldsymbol{D}_{t'}^{\alpha}\delta(t-t'). \tag{3.45}$$

In practice, Eq. (3.45) should be seen as a distribution defined through the Weyl fractional partial integration formula, see Thm. 3.1.1. However, we will show that Eq. (3.45) is actually colored noise. Using the definition of the pseudo Weyl fractional derivative acting

on the Fourier representation of the delta function, we get

$$\begin{aligned}
{}^{W}_{-}\boldsymbol{D}^{\alpha}_{t}\,{}^{W}_{-}\boldsymbol{D}^{\alpha}_{t'}\delta(t-t') &= \int_{-\infty}^{\infty}\frac{d\omega}{2\pi}\,{}^{W}_{-}\boldsymbol{D}^{\alpha}_{t}e^{i\omega t}\,{}^{W}_{-}\boldsymbol{D}^{\alpha}_{t'}e^{-i\omega t}\\
&= \int_{-\infty}^{\infty}\frac{d\omega}{2\pi}e^{i\omega(t-t')}|\omega|^{2\alpha}\\
&= \frac{1}{2\pi}\int_{0}^{\infty}d\omega\left[e^{i\omega(t-t')}\omega^{2\alpha}+e^{-i\omega(t-t')}\omega^{2\alpha}\right]\\
&= \frac{1}{2\pi}\left\{\mathcal{M}\left[e^{i\omega(t-t')};2\alpha+1\right]+\mathcal{M}\left[e^{-i\omega(t-t')};2\alpha+1\right]\right\}\\
&= \frac{1}{2\pi}\left[(-i)^{-2\alpha-1}+i^{-2\alpha-1}\right]\left(t-t'\right)^{-2\alpha-1}\Gamma(2\alpha+1)\\
&= \frac{\sin(\pi\alpha)\Gamma(2\alpha+1)}{\pi}\left(t-t'\right)^{-2\alpha-1},
\end{aligned}\tag{3.46}$$

where in the first line we used the Fourier representation of the delta function, in the second line we used the result from Ex. 3.1.2, in the fourth line we identified the Mellin transform of the exponential function and in the fifth line we used Eq. (B.65), justified by Rem. B.7.3. Note that this representation of colored noise is only valid for $(2\alpha+1)>0$, which can be deduced from the convergence of the used Mellin transforms, see Eq. (B.65).

3.3.4 The Weyl fractional Langevin equation

Finally, substituting Eqs. (3.41) and (3.43) into Eq. (3.33) yields

$$M\ddot{Q}(t)+\frac{\partial V(Q)}{\partial Q}+\eta\,{}^{W}_{-}\boldsymbol{D}^{\alpha}_{t}\,{}^{W}_{+}\boldsymbol{D}^{\alpha}_{t}\dot{Q}(t)=f(t),\tag{3.47}$$

with $\langle f(t)\rangle=0$ and $\langle f(t)f(t')\rangle=2\eta k_BT\,{}^{W}_{-}\boldsymbol{D}^{\alpha}_{t}\,{}^{W}_{-}\boldsymbol{D}^{\alpha}_{t'}\delta(t-t')$.

Remark 3.3.4. *Note that just by changing the coupling to the bath, we managed to obtain a modified version of the Langevin equation that we call the Weyl fractional Langevin equation. There was no need to assume a non-Ohmic bath explicitly.*

3.4 Solution of the Weyl fractional Langevin equation for the free case

The free case of Eq. (3.47) is obtained by setting $V=0$, leading to

$$M\ddot{Q}(t)+\eta\,{}^{W}_{-}\boldsymbol{D}^{\alpha}_{t}\,{}^{W}_{+}\boldsymbol{D}^{\alpha}_{t}\dot{Q}(t)=f(t),\tag{3.48}$$

with $\langle f(t)\rangle = 0$ and $\langle f(t)f(t')\rangle = 2\eta k_B T\, {}^{W}_{-}\boldsymbol{D}^{\alpha}_{t}\, {}^{W}_{-}\boldsymbol{D}^{\alpha}_{t'}\delta(t-t')$. The particular solution, $Q^p(t)$, of Eq. (3.48) for the case $V(Q) = 0$ is found by taking the Fourier transform on both sides of the equation, yielding

$$Q^p(\omega) = \frac{f(\omega)}{-M\omega^2 + \eta i\omega|\omega|^{2\alpha}}. \tag{3.49}$$

Taking the inverse Fourier transforms gives

$$\begin{aligned} Q^p(t) &= \mathcal{F}^{-1}\left[\frac{f(\omega)}{-M\omega^2 + \eta i\omega|\omega|^{2\alpha}}; t\right] \\ &= \frac{1}{2\pi} f(t) * \mathcal{F}^{-1}\left(\frac{1}{-M\omega^2 + \eta i\omega|\omega|^{2\alpha}}; t\right), \end{aligned} \tag{3.50}$$

where in the last line we used Lem. B.1.4.

Remark 3.4.1. *When comparing Eq. (3.50) with the particular solution of the normal Langevin equation, given by Eq. (2.13), we see that the structure of the solution remains the same. The only difference between the two solutions is the term $|\omega|^{2\alpha}$. Despite its innocent appearance, including the factor $|\omega|^{2\alpha}$ results in the need to understand Secs. B.5, B.6, B.7 and B.8.*

Now, we need to find the homogeneous solution, $Q^h(t)$. Therefore, we solve the homogeneous equation in Fourier space, namely

$$\omega\left(-M\omega + \eta i|\omega|^{2\alpha}\right) = 0. \tag{3.51}$$

The above equation then implies that either

$$\omega = 0 \quad \text{or that} \quad \omega = i\frac{\eta}{M}|\omega|^{2\alpha}. \tag{3.52}$$

Eq. (3.52) can be solved by using polar coordinates. We substitute $\omega = Re^{i\theta}$ with $R \in \mathbb{R}$ and $0 \leq \theta < 2\pi$ into Eq. (3.52) which gives

$$Re^{i\theta} = i\frac{\eta}{M}R^{2\alpha}. \tag{3.53}$$

It is clear that the above equation implies that $e^{i\theta} = i$ and

$$R = \frac{\eta}{M}R^{2\alpha}. \tag{3.54}$$

We solve the above equation by the following anzats: $R = (\eta/M)^b$. Substituting this anzats into Eq. (3.54) yields

$$\left(\frac{\eta}{M}\right)^b = \left(\frac{\eta}{M}\right)^{2\alpha b+1}, \tag{3.55}$$

which implies that

$$b = \frac{1}{1-2\alpha}. \tag{3.56}$$

We thus finally obtain that Eq. (3.51) is solved by

$$\omega = 0 \text{ or } \omega = i\left(\frac{\eta}{M}\right)^{\frac{1}{1-2\alpha}}. \tag{3.57}$$

This means that

$$\begin{aligned} Q^h(t) &= \mathcal{F}^{-1}\left\{A\delta(\omega) + B\delta\left(\omega - i\left(\frac{\eta}{M}\right)^{\frac{1}{1-2\alpha}}\right)\right\} \\ &= C + D\exp\left[-t\left(\frac{\eta}{M}\right)^{\frac{1}{1-2\alpha}}\right] \end{aligned} \tag{3.58}$$

where C and D are constants that will be determined later. One could substitute this solution back into the homogeneous equation and use the result from Ex. 3.1.3 to verify that this indeed solves the homogeneous equation.

Remark 3.4.2. *When we compare Eq. (3.58) with the homogeneous solution in the case of the normal Langevin, namely Eq. (2.20), we notice that the solution has the same structure, the only difference is a rescaling of the friction coefficient and of the mass. Since we obtained the solution given by Eq. (3.58) through an ansatz, it is still uncertain whether it constitutes the complete homogeneous solution or if there are missing terms in it.*

Next, we combine Eqs. (3.50) and (3.58), which gives the full solution, namely

$$\begin{aligned} Q(t) &= Q^p(t) + Q^h(t) \\ &= \frac{1}{2\pi} f(t) * \mathcal{F}^{-1}\left(\frac{1}{-M\omega^2 + \eta i\omega|\omega|^{2\alpha}}; t\right) + C + D\exp\left[-t\left(\frac{\eta}{M}\right)^{\frac{1}{1-2\alpha}}\right]. \end{aligned} \tag{3.59}$$

To determine the constants, C and D, we work in the same way as for the fluctuating force. We say that the particle coordinate $Q(t)$ is only coupled to the bath for $t > 0$, such that we can take $f(0) = 0$ and $\dot{f}(0) = 0$. This implies that C and D are only determined by the homogeneous part in Eq. (3.59), leading to

$$\begin{cases} C = Q(0) + \dot{Q}(0)\left(\frac{M}{\eta}\right)^{\frac{1}{1-2\alpha}}, \\ D = -\dot{Q}(0)\left(\frac{M}{\eta}\right)^{\frac{1}{1-2\alpha}}. \end{cases} \tag{3.60}$$

Since our system is translation invariant, we can chose for simplicity $Q(0) = 0$. Eq. (3.59) then becomes

$$Q(t) = \frac{f(t)}{2\pi} * \mathcal{F}^{-1}\left(\frac{1}{-M\omega^2 + \eta i\omega|\omega|^{2\alpha}}; t\right) + \dot{Q}(0)\left(\frac{M}{\eta}\right)^{\frac{1}{1-2\alpha}}\left\{1 - \exp\left[-t\left(\frac{\eta}{M}\right)^{\frac{1}{1-2\alpha}}\right]\right\}. \tag{3.61}$$

Next, we are interested in the mean squared displacement,

$$\langle Q(t)^2\rangle = \left\langle \left(\frac{1}{2\pi}\int_0^t d\tau f(t-\tau)\mathcal{F}^{-1}\left(\frac{1}{-M\omega^2+\eta i\omega|\omega|^{2\alpha}};\tau\right) + \dot{Q}(0)\left(\frac{M}{\eta}\right)^{\frac{1}{1-2\alpha}}\left\{1-\exp\left[-t\left(\frac{\eta}{M}\right)^{\frac{1}{1-2\alpha}}\right]\right\}\right)^2\right\rangle. \tag{3.62}$$

We can now use the linearity of the ensemble averages and the fact that $\langle f(t)\dot{Q}(0)\rangle = \langle f(t)\rangle = 0$, $\langle \dot{Q}(0)^2\rangle = k_BT/M$, and $\langle f(t)f(t')\rangle = 2\eta k_BT\, {}^W_-\boldsymbol{D}^\alpha_t\, {}^W_-\boldsymbol{D}^\alpha_{t'}\delta(t-t')$ to obtain

$$\langle Q(t)^2\rangle = \frac{\eta k_BT}{2\pi^2}\int_0^t d\tau\int_0^t d\tau'\, {}^W_-\boldsymbol{D}^\alpha_\tau\, {}^W_-\boldsymbol{D}^\alpha_{\tau'}\delta\left(\tau-\tau'\right)\mathcal{F}^{-1}\left(\frac{1}{-M\omega^2+\eta i\omega|\omega|^{2\alpha}};\tau\right)\times \times\mathcal{F}^{-1}\left(\frac{1}{-M\omega^2+\eta i\omega|\omega|^{2\alpha}};\tau'\right) + \frac{k_BT}{M}\left(\frac{M}{\eta}\right)^{\frac{2}{1-2\alpha}}\left\{1-\exp\left[-t\left(\frac{\eta}{M}\right)^{\frac{1}{1-2\alpha}}\right]\right\}^2. \tag{3.63}$$

Next, we can do partial integration of the pseudo Weyl fractional derivatives (see Thm. 3.1.1), which allows us to use the delta function, thus obtaining

$$\begin{aligned}\langle Q(t)^2\rangle &= \frac{\eta k_BT}{2\pi^2}\int_0^t d\tau\left[{}^W_+\boldsymbol{D}^\alpha_\tau\mathcal{F}^{-1}\left(\frac{1}{-M\omega^2+\eta i\omega|\omega|^{2\alpha}};\tau\right)\right]^2 + \frac{k_BT}{M}\left(\frac{M}{\eta}\right)^{\frac{2}{1-2\alpha}}\left\{1-\exp\left[-t\left(\frac{\eta}{M}\right)^{\frac{1}{1-2\alpha}}\right]\right\}^2 \\ &= \frac{\eta k_BT}{2\pi^2}\int_0^t d\tau\left\{\mathcal{F}^{-1}\left[\frac{(i\omega)^\alpha}{-M\omega^2+\eta i\omega|\omega|^{2\alpha}};\tau\right]\right\}^2 + \frac{k_BT}{M}\left(\frac{M}{\eta}\right)^{\frac{2}{1-2\alpha}}\left\{1-\exp\left[-t\left(\frac{\eta}{M}\right)^{\frac{1}{1-2\alpha}}\right]\right\}^2,\end{aligned} \tag{3.64}$$

where in the last line we used the definition of the Weyl fractional derivative.

3.5 Asymptotic expansions of the mean squared displacement

The goal of this section is to determine the short-and long-time behavior of the solution found in the previous section, see Eq. (3.64). To answer this question, we need to understand the asymptotic behavior of the inverse Fourier integral, given by

$$I(t) \equiv \mathcal{F}^{-1}\left[\frac{(i\omega)^\alpha}{-M\omega^2+\eta i\omega|\omega|^{2\alpha}};t\right] = \int_{-\infty}^{\infty} d\omega e^{i\omega t}\frac{(i\omega)^\alpha}{i\eta\omega|\omega|^{2\alpha}-M\omega^2}. \tag{3.65}$$

The first instinct that one might have is to discard one of the two terms in the denominator based on if η/M is either big or small. At first glance this looks similar to the approximations used in Eq. (2.10) and (2.11). However, this turns out to give wrong results. The key difference with this approximation and the one we used in Eq. (2.10) and (2.11), is that in those equations we compared t with η/M. Because of this, it is clear that taking η/M to be big or small corresponds to short time and long times respectively. In Eq. (3.65), it is not clear if those limits would still correspond to the same short and long time behavior since those parameters are not directly compared with t. Because of this we have to use a different method to find the asymptotic expansions of Eq. (3.65). We chose to derive an equivalence between this integral and a special function known as the Fox H-function. This is done because the asymptotic expansions are known for the Fox H-functions. To achieve this equivalence, we use the following steps:

1. Simplify Eq. (3.65) by using properties of the Fourier transform[4].
2. Take the Mellin transform[5] of the simplified expression.
3. Write this in a form that is compatible with the definition of the Fox H-function[6].
4. Take the inverse Mellin transform.
5. Identify the definition of a specific Fox-H function.
6. Use the known asymptotic expansions of the Fox H-function to get the asymptotic expansions of the mean squared displacement.

Steps 2-5 are inspired by Ref. [**56**].

3.5.1 Writing the Fourier integral as a Fox-H function

First, we simplify $I(t)$ as

$$\begin{aligned} I(t) &= \mathcal{F}^{-1}\left[\frac{(i\omega)^{\alpha}}{-M\omega^2+\eta i\omega|\omega|^{2\alpha}};t\right] \\ &= \frac{1}{2\pi}\mathcal{F}^{-1}\left[\frac{1}{\omega};t\right] * \mathcal{F}^{-1}\left[\frac{(i\omega)^{\alpha}}{-M\omega+\eta i|\omega|^{2\alpha}};t\right] \\ &= i\Theta(t) * \mathcal{F}^{-1}\left[\frac{(i\omega)^{\alpha}}{-M\omega+\eta i|\omega|^{2\alpha}};t\right] \\ &\equiv i\Theta(t) * I'(t), \end{aligned} \tag{3.66}$$

[4] See Sec. B.1 of App. B.
[5] See Sec. B.7 of App. B.
[6] See Sec. B.8 of App. B.

where in the second line we used Lem. B.1.4 and in the third line we interpreted this integral in the positive $i\epsilon$-interpretation for the same reason as was done in Eq. (2.14). Secondly, we take the Mellin transform of $I'(t)$, which gives

$$\begin{aligned} F(s) &\equiv \mathcal{M}\left[I'(t);s\right] \\ &= \int_0^\infty dt t^{s-1} \int_{-\infty}^\infty d\omega e^{i\omega t} \frac{(i\omega)^\alpha}{i\eta|\omega|^{2\alpha} - M\omega} \\ &= \frac{1}{M}\Gamma(s) \int_{-\infty}^\infty d\omega \frac{(i\omega)^\alpha (-i\omega)^{-s}}{i\frac{\eta}{M}|\omega|^{2\alpha} - \omega}, \end{aligned} \tag{3.67}$$

where in the last line we used the result of Ex. B.7.1, which is allowed (see Rem. B.7.2). This already gives a restriction on s, namely $\mathrm{Re}(s) > 0$. Next, we apply the definition of the complex power function together with the fact that $\omega \in \mathbb{R}$, which results in

$$\begin{aligned} F(s) &= \frac{1}{M}\Gamma(s) \int_{-\infty}^\infty d\omega \frac{|\omega|^{\alpha-s} e^{\arg(i\omega)i\alpha - \arg(-i\omega)is}}{i\frac{\eta}{M}|\omega|^{2\alpha} - \omega} \\ &= \frac{1}{M}\Gamma(s) \int_{-\infty}^\infty d\omega \frac{|\omega|^{\alpha-s} e^{i\arg(i\omega)(\alpha+s)}}{i\frac{\eta}{M}|\omega|^{2\alpha} - \omega}. \end{aligned} \tag{3.68}$$

We can further simplify the above equation by splitting the integral in its positive part and negative part Doing the substitution $\omega \to -\omega$ in the latter yields

$$\begin{aligned} F(s) &= \frac{1}{M}\Gamma(s)\left[e^{i\frac{\pi}{2}(\alpha+s)} \int_0^\infty d\omega \frac{\omega^{\alpha-s}}{i\frac{\eta}{M}\omega^{2\alpha} - \omega} + e^{-i\frac{\pi}{2}(\alpha+s)} \int_0^\infty d\omega \frac{\omega^{\alpha-s}}{i\frac{\eta}{M}\omega^{2\alpha} + \omega}\right] \\ &= \frac{1}{M}\Gamma(s)\left[e^{-i\frac{\pi}{2}(\alpha+s)} \int_0^\infty d\omega \frac{\omega^{\alpha-s-1}}{1 + i\frac{\eta}{M}\omega^{2\alpha-1}} - e^{i\frac{\pi}{2}(\alpha+s)} \int_0^\infty d\omega \frac{\omega^{\alpha-s-1}}{1 - i\frac{\eta}{M}\omega^{2\alpha-1}}\right] \\ &= \frac{\Gamma(s)}{M|2\alpha-1|}\left[e^{-i\frac{\pi}{2}(\alpha+s)}\left(i\frac{\eta}{M}\right)^{\frac{s-\alpha}{2\alpha-1}} - e^{i\frac{\pi}{2}(\alpha+s)}\left(-i\frac{\eta}{M}\right)^{\frac{s-\alpha}{2\alpha-1}}\right]\Gamma\left(\frac{\alpha-s}{2\alpha-1}\right)\Gamma\left(1-\frac{\alpha-s}{2\alpha-1}\right) \\ &= \frac{1}{M|2\alpha-1|}\left(\frac{\eta}{M}\right)^{\frac{s-\alpha}{2\alpha-1}}\left[e^{-i\frac{\pi}{2}\left(s+\frac{2\alpha^2}{2\alpha-1}\right)} - e^{i\frac{\pi}{2}\left(s+\frac{2\alpha^2}{2\alpha-1}\right)}\right]\Gamma(s)\Gamma\left(\frac{\alpha-s}{2\alpha-1}\right)\Gamma\left(1-\frac{\alpha-s}{2\alpha-1}\right) \\ &= -\frac{2i}{M|2\alpha-1|}\left(\frac{\eta}{M}\right)^{\frac{s-\alpha}{2\alpha-1}} \sin\left[\frac{\pi}{2}\left(s+\frac{2\alpha^2}{2\alpha-1}\right)\right]\Gamma(s)\Gamma\left(\frac{\alpha-s}{2\alpha-1}\right)\Gamma\left(1-\frac{\alpha-s}{2\alpha-1}\right), \end{aligned} \tag{3.69}$$

where in the third line we applied the result of Ex. B.7.2 to each term separately, which we can do because of Rem. B.7.4. However, using this example restricts the values of s even further. The additional constraint reads $0 < \mathrm{Re}\left[(\alpha-s)/(2\alpha-1)\right] < 1$. Together with the previous constraint that we already had, $\mathrm{Re}(s) > 0$, we get three different regions of convergence that are important to define the inverse Mellin transform (see Def. B.7.2).

Just like in the definition we call them fundamental strips (FS) and they are given by

$$\text{FS} = \begin{cases} S(0,\alpha) & \text{if } \alpha > 1, \\ S(1-\alpha,\alpha) & \text{if } \frac{1}{2} < \alpha < 1, \\ S(0,1-\alpha) & \text{if } \alpha < \frac{1}{2}. \end{cases} \tag{3.70}$$

Remark 3.5.1. *Note that the only two cases that are left out are $\alpha = 1/2$ and $\alpha = 1$ both of which can be easily worked out separately. Therefore we restrict from now on the values of $\alpha \neq 1/2, 1$.*

Finally, we use Euler's reflection formula, which is given by Lem. B.5.1, to get

$$F(s) = -\frac{2\pi i}{M|2\alpha-1|}\left(\frac{\eta}{M}\right)^{\frac{s-\alpha}{2\alpha-1}} \frac{\Gamma(s)\Gamma\left(\frac{\alpha-s}{2\alpha-1}\right)\Gamma\left(1-\frac{\alpha-s}{2\alpha-1}\right)}{\Gamma\left(\frac{\alpha^2}{2\alpha-1}+\frac{s}{2}\right)\Gamma\left(1-\frac{\alpha^2}{2\alpha-1}-\frac{s}{2}\right)}. \tag{3.71}$$

Since the inverse Mellin transform depends on the fundamental strip and the definition of the Fox H-function is depended on the sign of the factor $2\alpha - 1$, we will now split the calculation in three cases.

The first fundamental strip, $S(0,\alpha)$

Taking the above fundamental strip to be $S(1,\alpha)$ means that we restrict $\alpha > 1$, implying that $(2\alpha - 1) > 0$. Next, we note that in Def. B.8.1 some parameters have to be positive. The reason for this is that the contour in Def. B.8.1 has to split the poles in a certain way. The pole structure for $\alpha = 1.23$ can be seen in Fig. 3.1. Therefore, we rewrite Eq. (3.71) into

$$F(s) = -\frac{2\pi i}{M|2\alpha-1|}\left(\frac{\eta}{M}\right)^{\frac{s-\alpha}{2\alpha-1}} \frac{\Gamma(s)\Gamma\left(1-\frac{\alpha-1}{2\alpha-1}-\frac{s}{2\alpha-1}\right)\Gamma\left(\frac{\alpha-1}{2\alpha-1}+\frac{s}{2\alpha-1}\right)}{\Gamma\left(\frac{\alpha^2}{2\alpha-1}+\frac{s}{2}\right)\Gamma\left(1-\frac{\alpha^2}{2\alpha-1}-\frac{s}{2}\right)}. \tag{3.72}$$

Now, we can take the inverse Mellin transform of the above, see Def. B.7.2, which results in

$$\begin{aligned} I'(t) &= \mathcal{M}^{-1}\left[F(s);t\right] \\ &= \frac{1}{2\pi i}\int_{a-i\infty}^{a+i\infty} ds F(s) t^{-s} \\ &= -\frac{2\pi i}{M|2\alpha-1|}\left(\frac{\eta}{M}\right)^{-\frac{\alpha}{2\alpha-1}} \frac{1}{2\pi i}\int_{a-i\infty}^{a+i\infty} ds \left[\left(\frac{\eta}{M}\right)^{\frac{1}{1-2\alpha}} t\right]^{-s} \times \\ &\times \frac{\Gamma(s)\Gamma\left(-\frac{1}{2\alpha-1}+\frac{2s}{2\alpha-1}\right)\Gamma\left(1-\left[\frac{-1}{2\alpha-1}\right]-\frac{2s}{2\alpha-1}\right)}{\Gamma\left(1-\frac{\alpha-1}{2\alpha-1}-\frac{s}{2\alpha-1}\right)\Gamma\left(\frac{\alpha-1}{2\alpha-1}+\frac{s}{2\alpha-1}\right)}, \end{aligned} \tag{3.73}$$

where $a \in S(0,\alpha)$. Finally, we identify the following Fox-H function

$$I'(t) = -\frac{2\pi i}{M|2\alpha-1|}\left(\frac{\eta}{M}\right)^{-\frac{\alpha}{2\alpha-1}} H^{21}_{23}\left[\left(\frac{\eta}{M}\right)^{\frac{1}{1-2\alpha}} t \,\middle|\, \begin{matrix} (0,1) & \left(\frac{\alpha-1}{2\alpha-1},\frac{1}{2\alpha-1}\right), & \left(\frac{\alpha^2}{2\alpha-1},\frac{1}{2}\right) \\ & \left(\frac{\alpha-1}{2\alpha-1},\frac{1}{2\alpha-1}\right), & \left(\frac{\alpha^2}{2\alpha-1},\frac{1}{2}\right) \end{matrix}\right], \tag{3.74}$$

which can be verified using Def. B.8.1.

The second fundamental strip, $S(1-\alpha,\alpha)$

This case is very similar to the one we had for the first fundamental strip, the only difference being that the integration in the inverse Mellin transform is inside the strip $S(1-\alpha,\alpha)$ instead of $S(0,\alpha)$. Thus we can safely say that the results from the first fundamental strip are also valid for the second fundamental strip. Eq. (3.74) is thus valid for all $\alpha > 1/2$ and $\alpha \neq 1$.

The third fundamental strip, $S(0,1-\alpha)$

Finally, we work in the third fundamental strip, $S(0,1-\alpha)$, which means that $\alpha < 1/2$. Note that this implies that $(2\alpha-1) < 0$. In this case we rewrite Eq. (3.71) into

$$F(s) = -\frac{2\pi i}{M|2\alpha-1|}\left(\frac{\eta}{M}\right)^{\frac{s-\alpha}{2\alpha-1}} \frac{\Gamma(s)\Gamma\left(\frac{\alpha}{2\alpha-1}+\frac{s}{1-2\alpha}\right)\Gamma\left(1-\frac{\alpha}{2\alpha-1}-\frac{s}{1-2\alpha}\right)}{\Gamma\left(\frac{\alpha^2}{2\alpha-1}+\frac{s}{2}\right)\Gamma\left(1-\frac{\alpha^2}{2\alpha-1}-\frac{s}{2}\right)}. \tag{3.75}$$

Again this has to do with the pole structure of the gamma functions in the above equation. Comparing the sub-figures in Fig. 3.1 reveals that the blue and the green poles swapped their side of the fundamental strip, when going from $\alpha > 1/2$ to $\alpha < 1/2$. Next, we take the inverse Mellin transform of the above equation, with $a \in S(0,1-\alpha)$, which yields

$$\begin{aligned} I'(t) &= \mathcal{M}^{-1}\left[F(s);t\right] \\ &= \frac{1}{2\pi i}\int_{a-i\infty}^{a+i\infty} ds F(s) t^{-s} \\ &= -\frac{2\pi i}{M|2\alpha-1|}\left(\frac{\eta}{M}\right)^{-\frac{\alpha}{2\alpha-1}} \frac{1}{2\pi i}\int_{a-i\infty}^{a+i\infty} ds \left[\left(\frac{\eta}{M}\right)^{\frac{1}{1-2\alpha}} t\right]^{-s} \times \\ &\times \frac{\Gamma(s)\Gamma\left(\frac{\alpha}{2\alpha-1}+\frac{s}{1-2\alpha}\right)\Gamma\left(1-\frac{\alpha}{2\alpha-1}-\frac{s}{1-2\alpha}\right)}{\Gamma\left(\frac{\alpha^2}{2\alpha-1}+\frac{s}{2}\right)\Gamma\left(1-\frac{\alpha^2}{2\alpha-1}-\frac{s}{2}\right)}. \end{aligned} \tag{3.76}$$

Using Def. B.8.1, we can now identify a specific Fox-H function, given by

$$I'(t) = -\frac{2\pi i}{M|2\alpha-1|}\left(\frac{\eta}{M}\right)^{-\frac{\alpha}{2\alpha-1}} H^{21}_{23}\left[\left(\frac{\eta}{M}\right)^{\frac{1}{1-2\alpha}} t \,\middle|\, \begin{matrix}(0,1) & \left(\frac{\alpha}{2\alpha-1},\frac{1}{1-2\alpha}\right), & \left(\frac{\alpha^2}{2\alpha-1},\frac{1}{2}\right) \\ & \left(\frac{\alpha}{2\alpha-1},\frac{1}{1-2\alpha}\right), & \left(\frac{\alpha^2}{2\alpha-1},\frac{1}{2}\right)\end{matrix}\right]. \tag{3.77}$$

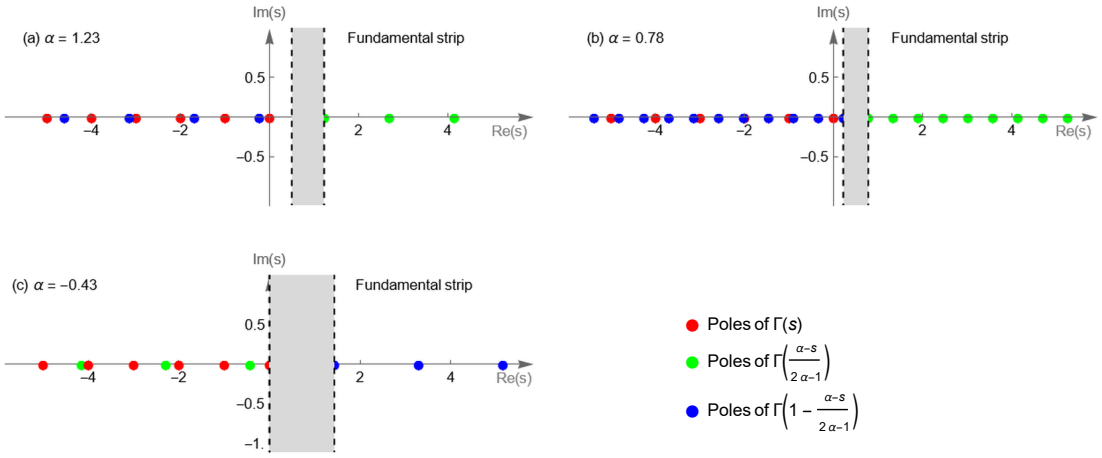

Figure 3.1: The three different fundamental strips of a Mellin transform involving the shown gamma functions in the legend. (a) the first fundamental strip, (b) the second and (c) the third. Notice that green poles are on the right of the fundamental strip in (a) and (b) but on the left and (c).

3.5.2 The asymptotic expansions of the Fox H-function

What remains is to apply the known asymptotic expansions for the Fox H-function to Eqs. (3.74) and (3.77). First, we note that in both cases we have $\mu_H, \alpha_H > 0$ such that we can use Thm. B.8.1 to find the expansions. The short-time behavior is given by

$$I'(t) \overset{t\to 0}{\sim} \begin{cases} 1 & \text{for } \alpha > 1, \\ t^{\alpha-1} & \text{for } \frac{1}{2} < \alpha < 1, \\ t^{\frac{2\alpha^2}{2\alpha-1}} & \text{for } \frac{1}{4} < \alpha < \frac{1}{2}, \\ t^{-\alpha} & \text{for } 0 < \alpha \leq \frac{1}{4}, \\ t^{\frac{2\alpha^2}{2\alpha-1}} & \text{for } \alpha < 0, \end{cases} \tag{3.78}$$

and the long-time behavior is

$$I'(t) \overset{t\to\infty}{\sim} \begin{cases} t^{-\alpha} & \text{for } \alpha > 1, \\ t^{\alpha-1} & \text{for } \alpha < 1, \alpha \neq 0. \end{cases} \tag{3.79}$$

From now on we will discard the case where $\alpha = -1/2, (-1 \pm \sqrt{3})/2, (-3 \pm \sqrt{21})/4$. This is because we want to keep the calculation as simple as possible and therefore do not want any logarithms while integrating the expansions. We thus have that $\alpha \in \mathbb{R} \setminus \mathcal{P}$ with $\mathcal{P} = \left\{(-3 - \sqrt{21})/4, (-1 - \sqrt{3})/2, -1/2, 0, (-1 + \sqrt{3})/2, (-3 + \sqrt{21})/4, 1/2, 1\right\}$.

3.5.3 The asymptotic expansions of the mean squared displacement

Recall that the mean squared displacement was given by

$$\begin{aligned} \left\langle Q(t)^2 \right\rangle = \frac{\eta k_B T}{2\pi^2} \int_0^t d\tau \left\{ \mathcal{F}^{-1}\left[\frac{(i\omega)^\alpha}{-M\omega^2 + \eta i\omega|\omega|^{2\alpha}}; \tau \right] \right\}^2 \\ + \frac{k_B T}{M} \left(\frac{M}{\eta} \right)^{\frac{2}{1-2\alpha}} \left\{ 1 - \exp\left[-t \left(\frac{\eta}{M} \right)^{\frac{1}{1-2\alpha}} \right] \right\}^2, \end{aligned} \tag{3.80}$$

and that the difficult part was understanding the asymptotic expansions of the inverse Fourier integral. We have managed to understand those expansions. Note that the definition of $I'(t)$ links it to the integral given by

$$\begin{aligned} I(t) &= \mathcal{F}^{-1}\left[\frac{(i\omega)^\alpha}{-M\omega^2 + \eta i\omega|\omega|^{2\alpha}}; t \right] \\ &= i\Theta(t) * I'(t) \\ &= i \int_0^t d\tau I'(\tau). \end{aligned} \tag{3.81}$$

First, we find the short time behavior of $I(t)$ by inserting into Eq. (3.81). For $t \to 0$[7] we get

$$I(t) \overset{t\to 0}{\sim} \begin{cases} t & \text{for } \alpha > 1, \\ t^{\alpha} & \text{for } \frac{1}{2} < \alpha < 1, \\ t^{\frac{2\alpha^2}{2\alpha-1}+1} & \text{for } \frac{1}{4} < \alpha < \frac{1}{2}, \\ t^{-\alpha+1} & \text{for } 0 < \alpha \leq \frac{1}{4}, \\ t^{\frac{2\alpha^2}{2\alpha-1}+1} & \text{for } \alpha < 0, \end{cases} \tag{3.82}$$

with $\alpha \notin \mathcal{P}$. Finally, we can substitute these asymptotic expansions into Eq. (3.80) and Taylor expand the exponential factor up to first order, to get the small time behavior of the MSD, which is given by

$$\left\langle Q(t)^2 \right\rangle \overset{t\to 0}{\sim} \begin{cases} t^2 & \text{for } \alpha > \frac{-1-\sqrt{5}}{4}, \alpha \notin \mathcal{P}, \\ t^{2\alpha+3} & \text{for } \alpha < \frac{-1-\sqrt{5}}{4}, \alpha \notin \mathcal{P}. \end{cases} \tag{3.83}$$

We can do exactly the same for the long-time behavior except that now we discard the exponential in Eq. (3.64) because it vanishes as $t \to \infty$. The long-time behavior of the MSD is

$$\left\langle Q(t)^2 \right\rangle \overset{t\to \infty}{\sim} \begin{cases} t^{-2\alpha+3} & \text{for } \alpha > 1, \alpha \notin \mathcal{P}, \\ t^{2\alpha+1} & \text{for } \alpha < 1, \alpha \notin \mathcal{P}. \end{cases} \tag{3.84}$$

Thus we obtained the asymptotic expansions for the MSD for the solution of the free Weyl fractional Langevin equation with colored noise, namely Eq. (3.48).

[7] To calculate the integral over the small time asymptotic expansion of $I'(t)$, see Eq. (3.81), one has to technically introduce a small time cut-off since otherwise the evaluation at $t = 0$ would diverge.

Chapter 4

Discussion, conclusion and outlook

In Ch.3, we introduced the Weyl fractional derivative which, due to its properties with the boundary and Fourier transforms, can be directly used inside the Lagrangian. We did this by imposing a fractional derivative in the coupling term between the system and bath, which we called a fractional Caldeira-Leggett model. Doing so required the introduction of the Weyl fractional Euler-Lagrange equation to derive the equations of motion, which we solved for the harmonic oscillators using Fourier transforms. We noted that the fractional bath spectral function could be written in terms of a fractional power prefactor and the original Caldeira-Leggett spectral function. Inserting the commonly used Ohmic assumption for the Caldeira-Leggett spectral function, we found an effective spectral function which has a power law of order $2\alpha + 1$. This led to a Weyl fractional Langevin equation with colored noise. We provided the analytical solutions for several quantities in terms of an inverse Fourier transform, which we could interpret as a Fox H-function with the help of Mellin transforms. Finally, the asymptotic limits of these solutions were calculated for a wide range of values. For short times, we found both ballistic and non-ballistic regimes. This means that, in some cases, friction can dominate the short-time dynamics. For long times we found everything ranging from sub-, normal-, and super-diffusion, as well as saturation, which could hint to a relation with glassy physics. Overall, we found a very broad range of anomalous diffusion.

We are now in a position to compare our results, given by Eqs. (3.83) and (3.84), with the results of Ref. [**22**], in which, to the best of our knowledge, a fractional Langevin equation was investigated for the first time. First, we note that we use the Weyl fractional derivative, while Ref. [**22**] used the Caputo fractional derivative. It is known that the Caputo fractional derivative and Weyl fractional derivatives lead to different results in a lot of cases. One such example is when the fractional derivative of the exponential function is calculated. This makes it very interesting to compare the results. The friction force in Eq. (3.48) is of order $2\alpha + 1$, which corresponds to the derivative order from Ref. [**22**] (which we will call α_L). Therefore, to compare the results, we must make the substitution

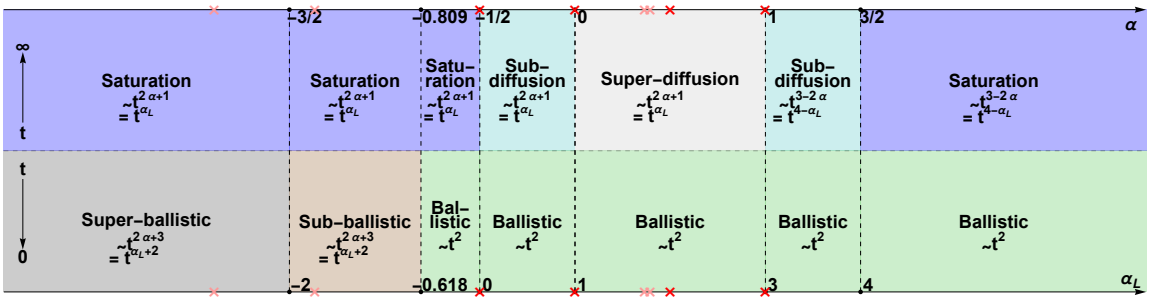

Figure 4.1: The behavior of the MSD for small and large times are shown in terms of the used parameter in this paper, α, but also in terms of the total friction force order, α_L, which are linked by $\alpha_L = 2\alpha + 1$. Some specific values of α, and in turn α_L, should be ignored in this plot, namely $\alpha \in \left\{(-3 \pm \sqrt{21})/4, (-1 \pm \sqrt{3})/2, \pm 1/2, 0, 1\right\}$. The light red crosses indicate the values excluded for simplicity while the red crosses indicate the values for which our calculation did not apply.

$\alpha = (\alpha_L - 1)/2$ in Eq. (3.84). Second, we note that Ref. [**22**] only considered the two cases, $0 < \alpha_L < 1$ and $1 < \alpha_L < 2$. For those restrictions, our result from Eq. (3.84) becomes

$$\left\langle Q(t)^2 \right\rangle \overset{t\to\infty}{\sim} t^{\alpha_L}, \tag{4.1}$$

which is exactly what was found in Ref. [**22**]. It is remarkable that the same result is obtained for a Caputo derivative instead of Weyl, and derived using completely different techniques. Moreover, we generalized the result of the Caputo derivative, which in Ref. [**22**] was obtained for $0 < \alpha_L < 2$ (corresponding to $-1/2 < \alpha < 1/2$), to the entire real line, except for $\alpha = 0$, $\alpha = \pm 1/2, \alpha = 1$ (corresponding to $\alpha_L = 0, 1, 2, 3$, which are well-known integer derivative cases) and $\alpha = (-3 \pm \sqrt{21})/4$, $\alpha = (-1 \pm \sqrt{3})/2$, which are cases for which a logarithm would appear because of integration. We can thus conclude that our model, given by Eq. (3.16), describes sub-diffusion for $-1/2 < \alpha < 0$, and super-diffusion for $0 < \alpha < 1$, while $1 < \alpha < 3/2$ yields sub-diffusion. Remarkably, when $\alpha > 3/2$ and when $\alpha < -1/2$ we find a negative MSD exponent, which typically indicates saturation in the MSD [**23**], possibly describing glassy states. The short-time behavior of the MSD exhibits the usual ballistic ($\sim t^2$) behavior when $\alpha > -(1 + \sqrt{5})/4 \approx -0.809$. However, when $-3/2 < \alpha < -(1 + \sqrt{5})/4$ we find sub-ballistic behavior, meaning that the MSD goes as t^p, where $0 < p < 2$, when $t \to 0$. In particular, we have that $0 < p < (5 - \sqrt{5})/2 \approx 1.382$. Finally, for $\alpha < -3/2$, we find super-ballistic behavior of the MSD for $t \to 0$, which in our words means that the short time behavior goes as a negative exponent. The different behavior of the MSD for short and long times in terms of the parameter of our model, α, and the total order of the friction force, α_L, is summarized in Fig. 4.1.

When we calculated the spectral function, we were able to identify the regular Caldeira-

Leggett spectral function inside it, but there is some delicate interpretation that needs to be done here. The spectral function describes the susceptibility of the bath to an external system in the frequency domain. However, as it turns out, this is not just a property of the bath, but also depends on the way that you couple to it, which is almost always linear. This is done because it is typically the lowest-order contribution, and it gives excellent options to proceed mathematically, with e.g. completing the square. Since baths are typically thought to be Ohmic (linear in frequency) in this fashion, we believe that the most likely assumption should be to keep this part identical, and thus retain an Ohmic $J_{CL}(\omega) \sim \omega$. In turn, this means that the fractional coupling spectral function goes as $J(\omega) \sim \omega^{2\alpha+1}$, which resulted in a Weyl fractional Langevin equation. The results of the latter remarkably match with Ref. [**22**], despite a different definition being used there, and even expand the domain of available parameters. Previously, this equation has only been derived using non-Ohmic baths, but this derivation shows that it can also be achieved for Ohmic baths, as long as the coupling term is changed accordingly. Hence, understanding the coupling mechanism is as important as understanding the bath properties in order to describe (anomalous) quantum diffusion.

As we have demonstrated, the Weyl fractional Langevin equation can describe anomalous diffusion for many different exponents. In experiments of quantum transport on fractals [**14**], theory of diffusion on confining geometries [**57**], and random walks [**12, 58**], several connections have been made to link either the order of the derivative or the diffusion exponent itself to a fractal dimension. Fractals can exhibit a dimension that is non-integer, such as the Sierpiński triangle which has a dimension of $d_f \approx 1.58$. Ref. [**14**] has shown that the MSD exhibits a regime where the exponent is equal to d_f. Although the mechanism for this is still not fully understood, this could be explained by an effect of the fractal dimension on the interaction between the underlying material and the quantum particle. If we assume that $\alpha_L = d_f$, then the Weyl fractional Langevin equation reproduces this result.

Moving forward, an important aspect that requires further investigation is the realization of a fractional derivative coupling as an effective theory. One way that was explored in this thesis was in the particular case of a self-similar fractal. An attempt was made in App. D to derive a fractional Langevin equation, starting from first principles. However, there seems to be one crucial missing link, namely, how the coupling constants, C_k, can be simplified in a fractal. Thus, this needs to be explored further. Another potential approach to derive a fractional coupling to the bath, is to couple the bath to another bath and subsequently integrate out the intermediate bath degrees of freedom to obtain an effective bath with the desired fractional derivative coupling. A final method that could result in Eq. (3.16) is inspired by the projection scheme used in Ref. [**54, 55**] and the fractal delta function used in Ref. [**59**]. In this approach one would project the initial theory down to a fractal, which could result in a fractional coupling. Furthermore, it is also interesting to explore quantization for the Weyl fractional derivative further than has already been done in the literature [**48,60,61**]. To do this one would first need to develop the Hamiltonian formalism

for these fractional derivatives, which can be inspired by Ref. [**62**]. After that, one chooses either for canonical quantization [**48**], path integral quantization [**60**] or the less known Weyl-Wigner quantization [**61**]. The last is in our opinion the most natural one to use for the Weyl fractional derivative and therefore the most promising method. Finally, we believe that it would be interesting to see if previous work [**33, 63, 64**], that assumes a non-Ohmic bath, could be reproduced by the approach used in this paper.

Appendix A

Fractals

The French mathematician, Benoît Mandelbrot, first used the term "fractal" in 1975 to describe irregular shapes in nature and mathematics that exhibit *self-similarity*, e.g. snowflakes. The word fractal comes from the Greek word "fractus", meaning "fractured". In this appendix we give a short and intuitive description of fractals. A mathematical discussion can be found in Ref. [**65**].
There are a lot of ways to define formally what the dimension of a geometrical object is through the Hausdorff measure and the Hausdorff dimension. However, we will take a more intuitive approach, which is done by working with three different geometrical objects: the square, the Sierpiński triangle and the Sierpiński carpet. We will define the dimension of an object from how it changes from one generation to the next. Starting from a given geometrical object, how many identical copies and at which scale do we have to 'glue' them together to obtain the same initial geometrical object? We say that the dimension of that

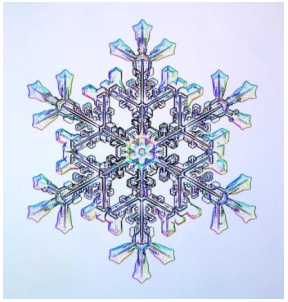

Figure A.1: A snowflake, which can be considered a fractal. Intuitively one can see that there is a certain symmetry in the snowflake, however it is difficult to pin-point.

object is determined by

$$d_f = \frac{\ln(N_{\text{copies}})}{\ln(K)}, \tag{A.1}$$

where N_{copies} is the number of identical copies needed to go from one generation to the another and K is the corresponding scaling factor. We note that this method does not work for a general geometric object because the construction is rather specific. We can illustrate that this intuitive definition works in the case of a square by noting that $N_{\text{copies}} = 4$ and $K = 2$, which can also be seen in Fig. A.2. According to Eq. (A.1), the dimension of a square is given by

$$d = \frac{\ln(4)}{\ln(2)} = 2, \tag{A.2}$$

which is what one expects. We can apply the same reasoning to the Sierpiński triangle,

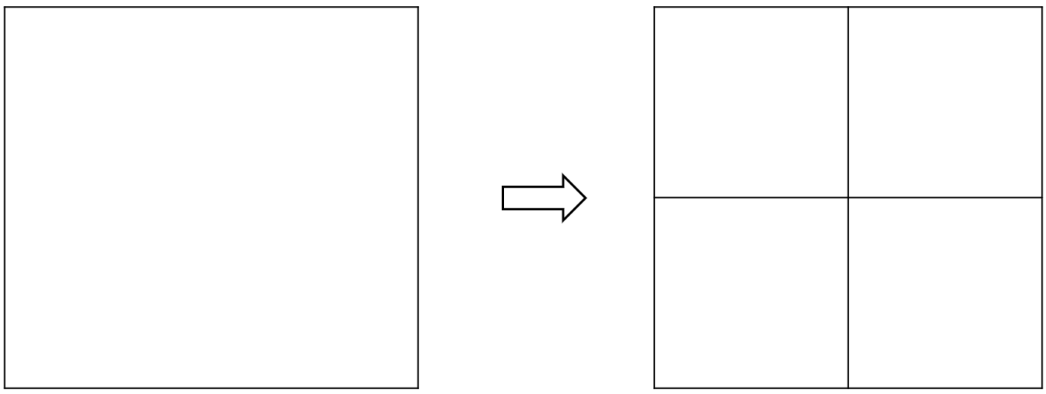

Figure A.2: The first and second generation of the square. It shows that four copies are needed and that the scaling factor is 2. This results in a dimension $d = 2$.

which is depicted in Fig. A.3. We find a dimension given by

$$d_f = \frac{\ln(3)}{\ln(2)} \approx 1.58. \tag{A.3}$$

Note that the dimension turns out to be non-integer. It might seem strange to have a non-integer dimension. However, this agrees with the intuition that the dimension of the Sierpiński triangle should be less than the dimension of the square, since it covers less than the square, but more than a line. Non-integer dimension will be one of the two defining properties that we will take for a fractal[1].

[1] Some fractals can have integer dimension. Examples include the Smith–Volterra–Cantor set, the Takagi or Blancmange curve, the Sierpiński tetrahedron, the Julia set, the Dragon curve, ...

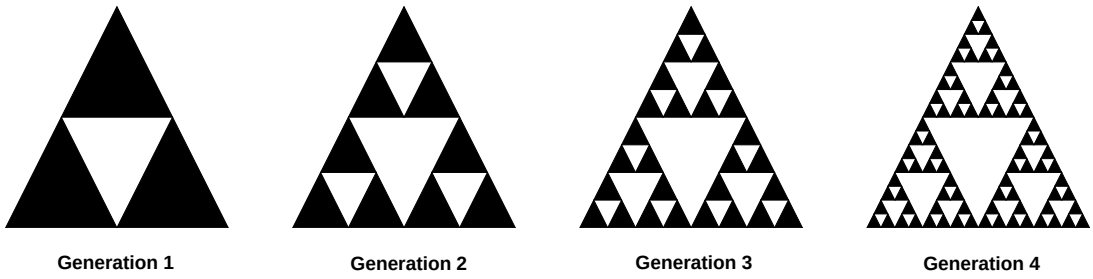

Figure A.3: The first, second, third, and fourth generations of the Sierpiński triangle. It shows that three copies are needed and that the scaling factor is 2. This results in a dimension $d_f \approx 1.58$.

Finally, we calculate the dimension of the Sierpiński carpet. From Fig. A.4 we can deduce that $N_{\text{copies}} = 8$ and the scaling factor $K = 3$. Therefore, we have

$$d_f = \frac{\ln(8)}{\ln(3)} \approx 1.89. \tag{A.4}$$

Now, that we defined the dimension, we move on to a very important symmetry that

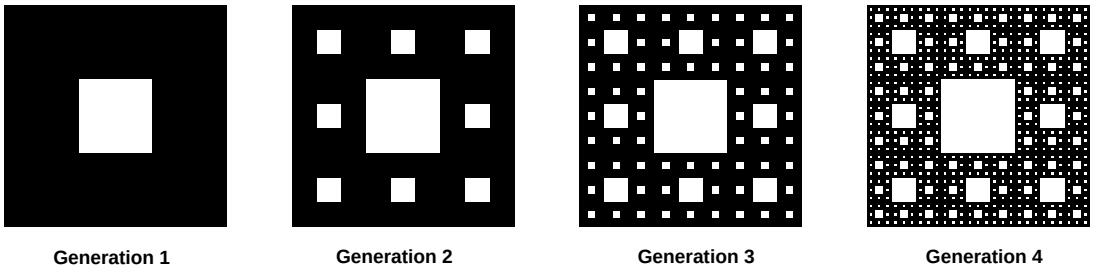

Figure A.4: The first, second, third, and fourth generations of the Sierpiński carpet. It shows that eight copies are needed and that the scaling factor is 3. This results in a dimension $d_f \approx 1.89$.

fractals have [2]: self-similarity. Self-similarity intuitively means that when you zoom into a part of the fractal, you exactly get that fractal again. This is illustrated in Fig. A.5. It makes sense that in our sequential approach, used to calculate the dimension, this

[2]There exist a collection of fractals known as random fractals, which do not have this specific symmetry. However, we are not interested in these fractals.

symmetry will only show itself when we go to the infinity generation. However, one can find approximate self-similarities in the earlier generations, meaning that zooming in doesn't result in exactly the same object but in one that is similarly looking. Therefore, we will refer to a fractal as the infinite generation of its basis geometry.

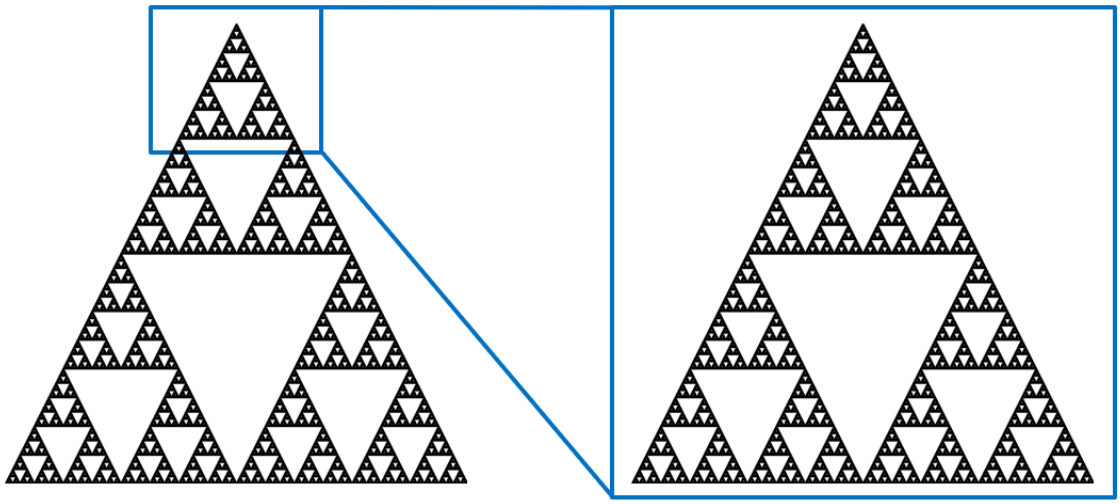

Figure A.5: Self-similarity of the Sierpiński triangle. One can see that zooming in on the Sierpiński triangle again results in the Sierpiński triangle.

Now, we are at a point where we can give an intuitive definition of a fractal:

A fractal is a geometric object constructed as the infinite generation of an initial geometric object such that the fractal has non-integer dimension and exhibits self-similarity.

Appendix B

Mathematical preliminaries

The goal of this appendix is to formalise most of the mathematical knowledge needed to understand this thesis in detail. Different transforms will be introduced, namely, the Fourier transform, the Laplace transform and the Mellin transform. These transformations are covered in sections B.1, B.2 and B.7 respectively. We cover them since they are very useful and necessary tools throughout this thesis. Using these transforms often results in divergent integrals. There are many different ways to give meaning to these integrals. One of the most common ways is by using a particular regularization in combination with contour integration. These interpretations are not unique and, therefore, we give a brief summary of some of the different possibilities in Sec. B.4. The examples that are used in this section are tailored towards this thesis, but also illustrate the differences between the different interpretations. A short overview of the complex power function and some of its properties are introduced in Sec. B.3, because understanding the difference between the real power function and the complex one is crucial in understanding the Weyl fractional derivative. The Caputo fractional derivative is shortly discussed in Sec. B.9. Finally, some special functions are briefly discussed in this appendix. The first one is the gamma function, which is discussed in Sec. B.5. The beta function is covered in Sec. B.6. Lastly, a very general family of special functions is covered, namely the Fox h-function. This is done in Sec. B.8.

B.1 The Fourier transform

The fractional Weyl derivative is defined in terms of the Fourier transform, see Def. 3.1.1, so the Fourier transform stands at the basis of this thesis. Therefore, it is important to formalise the conventions that we will use. Some important properties that depend on these conventions are also given.

Definition B.1.1. *Let $f \in L^2(\mathbb{R})$, then we define the Fourier transform of f to be*

$$\mathcal{F}[f(t);\omega] = \frac{1}{2\pi}\int_{-\infty}^{\infty} dt f(t)e^{-i\omega t}. \tag{B.1}$$

Remark B.1.1. *$\mathcal{F}[f(t);\omega]$ will sometimes be denoted by $f(\omega)$ even though the Fourier transform of a function $f(t)$ is not the same function evaluated at a different point.*

Definition B.1.2. *Let $f \in L^2(\mathbb{R})$, then we define the inverse Fourier transform of f to be*

$$\mathcal{F}^{-1}[f(\omega);t] = \int_{-\infty}^{\infty} d\omega f(\omega)e^{i\omega t}. \tag{B.2}$$

The definition of the Fourier transform implies the following property

$$\mathcal{F}\left[\frac{d^n}{dt^n}f(t);\omega\right] = (i\omega)^n\mathcal{F}[f(t);\omega]. \tag{B.3}$$

This property gives an easy way to generalize the derivative to non-integer values. The fractional derivative based on the generalization of this property is called *the Weyl fractional derivative*, which is defined in Sec. 3.1.

Definition B.1.3. *The convolution of two functions f and g is given by*

$$(f * g)(t) = \int_{-\infty}^{\infty} d\tau f(t-\tau)g(\tau). \tag{B.4}$$

Remark B.1.2. *When two functions f and g are only non-zero on $[0,\infty)$, then the convolution can be rewriten as*

$$(f * g)(t) = \int_{0}^{t} d\tau f(t-\tau)g(\tau). \tag{B.5}$$

Remark B.1.3. *The notation that we will use for the convolution of two functions is going to be $f(t) * g(t)$.*

Lemma B.1.1. *Let $f, g \in L^2(\mathbb{R})$, then the Fourier transform of a convolution is given by*

$$\mathcal{F}[f(t) * g(t);\omega] = 2\pi\mathcal{F}[f(t);\omega]\mathcal{F}[g(t);\omega], \tag{B.6}$$

where the conventions for the Fourier transform are given in Def. B.1.1.

Proof.

A direct calculation yields

$$\begin{aligned}\mathcal{F}\left[f(t) * g(t); \omega\right] &= \frac{1}{2\pi} \int_{-\infty}^{\infty} dt \int_{-\infty}^{\infty} d\tau f(t-\tau) g(\tau) e^{-i\omega t} \\ &= \frac{1}{2\pi} \int_{-\infty}^{\infty} du \int_{-\infty}^{\infty} d\tau f(u) g(\tau) e^{-i\omega(u+\tau)} \\ &= 2\pi \mathcal{F}\left[f(t); \omega\right] \mathcal{F}\left[g(t); \omega\right],\end{aligned}$$

where in the second line we made the substitution $t = u + \tau$.

□

A similar property holds for the inverse Fourier transform.

Lemma B.1.2. *Let $f, g \in L^2(\mathbb{R})$, then the inverse Fourier transform of a convolution is given by*

$$\mathcal{F}^{-1}\left[f(\omega) * g(\omega); t\right] = \mathcal{F}^{-1}\left[f(\omega); t\right] \mathcal{F}^{-1}\left[g(\omega); t\right], \tag{B.7}$$

where the conventions for the inverse Fourier transform are given in Def. B.1.2.

The proof of Lem. B.1.2 is completely analog to the proof of Lem. B.1.1.

Lemma B.1.3. *Let $f, g \in L^2(\mathbb{R})$, then the Fourier transform of a product is given by*

$$\mathcal{F}\left[f(t) g(t); \omega\right] = \mathcal{F}\left[f(t); \omega\right] * \mathcal{F}\left[g(t); \omega\right]. \tag{B.8}$$

Proof.

Using the short notation

$$\mathcal{F}\left[f(t); \omega\right] = \mathcal{F}(f),$$

and the same for the inverse Fourier then gives

$$\mathcal{F}\left(fg\right) = \mathcal{F}\left\{\mathcal{F}^{-1}\left[\mathcal{F}\left(f\right)\right] \mathcal{F}^{-1}\left[\mathcal{F}\left(g\right)\right]\right\}.$$

Next, we can use Lem. B.1.2 to get

$$\mathcal{F}\left\{\mathcal{F}^{-1}\left[\mathcal{F}\left(f\right)\right] \mathcal{F}^{-1}\left[\mathcal{F}\left(g\right)\right]\right\} = \mathcal{F}\left(f\right) * \mathcal{F}\left(g\right),$$

which means that

$$\mathcal{F}\left[f(t) g(t); \omega\right] = \mathcal{F}\left[f(t); \omega\right] * \mathcal{F}\left[g(t); \omega\right].$$

□

Again, a similar property holds for the inverse Fourier transform.

Lemma B.1.4. *Let $f, g \in L^2(\mathbb{R})$, then the inverse Fourier transform of a product is given by*

$$\mathcal{F}^{-1}\left[f(\omega)g(\omega);t\right] = \frac{1}{2\pi}\mathcal{F}^{-1}\left[f(\omega);t\right] * \mathcal{F}^{-1}\left[g(\omega);t\right]. \tag{B.9}$$

The proof of Lem. B.1.4 is completely analog to the proof of Lem. B.1.3.

Remark B.1.4. *Notice that the prefactors in Lems. B.1.1, B.1.2, B.1.3 and B.1.4 are fully determined by the used conventions in the Fourier transform and its inverse.*

B.2 The Laplace transform

In this section, we shortly discuss the Laplace transform and some of its properties. We do this because the Laplace transform is the standard method to solve some differential equations that come up in this thesis [**25, 66**]. The Laplace transform is often used to solve fractional differential equations [**23, 25, 67**].

Definition B.2.1. *Let f be a function defined on the interval $[0,\infty)$ and $s \in \mathbb{C}$, the*

$$F(s) = \mathscr{L}\left[f(t);s\right] = \int_0^\infty dt f(t)e^{-st}, \tag{B.10}$$

is defined to be the Laplace transform of f.

Definition B.2.2. *The inverse Laplace transform is given by*

$$f(t) = \mathscr{L}^{-1}\left[F(s);t\right] = \int_{c-i\infty}^{c+i\infty} ds F(s)e^{st}, \tag{B.11}$$

where $c \in \mathbb{R}$ is chosen such that all singularities of $F(s)$ lie to the left of the line $\mathrm{Re}(s) = c$.

Lemma B.2.1. *Let f and g be two functions such that the Laplace transform exists, denoted by F and G respectively. Then, the Laplace transform satisfies*

$$\mathscr{L}\left[f(t) * g(t);s\right] = F(s)G(s). \tag{B.12}$$

Proof.

By definition of the Laplace transform and the convolution of functions only non-zero on $[0,\infty)$, we have

$$\mathscr{L}\left[f(t) * g(t);s\right] = \int_0^\infty dt \int_0^t d\tau f(t-\tau)g(\tau)e^{-st}.$$

Next, we swap the order of integration, being careful with the integration domains since they are not indefinite. This yields,

$$\begin{aligned}\mathscr{L}\left[f(t) * g(t); s\right] &= \int_0^\infty d\tau \int_\tau^\infty f(t-\tau)g(\tau)e^{-st} \\ &= \int_0^\infty d\tau \int_0^\infty d\lambda f(\lambda)g(\tau)e^{-s(\lambda+\tau)} \\ &= F(s)G(s),\end{aligned}$$

where in the second line we made the substitution $t = \lambda+\tau$ and in the last line we identified the definition of the Laplace transform twice, therefore completing the proof.

□

Taking the inverse Laplace transform of Eq. (B.12) directly gives

$$\mathscr{L}^{-1}\left[F(s)G(s); t\right] = f(t) * g(t). \tag{B.13}$$

Lemma B.2.2. *Let $n \in \mathbb{N}$ and assume that the Laplace transform of the n^{th} derivative of f exists. Then,*

$$\mathscr{L}\left[\frac{d^n}{dt^n}f(t); s\right] = s^n F(s) - \sum_{k=0}^{n-1} s^{n-1-k} f^{(k)}(0) \tag{B.14}$$

Proof.

By definition, we have

$$\mathscr{L}\left[\frac{d^n}{dt^n}f(t); s\right] = \int_0^\infty dt \frac{d^n}{dt^n}[f(t)]e^{-st}.$$

Applying repeated integration by parts and assuming that the integrals exist, gives us

$$\begin{aligned}\mathscr{L}\left[\frac{d^n}{dt^n}f(t); s\right] &= s\int_0^\infty dt \frac{d^{n-1}}{dt^{n-1}}[f(t)]e^{-st} - f^{(n-1)}(0) \\ &= s^2\int_0^\infty dt \frac{d^{n-2}}{dt^{n-2}}[f(t)]e^{-st} - f^{(n-1)}(0) - sf^{(n-2)}(0) \\ &= ... \\ &= s^n F(s) - \sum_{k=0}^{n-1} s^{n-1-k} f^{(k)}(0).\end{aligned}$$

□

Taking the inverse Laplace transform of Eq. (B.14), directly gives

$$\mathscr{L}^{-1}\left[s^n F(s);t\right] = \frac{d^n}{dt^n}f(t) + \sum_{k=0}^{n-1} f^{(k)}(0)\,\mathscr{L}^{-1}\left[s^{n-1-k};t\right]. \tag{B.15}$$

Example B.2.1. *Lets look at the Laplace transform of an exponential function with* $\mathrm{Re}(s) > \mathrm{Re}(a)$*, which is given by*

$$\mathscr{L}\left(e^{at};s\right) = \int_0^\infty dt e^{(a-s)t} = \frac{1}{s-a}. \tag{B.16}$$

When we take $a = 0$ in the previous example we get

$$\mathscr{L}\left(1;s\right) = \frac{1}{s}, \tag{B.17}$$

which also implies that

$$\mathscr{L}^{-1}\left(\frac{1}{s};t\right) = 1. \tag{B.18}$$

Next, we can take $a \to ia$ in the above example, such that

$$\mathscr{L}\left(e^{iat};s\right) = \frac{1}{s-ia} = \frac{s+ia}{s^2+a^2}, \tag{B.19}$$

which by taking the real and imaginary parts implies

$$\mathscr{L}\left[\cos(at);s\right] = \frac{s}{s^2+a^2}, \tag{B.20}$$

$$\mathscr{L}\left[\sin(at);s\right] = \frac{a}{s^2+a^2}. \tag{B.21}$$

B.3 The complex power function

Since the definition of the Weyl fractional derivative involves an imaginary number to the power of a real number (see Def. 3.1.1), it is important to understand what this exactly means. We state the definition of the complex power function. Some of its non-trivial properties are also given, without proof. An extensive and formal discussion of the complex power function can be found in Ref. [**68**]. Proofs can also be found in this reference.

Definition B.3.1. *The complex logarithm, denoted by* $\mathrm{Log} : \mathbb{C} \to \mathbb{C}$ *is defined by*

$$\mathrm{Log}(z) = \ln|z| + i\,\arg(z). \tag{B.22}$$

Remark B.3.1. *Notice that this is not a function, since* $\arg(z) = \arg(z) + \arg(2\pi n)$ *with* $n \in \mathbb{Z}$. *To get a function, one needs to restrict the argument. One possibility is to impose* $\arg(z) \in (-\pi, \pi]$. *This is called the principle argument, which results in the principal value of* $\mathrm{Log}(z)$, *denoted by* $\mathrm{Ln}(z)$, *which is a well defined function.*

Definition B.3.2. *Let* $a, b \in \mathbb{C}$, *then*

$$a^b = e^{b\,\mathrm{Ln}(a)} \tag{B.23}$$

is defined to be the complex power function.

Remark B.3.2. *In the above definition, we chose for the principal value of the complex power function. We will just call this the complex power function, but other branches of* $\mathrm{Log}(z)$ *could also be chosen. When this is done we will explicitly mention it.*

Theorem B.3.1. *Let* $z_1, z_2, a, b \in \mathbb{C}$. *The complex power function satisfies the following properties:*

(i) $z_1^a z_1^b = z_1^{a+b}$,

(ii) $\frac{z_1^a}{z_1^b} = z_1^{a-b}$,

(iii) $z_1^a z_1^{-a} = 1$,

(iv) $(z_1^a)^b = z_1^{ab} e^{2\pi i b N_a}$,

(v) $(z_1 z_2)^a = z_1^a z_2^a e^{2\pi i a N_+}$,

(vi) $\left(\frac{z_1}{z_2}\right)^a = \frac{z_1^a}{z_2^a} e^{2\pi i a N_-}$,

where $N_a \equiv \lfloor 1/2 - \mathrm{Im}\left[\,\mathrm{Ln}(a z_1)\right]/(2\pi) \rfloor$, *with* $\lfloor \cdot \rfloor$ *the floor function,*

and $N_\pm \equiv \begin{cases} -1, & \text{if } \arg(z_1) \pm \arg(z_2) > \pi, \\ 0, & \text{if } -\pi < \arg(z_1) \pm \arg(z_2) \le \pi, \\ 1, & \text{if } \arg(z_1) \pm \arg(z_2) \le -\pi. \end{cases}$

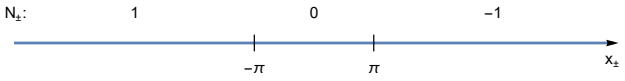

Figure B.1: Let $x_\pm = \arg(z_1) + \arg(z_2)$. Where $N_\pm$ is non-zero, the complex power function definitely has non-trivial properties.

B.4 Complex analysis: contour integration

In this section, we build the necessary knowledge to understand divergent integrals in certain interpretations that are often used by physicists and mathematicians. The difference between those interpretations are emphasised by the use of examples. For mathematical details we reference the reader to Refs. [**69, 70, 71**].

Theorem B.4.1. (The residue theorem) *Suppose a function f is analytic in a simply connected domain D, except for isolated singularities at $z_1, z_2, \dots, z_m$. Let γ be a regular closed curve in D which does not intersect any of the singularities, then*

$$\oint_\gamma dz f(z) = 2\pi i \sum_{k=1}^{m} \mathrm{Res}(f; z_k). \tag{B.24}$$

A proof of the above theorem is out of the scope of this thesis, however one can be found in Ref. [**69**]. Thm. B.4.1 allows us to make sense of integrals over the real line, which would not make sense otherwise. This will become more clear in later examples. To work out these examples we first need to introduce Jordan's lemma.

Lemma B.4.1. (Jordan's lemma) *Suppose that*

(i) a function $f(z)$ is analytic at all points in the upper half plane, $\mathrm{Im}(z) \geq 0$, that are exterior to a circle of radius $|z| = R_0$,

(ii) $\mathcal{C}_R$ denotes a semicircle parameterized by $z = Re^{i\theta}$ with $0 \leq \theta \leq \pi$ and $R > R_0$,

(iii) for all points on $\mathcal{C}_R$, there exists a positive constant M_R such that $|f(z)| \leq M_r$ and $\lim_{R\to\infty} M_R = 0$,

then, for every positive constant a, we have

$$\lim_{R\to\infty} \int_{\mathcal{C}_R} dz f(z) e^{iaz} = 0 \tag{B.25}$$

For a proof, see Ref. [**69**].

Remark B.4.1. *Jordan's lemma (Lem. B.4.1) can be modified in such a way that it also holds for $a < 0$. This is done by in the first condition swapping $\mathrm{Im}(z) \geq 0$ with $\mathrm{Im}(z) \leq 0$. The sign of the constant, a, will thus dictate if we chose the upper semi-circle or the lower semi-circle.*

With the residue theorem and Jordan's lemma, we can already give a meaning to divergent real integrals. Unfortunately, these are not unique and thus depend in the context and we will therefore refer to these meanings as interpretations. The first interpretation will be called *the positive $i\epsilon$-interpretation*. Here, one would move the pole to the upper half of the imaginary plane by adding an small imaginary part to the pole. This then allows one to use the residue theorem and Jordan's lemma to give a meaning to the real integral. Finally, one would take the imaginary part to zero.

Example B.4.1. *Consider the following integral:*

$$I(t) = \mathcal{F}^{-1}\left[\frac{1}{\omega}; t\right] = \int_{-\infty}^{\infty} d\omega \frac{1}{\omega} e^{i\omega t}. \tag{B.26}$$

One can check that the above integral diverges. We can however give meaning to this integral in the positive $i\epsilon$-interpretation. First, we do the substitution $1/\omega \to 1/(\omega - i\epsilon)$, where at the end of the calculation we will take $\epsilon \to 0$. For $t > 0$, we consider the contour depicted in Fig. B.2. We call the closed contour, $\mathcal{C}$, and the semi-circle contour, $\mathcal{C}_R$.

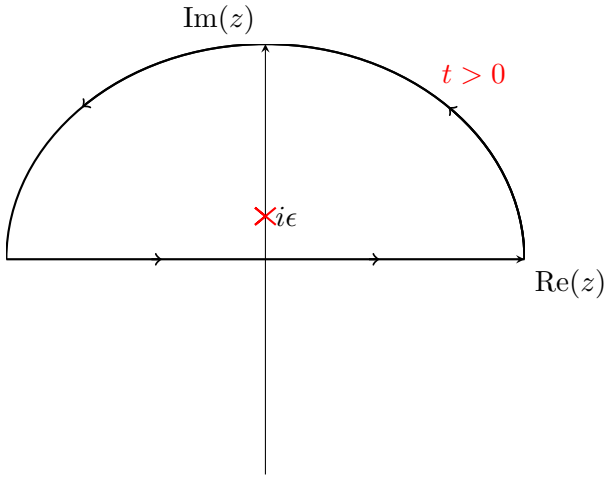

Figure B.2: the pole structure of the function $1/(z - i\epsilon)$ is depicted in the above figure. This is the positive $i\epsilon$-interpretation of the integral in Eq. (B.26). Note that the shown contour is only chosen for $t > 0$.

Thus, for $t > 0$ we get

$$\oint_{\mathcal{C}} dz \frac{1}{z - i\epsilon} e^{izt} = \int_{\mathcal{C}_R} dz \frac{1}{z - i\epsilon} e^{izt} + \int_{-\infty}^{\infty} dz \frac{1}{z - i\epsilon} e^{izt}. \tag{B.27}$$

Next, we can apply Lem. B.4.1, which says that the integral over $\mathcal{C}_R$ has no contribution for $t > 0$. Moreover, we can also use the Thm. B.4.1 to simplify the left side of Eq. (B.27). This then yields

$$2\pi i e^{-\epsilon t} = \int_{-\infty}^{\infty} dz \frac{1}{z - i\epsilon} e^{izt}. \tag{B.28}$$

Finally, we take $\epsilon \to 0$, which gives

$$\begin{aligned} I(t) &= \int_{-\infty}^{\infty} dz \frac{1}{z} e^{izt}, \qquad \text{for } t > 0 \\ &= 2\pi i. \end{aligned} \tag{B.29}$$

The final step in this interpretation is to repeat the above steps for $t < 0$ but this time by closing the contour from the bottom (because of Rem. B.4.1). This then yields

$$I(t) = 0, \qquad \text{for } t < 0, \tag{B.30}$$

which combined with Eq. (B.29), gives

$$I(t) = \int_{-\infty}^{\infty} dz \frac{1}{z} e^{izt} = \Theta(t) 2\pi i, \tag{B.31}$$

where $\Theta(t)$ is the Heaviside step function.

Remark B.4.2. *Note that the choice of adding $i\epsilon$ to the pole resulted in $\Theta(t)$. We could have also subtracted $i\epsilon$, which would have resulted in $\Theta(-t)$. This interpretation we will call the negative $i\epsilon$-interpretation.*

Remark B.4.3. *Ex. B.4.1 can be easily extended to give*

$$\mathcal{F}^{-1}\left[\frac{1}{\omega - b}; t\right] = \Theta(t) 2\pi i e^{ibt}, \tag{B.32}$$

for $b \in \mathbb{R}$.

The $i\epsilon$-interpretations are interpretations which are mainly used in physics. Mathematicians usually prefer the Cauchy principal value as an interpretation for divergent real integrals. For this interpretation we will state a modified version of the residue theorem.

Theorem B.4.2. *Let D be the region enclosed by a closed piecewise path γ. If a function, f, is analytical on γ and D, except at finitely many singular points $z_1, z_2, \dots, z_m$ in the interior of D and at finitely many poles $p_1, \dots, p_k$ of order 1 which are located on γ. Also, assume that γ has a tangent line on each pole p_i, then*

$$PV \oint_{\gamma} dz f(z) = 2\pi i \sum_{i=1}^{m} \text{Res}(f; z_i) + \pi i \sum_{i=1}^{k} \text{Res}(f; p_i) \tag{B.33}$$

For a proof we refer the reader to Ref. [**70**].

Remark B.4.4. *We will not be strict on writing 'PV' in front of an integral when we use the Cauchy principal value interpretation of it. We will, however, always state it in words when we use this, just like we will do when we use any of the $i\epsilon$-interpretations.*

Example B.4.2. *We will calculate the Cauchy principal value of the following integral*

$$\mathcal{F}^{-1}\left[\frac{1}{\omega}; t\right], \tag{B.34}$$

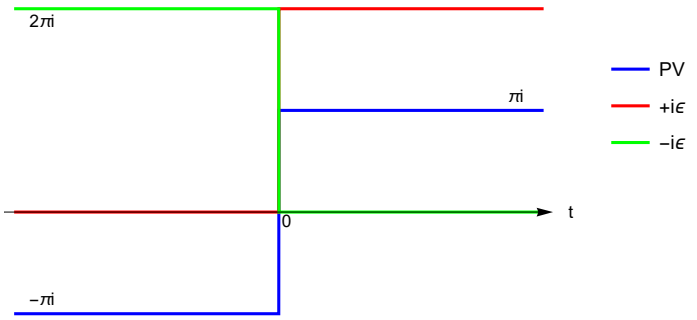

Figure B.3: The principal value of an integral keeps the symmetry around, $t = 0$, unlike the positive or negative $i\epsilon$-interpretations, which are zero for negative and positive times respectively.

which is the same as in Ex. B.4.1. Following exactly the same steps as in Ex. B.4.1 but using the modified residue theorem (Thm. B.4.2) yields for all t

$$\mathcal{F}^{-1}\left[\frac{1}{\omega};t\right] = \pi i \text{sign}(t), \tag{B.35}$$

where the extra minus sign for $t < 0$ comes from the negative orientation of the contour (the lower half semi-circle).

Remark B.4.5. *Note that, in the Cauchy principal value interpretation, we have a value that is non-zero for all t. Also, the Cauchy principal value and the positive $i\epsilon$-interpretation differ by a factor of $1/2$ for $t > 0$. The choice of interpretation has to be motivated by physical arguments or mathematical arguments. One of which can be the need to keep a symmetry around $t = 0$. The differences between the principal value and the positive and negative $i\epsilon$- interpretations are also visually depicted in Fig. B.3.*

Complex analysis will also allow us to find different representations of the Dirac delta function. To do this, we will give a more concrete meaning to the Dirac delta function.

Definition B.4.1. *Let $\phi \in \mathcal{S}(\mathbb{R})$, be a function in a suitable space, $\mathcal{S}$. This space will be chosen based on the context*[1]*. Then we define the Dirac delta function, $\delta(x-x_0)$, associated with $\mathcal{S}(\mathbb{R})$ such that for all $\phi \in \mathcal{S}(\mathbb{R})$, we have that*

$$\int_{-\infty}^{\infty} dx \delta(x - x_0)\phi(x) = \phi(x_0). \tag{B.36}$$

In this definition the delta function is a distribution and ϕ is called a test function.

[1] In this thesis we will not be strict on defining the space when we use this definition of the delta function.

Remark B.4.6. *The above definition can be extended to include integrals over complex values. For example this is done in Ref. [**71**].*

Remark B.4.7. *Many different functions can satisfy Def. B.4.1. This means that the delta function is not unique. Therefore, we refer to different representations of the delta function.*

An important representation of the delta function will be derived in the example below by interpreting certain integrals as their Cauchy principal value.

Example B.4.3. *We will show that*

$$\frac{1}{\omega^2-\omega_j^2}=\frac{\pi i}{2\omega_j}\left[\delta(\omega+\omega_j)-\delta(\omega-\omega_j)\right]. \tag{B.37}$$

The first step will be to partial fraction the left side of Eq. (B.37) as

$$\frac{1}{\omega^2-\omega_j^2}=-\frac{1}{2\omega_j}\left(\frac{1}{\omega+\omega_j}-\frac{1}{\omega-\omega_j}\right). \tag{B.38}$$

Next, we can check if each of the above terms satisfy Def. B.4.1. Let $\phi(\omega)$ be a suitable test function such that a closed negatively oriented contour, $\mathcal{C}_-$, can be constructed that satisfies

$$\begin{aligned}\int_{-\infty}^{\infty}d\omega\frac{\phi(\omega)}{\omega\pm\omega_j}&=\oint_{\mathcal{C}_-}dz\frac{\phi(z)}{z\pm\omega_j}\\&=-\oint_{\mathcal{C}_+}dz\frac{\phi(z)}{z\pm\omega_j}.\end{aligned} \tag{B.39}$$

Next, we assume that these test functions don't have any singularities inside the closed contour, allowing us to use Thm. B.4.2, which then yields

$$\int_{-\infty}^{\infty}d\omega\frac{\phi(\omega)}{\omega\pm\omega_j}=-\pi i\phi(\mp\omega_j). \tag{B.40}$$

This means that, for these test functions and in the principal value interpretation, we have

$$\frac{1}{\omega\pm\omega_j}=-\pi i\delta(\omega\pm\omega_j), \tag{B.41}$$

which, when used in Eq. (B.38), yields

$$\frac{1}{\omega^2-\omega_j^2}=\frac{\pi i}{2\omega_j}\left[\delta(\omega+\omega_j)-\delta(\omega-\omega_j)\right]. \tag{B.42}$$

Remark B.4.8. *The above example immediately gives the following properties*

$$\mathrm{Im}\left(\frac{1}{\omega^2-\omega_j^2}\right)=\frac{\pi}{2\omega_j}\left[\delta(\omega+\omega_j)-\delta(\omega-\omega_j)\right], \tag{B.43}$$

$$\mathrm{Im}\left(\frac{i}{\omega^2-\omega_j^2}\right)=0. \tag{B.44}$$

B.5 The gamma function

The gamma function is one of the most important special functions. It is not surprising that, in our case, the gamma function will also be useful. Thus, we give an overview of the definition and some of its properties in this section, which are based on Refs. [**72, 73**]. In this thesis, the main use of the gamma function is to understand the beta and Fox-H functions, which are in its turn essential to understand the asymptotic behavior of the inverse Fourier integral given by Eq. (3.65).

Definition B.5.1. *Let* $z\in\mathbb{C}$ *with* $\mathrm{Re}(z)>0$, then we define

$$\Gamma(z)=\int_0^\infty dx\, x^{z-1}e^{-x}, \tag{B.45}$$

which is called the gamma function and converges absolutely.

Example B.5.1.

$$\begin{aligned}\Gamma(1)&=\int_0^\infty dx e^{-x}\\&=1.\end{aligned} \tag{B.46}$$

Theorem B.5.1. *The gamma function satisfies the reduction formula, namely*

$$\Gamma(z+1)=z\Gamma(z). \tag{B.47}$$

Proof.

We have

$$\begin{aligned}\Gamma(z+1)&=\int_0^\infty dx\, x^z e^{-x}\\&=\left[-x^z e^{-x}\right]_0^\infty+z\int_0^\infty dx\, x^{z-1}e^{-x}\\&=z\Gamma(z),\end{aligned}$$

where in the second we applied partial integration and in the third line we noticed that the first term vanishes.

□

Combining Ex. B.5.1 with Thm. B.5.1 allows one to easily apply induction to proof, such that for positive integers, $n > 0$, we have

$$\Gamma(n) = (n-1)!\,. \tag{B.48}$$

Remark B.5.1. *The gamma function is only defined for $Re(z) > 0$. However, Thm. B.5.1 allows us to uniquely extend the definition of the gamma function to $Re(z) \leq 0$. The gamma function for all complex arguments can be seen in Fig. B.4.*

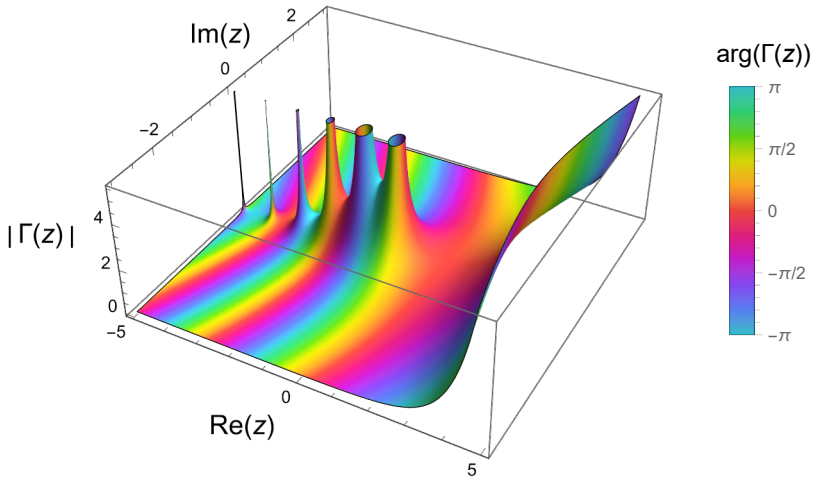

Figure B.4: The plot shows the norm of the gamma function, $\Gamma(z)$, plotted in function of the real and imaginary parts of its input, z. The plot is color coded based on the argument of the output, $\arg[\Gamma(z)]$. Poles can be seen at negative integer values for z.

The gamma function is a meromorphic[2] function, which means that the function is analytical on its domain except at isolated points. The poles of the gamma functions are located at $\Gamma(z)$ such that $z \in -\mathbb{N}$[3]. The pole structure of the gamma function will be important to calculate integrals of gamma functions, which will be done in later sections. Another notable property is that the Gamma function has no zeros on $\mathbb{C}$. This means that the reciprocal gamma function,

$$f(z) = \frac{1}{\Gamma(z)}, \tag{B.49}$$

[2] A meromorphic function, is a function that is holomorphic except at isolated points.
[3] In this thesis the symbol, $\mathbb{N}$, will mean the set $\{0, 1, ..., n, ...\}$.

has no poles and has zeros for $z \in -\mathbb{N}$. This can also be seen in Fig. B.5. The analytic

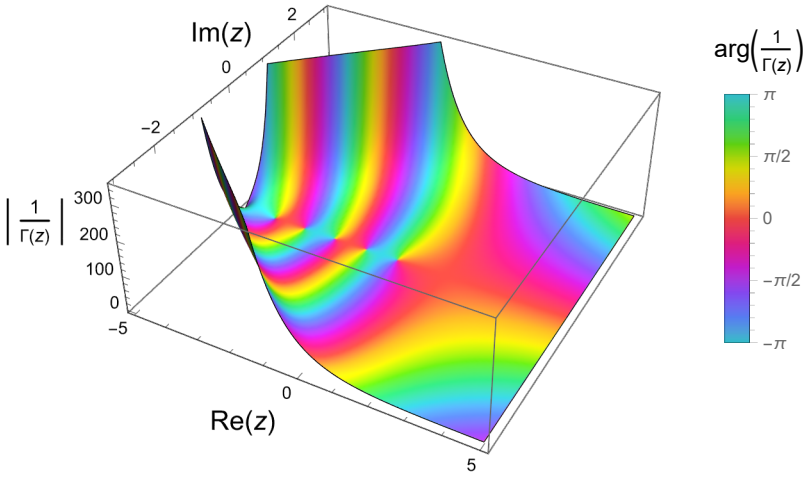

Figure B.5: The plot shows the norm of the reciprocal gamma function, $1/\Gamma(z)$, plotted as a function of the real and imaginary parts of, z. The plot is color coded based on the argument of the output, $\arg[1/\Gamma(z)]$. Notice that there are no poles visible in the plot.

structure of the gamma function and its reciprocal will be crucial when calculating integrals over gamma functions with complex analysis.

Example B.5.2. *Let's calculate the sum of the residues of a function, $f(z)$, that is analytic on $\mathbb{C}$ multiplied by a gamma function, $\Gamma(z)$. We know that the poles are given by*

$$z = -\nu, \text{ where } \nu \in \mathbb{N}. \tag{B.50}$$

This means that

$$\begin{aligned}\sum_j \text{Res}\left[\Gamma(z)f(z);z_j\right] &= \sum_{\nu=0}^{\infty} f(-\nu)\lim_{z\to-\nu}(z+\nu)\Gamma(z)\\ &= \sum_{\nu=0}^{\infty} f(-\nu)\lim_{z\to-\nu}(z+\nu)\frac{z(z+1)...(z+\nu)}{z(z+1)...(z+\nu)}\Gamma(z)\\ &= \sum_{\nu=0}^{\infty} f(-\nu)\lim_{z\to-\nu}(z+\nu)\frac{\Gamma(z+\nu+1)}{z(z+1)...(z+\nu)}\\ &= \sum_{\nu=0}^{\infty} f(-\nu)\lim_{z\to-\nu}\frac{\Gamma(z+\nu+1)}{z(z+1)...(z+\nu-1)}\\ &= \sum_{\nu=0}^{\infty} f(-\nu)\frac{\Gamma(1)}{\nu!(-1)^{\nu}}\\ &= \sum_{\nu=0}^{\infty} f(-\nu)\frac{(-1)^{\nu}}{\nu!},\end{aligned} \tag{B.51}$$

where in the second line we multiplied by unity, in the third line we repeatedly applied Thm. B.5.1 and in the last line we used the result from Ex. B.5.1.

Example B.5.3. *The above example can now easily be generalised for a gamma function of the form, $\Gamma(a+bz)$, with $a,b\in\mathbb{C}$, by making use of the substitution $\tilde{z}=a+bz$ and then working out the example in the same way. This yields*

$$\begin{aligned}\sum_j \text{Res}\left[\Gamma(a+bz)f(z);z_j\right] &= \sum_{\nu=0}^{\infty}\lim_{\tilde{z}\to-\nu}(\tilde{z}+\nu)\Gamma(\tilde{z})f\left(\frac{\tilde{z}-a}{b}\right)\\ &= \sum_{\nu=0}^{\infty} f\left(\frac{-\nu-a}{b}\right)\frac{(-1)^{\nu}}{\nu!}\end{aligned} \tag{B.52}$$

Finally, one last useful formula relating gamma functions and the sine, is known as Euler's reflection formula, and can be found in the lemma below.

Lemma B.5.1. ***(Euler's reflection formula)*** *Let $z\in\mathbb{C}\setminus\mathbb{Z}$, then*

$$\Gamma(z)\Gamma(1-z)=\frac{\pi}{\sin(\pi z)}. \tag{B.53}$$

A proof is most easily obtained by using a different definition of the gamma function. A full proof can be found in Ref. [**72**].

Remark B.5.2. *Taking $z\to(1/2-z)$ in Lem. B.5.1 and using the fact that $\sin(\pi/2-x)=\cos(x)$, yields*

$$\Gamma\left(\frac{1}{2}-z\right)\Gamma\left(\frac{1}{2}+z\right)=\frac{\pi}{\cos(\pi z)}. \tag{B.54}$$

B.6 The beta function

A short introduction to the beta function is needed to compute a certain Mellin transform, which we will come back to in a later section. For this section, we mainly followed Ref. [**73**].

Definition B.6.1. *Let $z_1, z_2 \in \mathbb{C}$ with $\mathrm{Re}(z_1)$, $\mathrm{Re}(z_2) > 0$, then we define the beta function as*

$$B(z_1, z_2) = \int_0^1 dt\, (1-t)^{z_2-1}\, t^{z_1-1}. \tag{B.55}$$

Remark B.6.1. *Applying the definition of the convolution (see Def. B.1.3), to the functions $f(t) = t^{z_1-1}$ and $g(t) = t^{z_2-1}$ on the interval $[0,1]$, gives*

$$(f * g)(t) = \int_0^1 d\tau\, (t-\tau)^{z_1-1}\, \tau^{z_2-1}. \tag{B.56}$$

Evaluating the above convolution at the point $t = 1$, yields

$$\begin{aligned}(f * g)(1) &= \int_0^1 d\tau\, (1-\tau)^{z_1-1}\, \tau^{z_2-1} \\ &= B(z_1, z_2).\end{aligned} \tag{B.57}$$

Thus the beta function has the structure of a convolution.

Remark B.6.2. *By making a simple substitution, $u = 1 - t$, in Def. B.6.1, one can see that*

$$B(z_1, z_2) = B(z_2, z_1). \tag{B.58}$$

Starting from Def. B.6.1, we can derive a useful representation of the beta function. By definition, we have

$$\begin{aligned}B(z_1, z_2) &= \int_0^1 dt\, (1-t)^{z_2-1}\, t^{z_1-1} \\ &= \int_0^\infty du \frac{u^{z_1-1}}{(1+u)^{z_1+z_2}},\end{aligned} \tag{B.59}$$

where in the second line we made the substitution $u + 1 = 1/(1-t)$.

Theorem B.6.1. *Let $z_1, z_2 \in \mathbb{C}$ with $\mathrm{Re}(z_1)$, $\mathrm{Re}(z_2) > 0$, then*

$$B(z_1, z_2) = \frac{\Gamma(z_1)\Gamma(z_2)}{\Gamma(z_1+z_2)}. \tag{B.60}$$

Proof.

By definition of the gamma function we have

$$\Gamma(z_1)\Gamma(z_2) = \int_0^\infty ds \int_0^\infty dt e^{-(t+s)} t^{z_1-1} s^{z_2-1}.$$

Next, we do the change of variables, $t = xy$ and $s = x(1-y)$. This implies that $0 < x < \infty$ and $0 < y < 1$. The Jacobian of this transformation is given by

$$J = \det \begin{pmatrix} y & x \\ 1-y & -x \end{pmatrix} = -x.$$

Since $x > 0$ we have that $|J| = x$, such that $dtds = xdxdy$. Putting things together gives

$$\begin{aligned} \Gamma(z_1)\Gamma(z_2) &= \int_0^\infty dx e^{-x} x^{z_1+z_2-1} \int_0^1 dy (1-y)^{z_2-1} y^{z_1-1} \\ &= \Gamma(z_1+z_2) B(z_1, z_2), \end{aligned}$$

where in the last line we used the definitions of the gamma function and the beta function.

□

Remark B.6.3. *Thm. B.6.1 relates the beta function and the gamma function, implying that the beta function has a rich singular structure which can also be observed in Fig. B.6. This theorem together with Rem. B.5.1 implies that we can uniquely extend the beta function to $z \in \mathbb{C}$ such that $Re(z) < 0$.*

Applying Thm. B.6.1 for the case $z = z_1 = 1 - z_2$ and using Ex. B.5.1, gives

$$B(z, 1-z) = \Gamma(z)\Gamma(1-z). \tag{B.61}$$

Which, using Eq. (B.60), yields

$$\int_0^\infty du \frac{u^{z-1}}{(1+u)} = \Gamma(z)\Gamma(1-z). \tag{B.62}$$

The above equation will be helpful in later sections.

B.7 The Mellin transform

To calculate asymptotic behavior of certain very difficult Fourier integrals, we linked the Fourier integral to a Fox-H function. This is done in Sec. 3.5. The derivation of this requires the use of the Mellin transform. The Mellin transform also allowed us to find a very useful representation of colored noise, given in Eq. (3.46). We mainly used Refs. [**74,75**], however we took a more physics approach to the topic and were therefore a little less formal than those references. An important example that is used in Sec. 3.5 is also included.

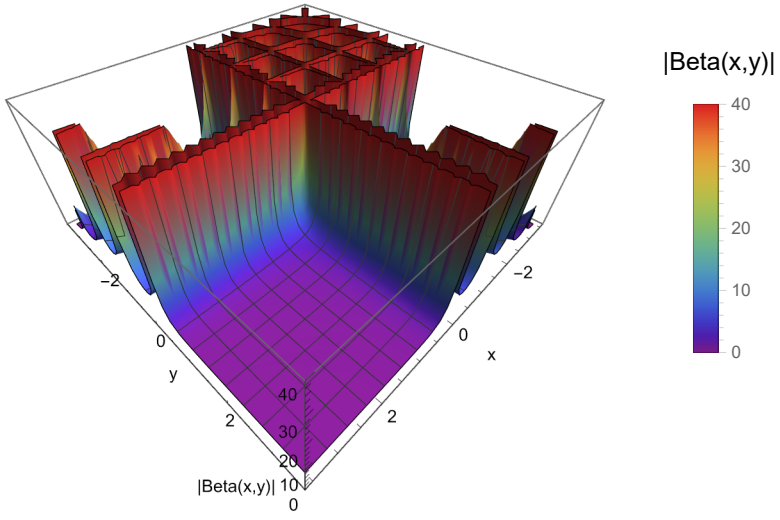

Figure B.6: The plot shows the norm of the beta function, $B(x, y)$, plotted in function of real inputs, x and y. The plot is color coded based on the norm of the beta function to emphasize the singular behavior of this function.

Definition B.7.1. *Let $f(t)$ be a function defined on the positive real axis $0 < t < \infty$. The Mellin transformation of the function f, is defined by*

$$\mathcal{M}\left[f(t); s\right] = \int_0^\infty dt f(t) t^{s-1}. \tag{B.63}$$

Remark B.7.1. *In general, the integral does exist only for complex values of $s = a + ib$ such that $a_1 < a < a_2$, where a_1 and a_2 depend on the function $f(t)$ to transform. This introduces what is called the strip of definition of the Mellin transform that will be denoted by $S(a_1, a_2)$. In some cases, this strip may extend to a half-plane ($a_1 = -\infty$ or $a_2 = \infty$) or to the whole complex s-plane ($a_1 = -\infty$ and $a_2 = \infty$).*

Example B.7.1. *The Mellin transform of the exponential function,*

$$f(t) = e^{-at}, \text{for } a > 0, \tag{B.64}$$

is given by

$$\begin{aligned}\mathcal{M}\left[f(t);s\right] &= \int_0^\infty dt e^{-at} t^{s-1} \\ &= a^{-s}\int_0^\infty dt e^{-t} t^{s-1} \\ &= a^{-s}\Gamma(s),\end{aligned} \tag{B.65}$$

where in the second line we did the substitution at $\to t$ *and in the last line we identified the gamma function based on Def. B.5.1. Note that this Mellin transform only holds for* $\mathrm{Re}(s) > 0$.

Remark B.7.2. *In Ex. B.7.1, we considered* $a > 0$. *We would like to consider more general values of the form,* $\mathrm{Re}(a) > 0$. *The calculations is to involved to do it here but for a conformation that this is allowed we refer the reader to equation 1 of page 312 in Ref. [**76**]. In Fig. B.7, one can see the Mellin transform of the exponential function for different values of the parameter* a, *which satisfies* $\mathrm{Re}(a) > 0$.

Remark B.7.3. *The above remark only states that* $\mathrm{Re}(a) > 0$. *However, one could show that it also holds* $\mathrm{Re}(a) = 0$. *This is done by first regularizing the function,* $e^{-ibt} \to e^{-(ibt+\delta t)}$ *for* $b \in \mathbb{R}$ *and* $\delta > 0$. *Then one would be able to use the result from Ex. B.7.1 together with Rem. B.7.2. Finally, one can safely take* $\delta \to 0$.

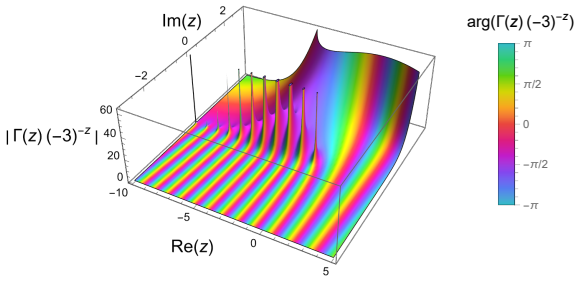

(a) For this plot $a = -3$ was chosen.

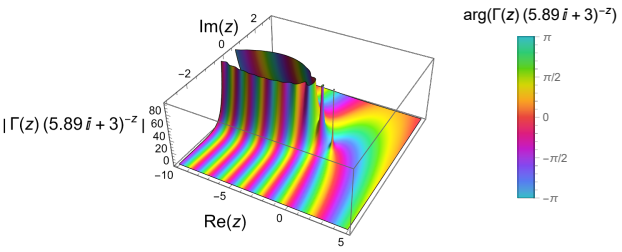

(b) For this plot $a = 5.89i + 3$ was chosen.

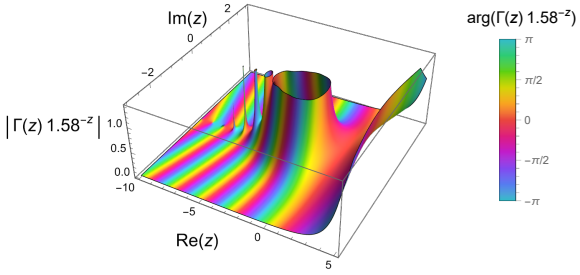

(c) For this plot $a = 1.58$ was chosen.

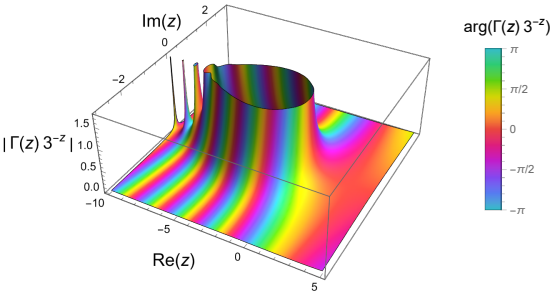

(d) For this plot $a = 3$ was chosen.

Figure B.7: Plots of the Mellin transform of the exponential function, e^{-at}, which is given by $a^{-s}\Gamma(s)$, for different values of the parameter a. Notice that we also showed one plot for a negative value of a, which is totally different than the other plots. This is also a numerical indicator that the real part of a, $\mathrm{Re}(a)$, has to be greater than or equal to 0. The range of each subplot varies to make the output in that specific case more clearly, however one should keep that in mind when comparing all the subplots.

Example B.7.2. *In this example, we calculate the Mellin transform of a more difficult function,* $\mathcal{M}[f(\omega); s]$*, with the function given by*

$$f(\omega) = \frac{1}{1 + c\omega^a}, \text{for } a \in \mathbb{R} \setminus \{0\}, c > 0, \tag{B.66}$$

where we already anticipated that we will use this example to calculate a Fourier type integral (therefore using ω *as the initial variable instead of* t*). The function,* $f(\omega)$*, for different values of* a*, can be seen in Fig. B.8. Starting with Eq. (B.62), for the case* $z = s/a$*, gives*

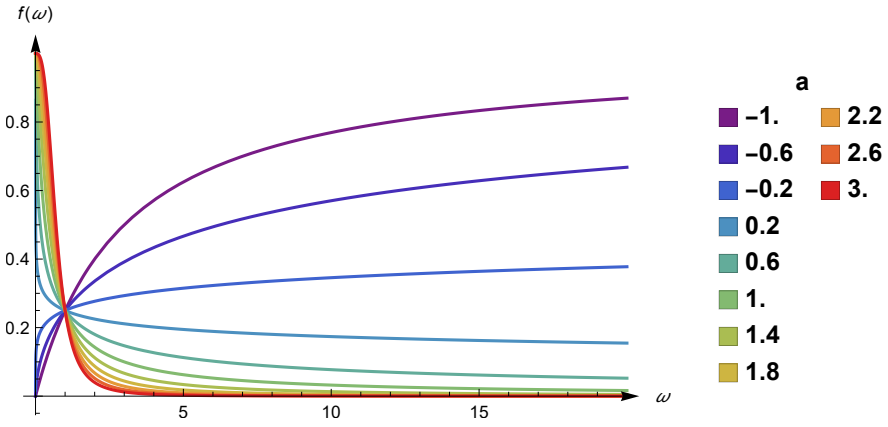

Figure B.8: The plot shows values of the function, $f(\omega) = 1/(1 + 3\omega^a)$, for different values of the parameter, a, ranging from -1 to 3.

$$\int_0^\infty du \frac{u^{\frac{s}{a}-1}}{1+u} = \Gamma\left(\frac{s}{a}\right)\Gamma\left(1 - \frac{s}{a}\right). \tag{B.67}$$

Next, we do the substitution $u = c\omega^a$ *on the left side, which results in*

$$\int_0^\infty d\omega \frac{\omega^{s-1}}{1 + c\omega^a} = \frac{1}{|a|} c^{-\frac{s}{a}} \Gamma\left(\frac{s}{a}\right)\Gamma\left(1 - \frac{s}{a}\right), \tag{B.68}$$

where the absolute value of a *comes from the case for which* $a < 0$*. Finally, we can identify the Mellin transform of the function* $f(\omega)$ *on the left side of Eq. (B.68). We conclude that*

$$\mathcal{M}[f(\omega); s] = \frac{1}{|a|} c^{-\frac{s}{a}} \Gamma\left(\frac{s}{a}\right)\Gamma\left(1 - \frac{s}{a}\right). \tag{B.69}$$

Note that this Mellin transform only holds for $0 < \mathrm{Re}(s/a) < 1$*.*

Remark B.7.4. *Similar to Ex. B.7.1, we would like to relax the restrictions on the parameter,* c*. This time, we refer to equation (30) on page 311 of Ref. [**76**]. We can thus take* $c \in \mathbb{C} \setminus (-\infty, 0]$*.*

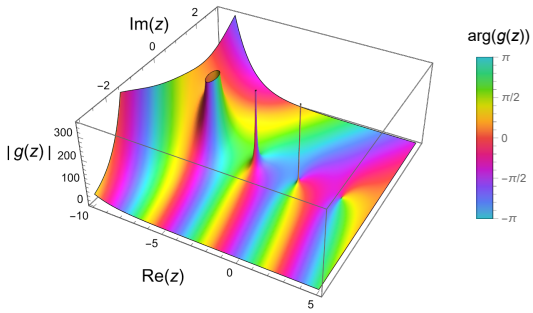

(a) For this plot $a = 3$ and $c = 10i$ were chosen.

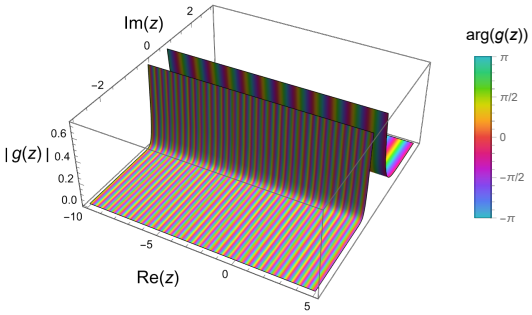

(b) For this plot $a = 0.3$ and $c = i$ were chosen.

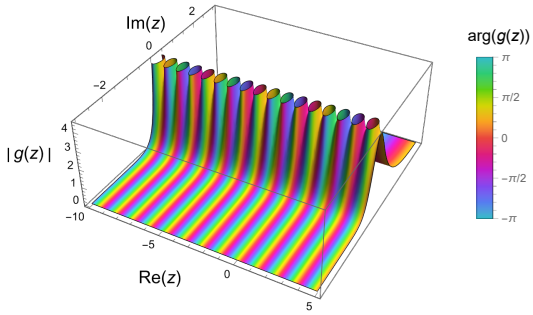

(c) For this plot $a = 0.9$ and $c = i$ were chosen.

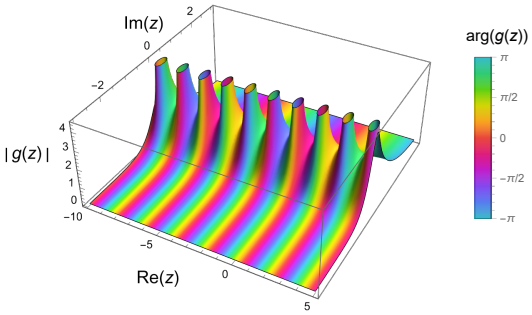

(d) For this plot $a = 1.58$ and $c = i$ were chosen.

Figure B.9: Plots of the Mellin transform of the exponential function, $1/(1 + c\omega^a)$, which is given by $c^{-\frac{s}{a}}\Gamma(s/a)\,\Gamma(1 - s/a)\,/|a|$, for different values of the parameters a and c. Notice that the parameter a, determines the singularity spacing. The range of each subplot varies to make the output in that specific case more clearly, however one should keep that in mind when comparing all the subplots.

Definition B.7.2. *The inverse Mellin transform of a function, $F(s)$, defined on a strip $S(a_1, a_2)$, is given by*

$$f(t) = \mathcal{M}^{-1}\left[F(s); t\right] = \frac{1}{2\pi i}\int_{a-i\infty}^{a+i\infty} dsF(s)t^{-s}, \tag{B.70}$$

where $a_1 < a < a_2$.

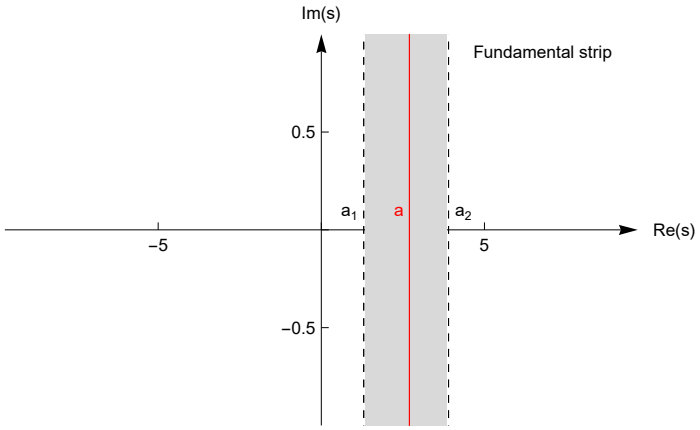

Figure B.10: We chose $a_1 = 1.3$, $a = 2.7$ and $a_1 = 3.9$. This means that the fundamental strip in the figure is $S(1.3, 2.7)$.

B.8 The Fox H-function

The last appendix involves the Fox H-function, were we mainly used Refs. [**77, 78, 79**]. As stated before, the usefulness of the Fox H-function is that there are known asymptotic expansions. Therefore, when we derive an equality between a Fourier integral and a Fox-H function, we also find the asymptotic expansions of that Fourier integral (see Sec. 3.5).

Definition B.8.1. *Let $m, n, p, q \in \mathbb{N}$ with $0 \leq n \leq p$ and $1 \leq m \leq q$, $A_i, B_j \in \mathbb{R}_+$, $a_i, b_j \in \mathbb{C}$ for $i = 1, ..., p$ and $j = 1, ..., q$. The Fox H-function with parameters $m, n, p, q, a_i, A_i, b_j, B_j$ and argument $z \neq 0$ is defined by*

$$H_{p,q}^{m,n}\left[z\left|\begin{matrix}(a_1, A_1), & ..., & (a_p, A_p)\\ (b_1, B_1), & ..., & (b_q, B_q)\end{matrix}\right.\right] = \frac{1}{2\pi i}\int_L ds\Upsilon(s)z^{-s}, \tag{B.71}$$

where z^{-s} is not necessarily the principal value complex power function and $\Upsilon(s)$ is given by

$$\Upsilon(s) = \frac{\prod_{j=1}^{m}\Gamma(b_j + B_j s)\prod_{k=1}^{n}\Gamma(1 - a_k - A_k s)}{\prod_{j'=m+1}^{q}\Gamma(1 - b_{j'} - B_{j'} s)\prod_{k'=n+1}^{p}\Gamma(a_{k'} + A_{k'} s)},$$

where an empty product is always interpreted as unity and L is a suitable contour which separates the poles of the two factors in the numerator of $\Upsilon(s)$ [4].

Remark B.8.1. *We will also denote the Fox H-function as*

$$H_{p,q}^{m,n}(z) \equiv H_{p,q}^{m,n}\left[z\middle|\begin{array}{ccc}(a_1,A_1)\,, & ..., & (a_p,A_p)\\ (b_1,B_1)\,, & ..., & (b_q,B_q)\end{array}\right] \tag{B.72}$$

when the specifications of the parameters, a_i, A_i, b_j, B_j, is not necessary.

Example B.8.1. *In this example, we will express the exponential function in terms of a Fox H-function. We will show that*

$$e^{-z} = H_{0,1}^{1,0}\left[z\middle|\begin{array}{c}\\ (0,1)\end{array}\right] \tag{B.73}$$

for $|\arg(z) < \frac{\pi}{2}|$ and $z \neq 0$. We can prove the above relation by using Def. B.8.1 on the right hand side, which gives

$$H_{0,1}^{1,0}\left[z\middle|\begin{array}{c}\\ (0,1)\end{array}\right] = \frac{1}{2\pi i}\int_L ds\Gamma(s)z^{-s}. \tag{B.74}$$

Now, we choose the contour L to be the vertical line, $\mathrm{Re}(s) = \gamma$, $\gamma > 0$, which lies to the right of the poles of $\Gamma(z)$. Thus, we have

$$H_{0,1}^{1,0}\left[z\middle|\begin{array}{c}\\ (0,1)\end{array}\right] = \frac{1}{2\pi i}\int_{\gamma-i\infty}^{\gamma+i\infty} ds\Gamma(s)z^{-s}. \tag{B.75}$$

Next, we assume that we can close the contour such that it picks up all the poles of the gamma function[5]*. Using the residue theorem and Eq. (B.51), yields*

$$\begin{aligned} H_{0,1}^{1,0}\left[z\middle|\begin{array}{c}\\ (0,1)\end{array}\right] &= \sum_{\nu=0}^{\infty} z^{\nu}\frac{(-1)^{\nu}}{\nu!} \\ &= e^{-z}. \end{aligned} \tag{B.76}$$

Some quantities that will be important to determine the asymptotic behavior of Fox-H

[4] For more information about the contour, L, we refer the reader to Ref. [**77**].

[5] A more formal treatment of this example can be found in Ref. [**80**]. In the same reference, more advanced integrals can also be found.

functions are defined as

$$\mu_H \equiv \sum_{j=1}^{q} B_j - \sum_{j=1}^{p} A_j, \tag{B.77}$$

$$\delta_H \equiv \sum_{j=1}^{q} b_j - \sum_{j=1}^{p} a_j + \frac{p-q}{2}, \tag{B.78}$$

$$\alpha_H \equiv \sum_{j=1}^{n} A_j - \sum_{j=n+1}^{p} A_j + \sum_{j=1}^{m} B_j - \sum_{j=m+1}^{q} B_j. \tag{B.79}$$

These quantities will be important to determine the asymptotic behavior of Fox H-functions as the theorem below shows.

Theorem B.8.1. *Let α_H, μ_H and δ_H be like defined in Eqs. (B.79), (B.77) and (B.78) respectively. Assume that the conditions on the parameters of the Fox H-function, given in Def. B.8.1, are satisfied. Then the following expansions hold:*

(i) If $\mu_H \geq 0$ or $\mu_H < 0$, $\alpha_H > 0$ and $|\arg(z)| < \frac{1}{2}\pi\alpha_H$ then the Fox H-function has either the asymptotic expansions at zero given by

$$\begin{aligned} H_{p,q}^{m,n}(z) &= \mathcal{O}(z^c), && |z| \to 0, \text{ or} \\ H_{p,q}^{m,n}(z) &= \mathcal{O}\left(z^c \left|\ln(z)\right|^{N-1}\right), && |z| \to 0, \end{aligned} \tag{B.80}$$

with $c = \min_{1\leq j\leq m}\left[\frac{\mathrm{Re}(b_j)}{B_j}\right]$ and N is the order of the poles of $\Gamma(b_j + B_j s)$ to which some other poles of another gamma function $\Gamma(b_l + B_l s)$ with $1 \leq j \leq m$ and $1 \leq l \leq m$ could coincide.

(ii) If $\mu_H < 0$, $\alpha_H = 0$, then the asymptotic expansion near zero becomes

$$H_{p,q}^{m,n}(z) = \mathcal{O}(z^\sigma), \qquad |z| \to 0, |\arg(z)| \leq \widetilde{\epsilon}, \tag{B.81}$$

where $\sigma = \min_{1\leq j\leq m}\left[\frac{\mathrm{Re}(b_j)}{B_j}, \frac{\mathrm{Re}(\delta_H)+1/2}{\mu_H}\right]$ and $\widetilde{\epsilon}$ is a constant such that $0 < \widetilde{\epsilon} < \frac{\pi}{2}\min_{1\leq j\leq m; m+1\leq k\leq q}(A_j, B_k)$.

(iii) If $\mu_H \leq 0$ or $\mu_H > 0$ and $\alpha_H > 0$, then the Fox H-function has either the asymptotic expansion at infinity given by

$$\begin{aligned} H_{p,q}^{m,n}(z) &= \mathcal{O}(z^d), && |z| \to \infty, \text{ or} \\ H_{p,q}^{m,n}(z) &= \mathcal{O}(z^d \left|\ln(z)\right|^{M-1}), && |z| \to \infty, \end{aligned} \tag{B.82}$$

with $d = \min_{1\leq j\leq n}\left[\frac{\mathrm{Re}(a_j)-1}{A_j}\right]$ and M is the order of the poles $\Gamma(1 - a_k - A_k s)$ to which some of the poles of $\Gamma(1 - a_l - A_l s)$ with $1 \leq j \leq n$ and $1 \leq l \leq n$ could coincide.

(iv) If $\mu_H > 0$ and $\alpha_H = 0$, then

$$H_{p,q}^{m,n}(z) = \mathcal{O}(z^{\rho}), \qquad |z| \to \infty, |\arg(z)| \leq \epsilon, \tag{B.83}$$

where $\rho = \max_{1\leq j\leq n}\left[\frac{\mathrm{Re}(a_j)-1}{A_j}, \frac{\mathrm{Re}(\delta_H)+1/2}{\mu_H}\right]$ and ϵ is a constant such that $0 < \epsilon < \frac{\pi}{2}\min_{n+1\leq j\leq p;1\leq k\leq m}(A_j, B_k)$.

B.9 The Caputo fractional derivative

In App. C, a Caputo fractional derivative is needed. This is not the fractional derivative that is mainly used in this thesis. Therefore, we will be brief in this discussion. We follow Ref. [**25**], where more details can be found.

Definition B.9.1. *Let $\alpha \in \mathbb{R}\setminus\mathbb{Z}$, $b < t$ and $n-1 < \alpha < n$ with $n \in \mathbb{Z}$. The Caputo fractional derivative is given by*

$${}_b^C\boldsymbol{D}_t^{\alpha} f(t) = \frac{1}{\Gamma(n-\alpha)}\int_b^t d\tau \frac{f^{(n)}(\tau)}{(t-\tau)^{\alpha-n-1}}, \tag{B.84}$$

where $f^{(n)}(t)$ denotes the n^{th} order derivative.

Remark B.9.1. *Notice, that the Caputo fractional derivative depends on the lower bound, b. This is in contrast with the Weyl fractional derivative which has a lower bound of $-\infty$.*

It turns out that the Caputo fractional derivative works well with Taylor series.

Example B.9.1. *Assuming that $\nu > n$, we have*

$${}_b^C\boldsymbol{D}_t^{\alpha}(t-b)^{\nu} = \frac{1}{\Gamma(n-\alpha)}\int_a^t d\tau \frac{\Gamma(\nu+1)}{\Gamma(\nu-n+1)}(\tau-b)^{\nu-n}(t-\tau)^{-\alpha+n-1}, \tag{B.85}$$

where we calculated the n^{th} order derivative. Next, we make the substitution: $\tau = b+z(t-b)$, which results in

$$\begin{aligned}
{}_b^C\boldsymbol{D}_t^{\alpha}(t-b)^{\nu} &= \frac{\Gamma(\nu+1)}{\Gamma(n-\alpha)\Gamma(\nu-n+1)}\int_0^1 dz\,[z(t-b)]^{\nu-n}\,[(1-z)(t-b)]^{-\alpha+n-1}\,(t-b) \\
&= \frac{\Gamma(\nu+1)}{\Gamma(n-\alpha)\Gamma(\nu-n+1)}(t-b)^{\nu-\alpha}\int_0^1 dz\, z^{\nu-n}(1-z)^{-\alpha+n-1} \\
&= \frac{\Gamma(\nu+1)}{\Gamma(n-\alpha)\Gamma(\nu-n+1)}(t-b)^{\nu-\alpha}B(\nu-n+1, n-\alpha) \\
&= \frac{\Gamma(\nu+1)}{\Gamma(\nu-\alpha+1)}(t-b)^{\nu-\alpha},
\end{aligned} \tag{B.86}$$

where in the third line we identified the definition of the beta function, see Def. B.6.1, and in the last line we applied Eq. (B.61).

The previous example allows one to calculate the caputo derivative of any function that is Taylor expandable. To illustrate the difference between the Weyl fractional derivative and the Caputo fractional derivative, we investigate what happens when we apply the Caputo fractional derivative on the exponential. Recalling that the exponential was an eigenfunction of the Weyl fractional derivative, as was shown in Ex. 3.1.1.

Example B.9.2. *First, we note that we will work with lower bound of the Caputo fractional derivative to be zero such that we can easily compare the result with the result obtained by using the Weyl fractional derivative. For* $0 < \alpha < 1$*, we have that*

$$\begin{aligned} {}_0^C\boldsymbol{D}_t^\alpha e^{at} &= \sum_{\nu=0}^{\infty} \frac{1}{\nu!} {}_0^C\boldsymbol{D}_t^\alpha t^\nu \\ &= \sum_{\nu=1}^{\infty} \frac{(at)^{\nu-\alpha}}{\Gamma(\nu-\alpha+1)}, \end{aligned} \tag{B.87}$$

*which clearly is not the exponential function anymore. It is a Mittag-Leffler function [**81, 82**]. We thus conclude that the exponential function is not an eigenfunction of the Caputo fractional derivative.*

Appendix C

Numerical study of fractals

In this appendix we will justify numerically the assumption made in Eq. (D.2). Namely, that labeling the points of a fractal, k, based on the ordered distances to the origin, R_k, results in

$$k = \left(\frac{R_k}{a}\right)^{d_f}, \tag{C.1}$$

where d_f is the fractal dimension and a is the lattice spacing. First, we generate the points of a fractal, then we order those points based on the distance to the origin. Then, we make a log-log plot to see if we actually have a power relation between the labels and the distance to the origin. Finally, we fit the log-log plot by a linear function, which then returns the parameters in which we are interested. We fitted $\ln(R_k)$ in terms of $\ln(k)$, which resulted in

$$\begin{aligned} \ln(R_k) &= p_1 \ln(k) + p_2 \\ &= \ln\left(e^{p_2} k^{p_1}\right), \end{aligned} \tag{C.2}$$

where $p1$ and p_2 are the parameters of the fit. This implies that

$$k = \left(\frac{R_k}{e^{p_2}}\right)^{\frac{1}{p_1}}. \tag{C.3}$$

Comparing the above equation with Eq. (C.1), yields

$$d_f = \frac{1}{p_1} \text{ and } a = e^{p_2}. \tag{C.4}$$

These are the relations that will be justified from the numerical results.

First, we check the above assumption in the case of a two-dimensional lattice, namely, a triangular lattice. The results are depicted in Fig. C.1. The dimension becomes

$$d = \frac{1}{p_1} = 1.981, \tag{C.5}$$

which is of course very close to the dimension of the triangular lattice, which is two. For the lattice spacing, which was set to be 0.00391 in the simulation, the numerical result yielded

$$a = e^{p_2} = 0.00406. \tag{C.6}$$

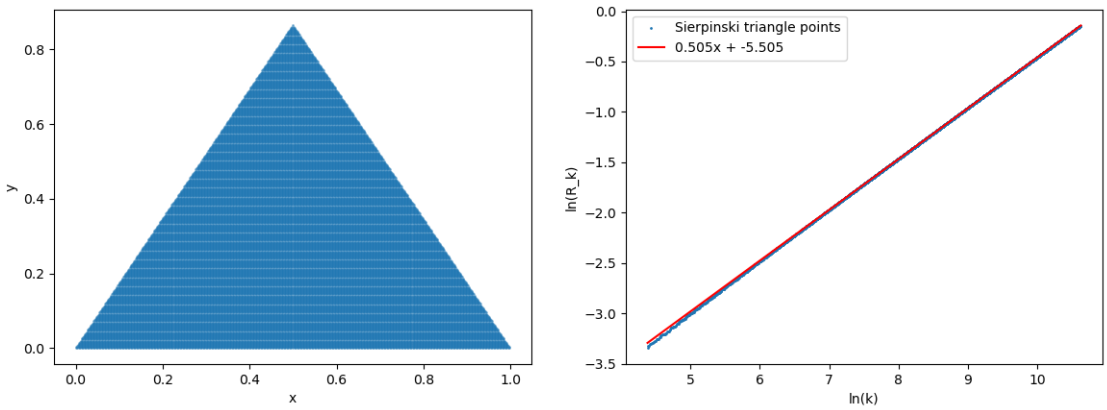

(a) (b)

Figure C.1: (a) shows the points of a triangular lattice. The lattice spacing is 0.00391. (b) is a log-log plot of R_k in terms of k. A fit is shown in the same figure.

Next, we did the same investigation for the Sierpiński triangle, which has a fractal dimension, $d_f \approx 1.585$ and the lattice spacing was kept the same as for the triangular lattice, 0.00391. The results of the fit are

$$d_f = \frac{1}{p_1} = 1.589 \text{ and } a = e^{p_2} = 0.00203, \tag{C.7}$$

which can also be seen in Fig. C.2. Notice that the lattice spacing is almost half of what it should be. This is because we calculated the lattice spacing numerically as the minimum distance between the points. However, the first hole that appears in the first generation of the Sierpiński triangle is not a real hole when using a triangular lattice basis. This can be observed in Fig C.3.

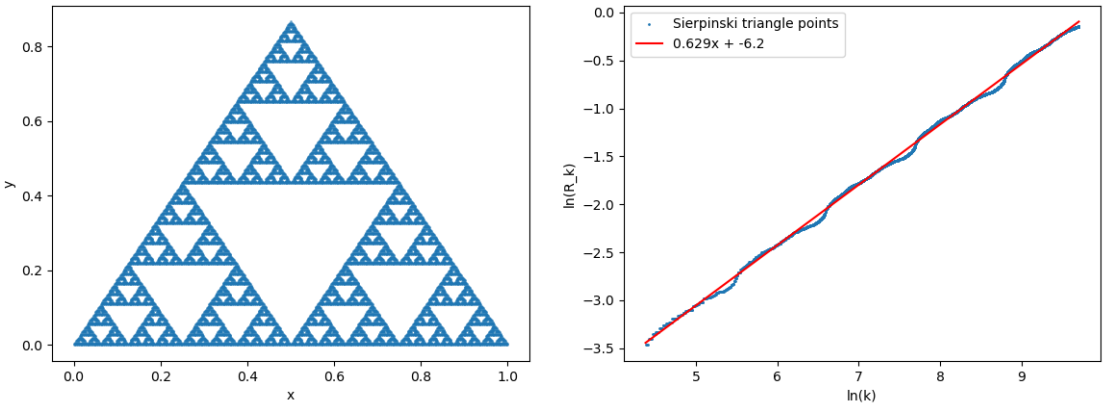

(a) (b)

Figure C.2: (a) shows the points of a Sierpiński triangle of generation 8. The lattice spacing is 0.00391. (b) depicts the log-log plot of R_k in terms of k. A fit is also shown in the same figure.

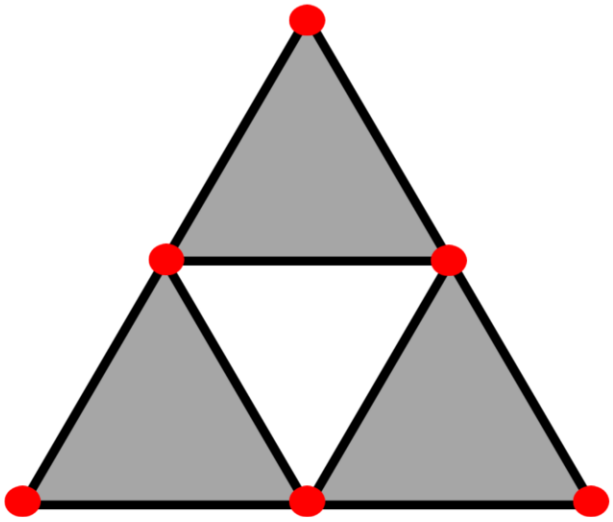

Figure C.3: The lattice of the first generation Sierpiński triangle. Notice that this is the same as the triangular lattice. This means that the minimum distance between the points is not the lattice constant but half of it.

This means that the minimum distance between two points is half the size of the fractal's unit triangle. Hence, we find a factor of two difference. Note that Eq. (C.1) still holds. The dimension is very close to the actual fractal dimension of the Sierpiński triangle.
Finally, we did the same experiment for the Sierpiński carpet, which has a fractal dimension of approximately 1.893 and the lattice spacing was chosen to be 0.000647. The results are shown in Fig. C.4. The fit gives

$$d_f = \frac{1}{p_1} = 1.871 \text{ and } e^{p_2} = 0.000346. \tag{C.8}$$

The lattice spacing, resulting from the fit, is again around half of what is expected. The explanation is the same as for the Sierpiński triangle. The fractal dimension is again very close to what the fractal dimension of the Sierpiński carpet is. We can thus conclude that the relation, given by Eq. (C.1) is the correct one, up to potentially a factor of two. This could be verified by using a different (symmetry in the) lattice, such as a honeycomb lattice, where there is no mixing between fractal holes and lattice holes.

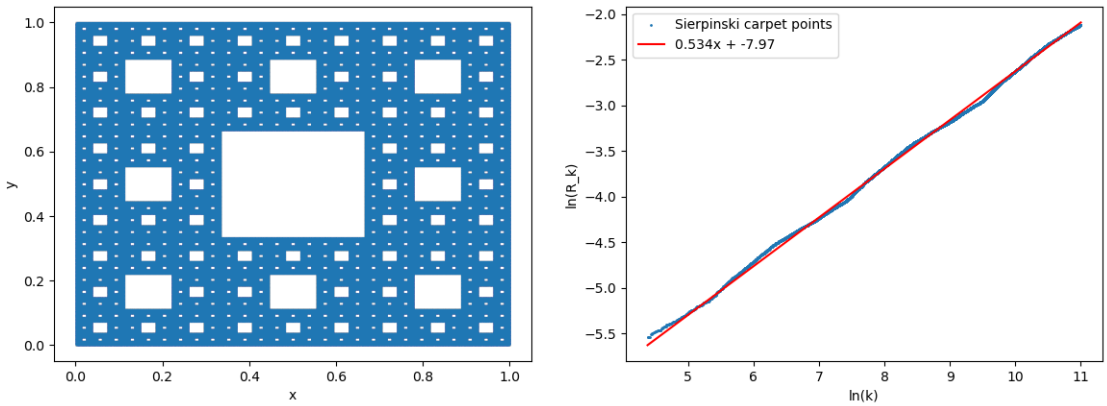

(a) (b)

Figure C.4: (a) shows the points of a Sierpiński carpet of generation 7. The lattice spacing is 0.000647. (b) depicts the log-log plot of R_k in terms of k. A fit is shown in the same figure.

Appendix D

The Caldeira-Leggett model on a fractal

In this appendix, we give a first attempt to derive the fractional Caldeira-Leggett model from a physical point of view. We do this by focussing on anomalous diffusion on fractals [**14**]. We believe that our approach is one that could work. However, we need to make an inelegant and non-intuitive assumption, which makes this approach incomplete.

We consider the Caldeira-Leggett model, which is described by the Lagrangian

$$\mathcal{L} = \frac{1}{2}M\dot{Q}^2 - V(Q) + \frac{1}{2}\sum_{k=1}^{N} m_k(\dot{q}_k^2 - \omega_k^2 q_k^2) + Q\sum_{k=1}^{N} C_k q_k - \frac{1}{2}\sum_{k=1}^{N}\frac{C_k^2}{m_k\omega_k^2}Q^2, \tag{D.1}$$

where all the parameters are the same as in Sec. 2.2.
Next, we will apply the knowledge of the fractal geometry to the microscopic quantities, m_k, ω_k, and C_k. To achieve this, we place the oscillators in the fractal. The intuition for this is that we will integrate out the oscillators such that the particle can only move in the fractal. Now, we label the oscillators in order of their distance to the origin. When this is done for a self-similar fractal, one gets a relation between the distances of the oscillator to the origin, R_k, and the label of the oscillators, k, which is given by

$$k = \left(\frac{R_k}{a}\right)^{d_f}, \tag{D.2}$$

with $a > 0$ defining the lattice spacing. The justification for this relation can be found in App. C. Next, we need to find relations between the other microscopic quantities and R_k. Let us start with the mass of the oscillators, m_k. We note that when the particle just enters the fractal on the edge it essentially sees a 2D geometry. However, when it moves into the bulk it starts to see larger and larger holes. This results in a lowering of the average mass

of an oscillator when we go further inside the bulk of the fractal. This indicates that the relation between these should have a negative exponent. From Ref. [**83**], we know that the lacunarity of a perfect fractal, $\Lambda(r)$, is approximately given by

$$\Lambda(r) = \lambda \left(\frac{r}{L}\right)^{d_f - d_E}, \tag{D.3}$$

where r is the scale at which one is observing the system[1], λ is called the lacunarity parameter, L is the size of the fractal, and d_E is the Euclidean dimension of the embedding space. In the same reference, a link between the lacunarity and the relative mass fluctuations at scale r is given by

$$\frac{\mathrm{Var}[m(r)]}{\langle m \rangle^2} = \Lambda(r) - 1, \tag{D.4}$$

where $\mathrm{Var}[m(r)]$ stands for the variance of the mass at scale r, thus having a unit of mass squared, and $\langle m \rangle$ the average mass of a single oscillator in the whole fractal, which is by definition independent from the scale. We can then write

$$\begin{aligned} m_k &= \langle m \rangle + \delta m_k(r) \\ &= \langle m \rangle + \frac{\mathrm{Var}[m(r)]}{\langle m \rangle} \\ &= \langle m \rangle \Lambda(r). \end{aligned} \tag{D.5}$$

Now, we note that in the bulk of the fractal, r and R_k are essentially the same, such that we obtain

$$\begin{aligned} m_k &= \langle m \rangle \Lambda(R_k) \\ &= \langle m \rangle \lambda \left(\frac{R_k}{L}\right)^{d_f - d_E}, \end{aligned} \tag{D.6}$$

where in the last line we used Eq. (D.3). Next, we see that a relation between the coupling constant, C_k, and m_k, and ω_k can be obtained by looking at the dimensions in Eq. (D.1), which imply that

$$[C_k] = \frac{\text{force}}{\text{distance}}. \tag{D.7}$$

Dimensional analysis of Newton's second law gives

$$\text{force} = \text{mass} \cdot \frac{\text{distance}}{\text{time}^2} = \text{mass} \cdot \text{distance} \cdot \text{frequency}^2. \tag{D.8}$$

[1] For example a ball of radius r.

Thus, we can rewrite C_k as

$$C_k = \tilde{C} m_k \omega_k^2. \tag{D.9}$$

where $\tilde{C}$ is a dimensionless constant. However, since we only used dimensional analysis, $\tilde{C}$ can still depend on k. Therefore, we take the general form

$$C_k = C m_k \omega_k^2 \left(\frac{\omega_k}{\tilde{\omega}}\right)^b, \tag{D.10}$$

where C is independent of k, b is a real number, and $\tilde{\omega}$ is a constant that has units of frequency. Finally, we turn our attention towards ω_k. We assume that the bath is in equilibrium, meaning that we can use the equipartition theorem (Eqs. 2.7), which states

$$m_k \omega_k^2 R_k^2 = k_B T. \tag{D.11}$$

Hence, we get for ω_k

$$\omega_k = \sqrt{\frac{k_B T}{m_k}} \frac{1}{R_k}. \tag{D.12}$$

To summarize, by using the properties of fractals, we were able to write the microscopic bath quantities as a set of implicit functions of k, namely

$$\begin{cases} k = \left(\frac{R_k}{a}\right)^{d_f}, \\ C_k = C m_k \omega_k^2 \left(\frac{\omega_k}{\tilde{\omega}}\right)^b, \\ m_k = \langle m \rangle \lambda \left(\frac{R_k}{L}\right)^{d_f - d_E}, \\ \omega_k = \sqrt{\frac{k_B T}{m_k}} \frac{1}{R_k}. \end{cases} \tag{D.13}$$

The only remaining question is what the measure should become. This can be solved by considering

$$\Delta k \equiv k_{\text{previous}} - k_{\text{next}}, \tag{D.14}$$

where k_{next} is the label of the next oscillator. This is defined because we ordered the oscillators based on their distance to the origin. Δk is just a number, which in the continuum limit will go to unity. Thus, $1 \to dk$. Taking the differential of Eq. (D.2), gives

$$dk = a^{-d_f} d_f R_k^{d_f - 1} dR_k. \tag{D.15}$$

It will be more useful to write dk in terms of $d\omega_k$, since in the Caldeira-Leggett model (see Sec. 2.2) delta functions of the form $\delta(\omega - \omega_k)$ were used. To achieve this, we first derive a

relation between R_k and ω_k, which is done by inserting Eq. (D.6) into Eq. (D.12), yielding

$$\begin{aligned} R_k &= \left(\sqrt{\frac{k_B T L^{d_f - d_E}}{\langle m \rangle \lambda}}\right)^{\frac{2}{2+d_f-d_E}} \omega_k^{\frac{-2}{2+d_f-d_E}} \\ &\equiv \left(\frac{B}{\omega_k}\right)^{\frac{2}{2+d_f-d_E}}, \end{aligned} \tag{D.16}$$

with $B \equiv \sqrt{\frac{k_B T L^{d_f-d_E}}{\langle m \rangle \lambda}}$. This equation implies that

$$dR_k = -\frac{2}{2+d_f-d_E}\left(\frac{B}{\omega_k}\right)^{\frac{2}{2+d_f-d_E}} \omega_k^{-1} d\omega_k. \tag{D.17}$$

Remark D.0.1. *From Eq. (D.12), we see that, if k goes from 0 to ∞, then ω_k goes from ∞ to 0. This gives an extra minus sign when going from k to ω_k under the integral, canceling the minus sign that appears in Eq. (D.17).*

Substituting Eqs. (D.16) and (D.17) into Eq. (D.15) gives

$$dk = -\frac{2 d_f a^{-d_f}}{2+d_f-d_E}\left(\frac{B}{\omega_k}\right)^{\frac{2d_f}{2+d_f-d_E}} \omega_k^{-1} d\omega_k. \tag{D.18}$$

Recall that the spectral function in the Caldeira-Leggett model was given by

$$J_{CL}(\omega) = \frac{\pi}{2}\sum_k \frac{C_k^2}{m_k \omega_k}\delta(\omega - \omega_k). \tag{D.19}$$

Now, we apply the continuum limit of the sum, to get

$$J_f(\omega) = \frac{\pi}{2}\int_0^\infty dk \frac{C_k^2}{m_k \omega_k}\delta(\omega - \omega_k), \tag{D.20}$$

where we swapped the subscript, CL, by f, which stands for fractal. Using Eq. (D.10), we can write

$$\begin{aligned} \frac{C_k^2}{m_k \omega_k} &= C^2 m_k \omega_k^3 \left(\frac{\omega_k}{\tilde{\omega}}\right)^{2b} \\ &= \frac{C^2 \langle m \rangle \lambda B^{\frac{2(d_f-d_E)}{2+d_f-d_E}}}{\tilde{\omega}^{2b} L^{d_f-d_E}} \omega^{\frac{-2d_f+2d_E}{2+d_f-d_E}+3+2b} \\ &\equiv K \omega^{\frac{-2d_f+2d_E}{2+d_f-d_E}+3+2b} \end{aligned} \tag{D.21}$$

with $K \equiv C^2\langle m\rangle\lambda B^{\frac{2(d_f-d_E)}{2+d_f-d_E}}/(\tilde{\omega}^{2b}L^{d_f-d_E})$. In the second line we substituted Eqs. (D.6) and (D.16). Substituting the above result and Eq. (D.18) together with the extra minus sign explained in Rem. D.0.1 yields

$$\begin{aligned} J_f(\omega) &= K\frac{\pi d_f a^{-d_f}}{2+d_f-d_E}B^{\frac{2d_f}{2+d_f-d_E}}\int_0^\infty d\omega_k \omega_k^{\frac{-4d_f+d_E}{2+d_f-d_E}+2+2b}\delta(\omega-\omega_k) \\ &= K\frac{\pi d_f a^{-d_f}}{2+d_f-d_E}B^{\frac{2d_f}{2+d_f-d_E}}\omega^{\frac{-4d_f+d_E}{2+d_f-d_E}+2+2b}. \end{aligned} \tag{D.22}$$

We first note that when we take $b = 0$, we do not get the result that is given in the experiments [**14**]. However, we can choose $2b = -\frac{-4d_f+d_E}{2+d_f-d_E} - 2 + \frac{2d_f}{d_E}$, such that

$$J_f(\omega) = K\frac{\pi d_f a^{-d_f}}{2+d_f-d_E}B^{\frac{2d_f}{2+d_f-d_E}}\omega^{\frac{2d_f}{d_E}}, \tag{D.23}$$

which does reproduce the results of the experiment. However, we are unable to justify this choice at the moment. This is the missing link in the derivation.
Finally, we will show that the spectral function of the previous section will lead to a Caputo fractional derivative (see Sec. B.9) Langevin equation with colored noise. We can directly start with

$$F_{fr} = \frac{2}{\pi}\frac{d}{dt}\left\{\int_0^t d\tau\int_0^\infty d\omega\frac{J_f(\omega)}{\omega}\cos[\omega(t-\tau)]Q(\tau)\right\}, \tag{D.24}$$

which is a known result in the Caldeira-Legget model. It is known (see Ref. [**25**]) that a spectral function of the form Eq. (D.23) leads to a friction form

$$F_{fr} = \tilde{\eta}\,{}_0^C\boldsymbol{D}_t^{2d_f/d_E}. \tag{D.25}$$

Turning our focus to the fluctuating force, which in the Caldeira-Leggett model has statistics given by

$$\langle f(t)\rangle = 0, \tag{D.26}$$

$$\langle f(t)f(t')\rangle = \frac{2k_BT}{\pi}\int_0^\infty d\omega\frac{J_f(\omega)}{\omega}\cos[\omega(t-t')]. \tag{D.27}$$

Substituting a non-Ohmic spectral function, such as Eq. (D.23), yields colored noise of the form (Ref. [**25**])

$$\langle f(t)f(t')\rangle = H(t-t')^{-2d_f/d_E}, \tag{D.28}$$

where H is a specific constant. Thus, we have that

$$-M\ddot{Q}(t) + \tilde{\eta}\, {}_0^C\boldsymbol{D}_t^{2d_f/d_E} Q(t) + \frac{\partial V(Q)}{\partial Q} = f(t), \tag{D.29}$$

with $\langle f(t)\rangle = 0$ and $\langle f(t)f(t')\rangle = H(t-t')^{-2d_f/d_E}$. Now, we know that, in the free case, this leads to a long-time behavior of the mean squared displacement given by

$$\left\langle Q(t)^2 \right\rangle \overset{t\to\infty}{\sim} t^{2d_f/d_E}, \tag{D.30}$$

which justified our claim that with our specific assumptions one could explain the experiments in Ref. [**14**].

Bibliography

[**1**] Chengying Bao, Myoung-Gyun Suh, Boqiang Shen, Kemal Şafak, Anan Dai, Heming Wang, Lue Wu, Zhiquan Yuan, Qi-Fan Yang, Andrey B. Matsko, Franz X. Kärtner, and Kerry J. Vahala. Quantum diffusion of microcavity solitons. *Nature Physics*, 17(4):462–466, April 2021.

[**2**] Yu. Kagan. Quantum diffusion in solids. *Journal of Low Temperature Physics*, 87(3):525–569, May 1992.

[**3**] P. Kleinert. Theory of hot-electron quantum diffusion in semiconductors. *Physics Reports*, 485(1):1–42, 2010.

[**4**] Vyacheslav G Storchak and Nikolai V Prokof'ev. Quantum diffusion of muons and muonium atoms in solids. *Reviews of Modern Physics*, 70(3):929, 1998.

[**5**] I Guarneri. Spectral properties of quantum diffusion on discrete lattices. *Europhysics Letters*, 10(2):95, 1989.

[**6**] M. Biagetti, G. Franciolini, A. Kehagias, and A. Riotto. Primordial black holes from inflation and quantum diffusion. *Journal of Cosmology and Astroparticle Physics*, 2018(07):032, jul 2018.

[**7**] Yoav Sagi, Miri Brook, Ido Almog, and Nir Davidson. Observation of anomalous diffusion and fractional self-similarity in one dimension. *Phys. Rev. Lett.*, 108:093002, Mar 2012.

[**8**] Beth M Regner, Dragan Vučinić, Cristina Domnisoru, Thomas M Bartol, Martin W Hetzer, Daniel M Tartakovsky, and Terrence J Sejnowski. Anomalous diffusion of single particles in cytoplasm. *Biophysical journal*, 104(8):1652–1660, 2013.

[**9**] Daniel S Banks and Cécile Fradin. Anomalous diffusion of proteins due to molecular crowding. *Biophysical journal*, 89(5):2960–2971, 2005.

[**10**] TH Solomon, Eric R Weeks, and Harry L Swinney. Observation of anomalous diffusion and Lévy flights in a two-dimensional rotating flow. *Physical Review Letters*, 71(24):3975, 1993.

[**11**] A. Einstein. Über die von der molekularkinetischen theorie der wärme geforderte bewegung von in ruhenden flüssigkeiten suspendierten teilchen. *Annalen der Physik*, 322(8):549–560, 1905.

[**12**] Ralf Metzler and Joseph Klafter. The random walk's guide to anomalous diffusion: a fractional dynamics approach. *Physics Reports*, 339(1):1–77, 2000.

[**13**] Wen Chen. Time–space fabric underlying anomalous diffusion. *Chaos, Solitons & Fractals*, 28(4):923–929, 2006.

[**14**] Xiao-Yun Xu, Xiao-Wei Wang, Dan-Yang Chen, C. Morais Smith, and Xian-Min Jin. Quantum transport in fractal networks. *Nature Photonics*, 15(9):703–710, 2021.

[**15**] A. O. Caldeira. *An Introduction to Macroscopic Quantum Phenomena and Quantum Dissipation*. Cambridge University Press, 2014.

[**16**] Ulrich Weiss. *Quantum dissipative systems*. World Scientific, 2012.

[**17**] A.O Caldeira and A.J Leggett. Quantum tunnelling in a dissipative system. *Annals of Physics*, 149(2):374–456, 1983.

[**18**] L. Ferialdi. Dissipation in the Caldeira-Leggett model. *Phys. Rev. A*, 95:052109, May 2017.

[**19**] Anthony J Leggett, SDAFMGA Chakravarty, Alan T Dorsey, Matthew PA Fisher, Anupam Garg, and Wilhelm Zwerger. Dynamics of the dissipative two-state system. *Reviews of Modern Physics*, 59(1):1, 1987.

[**20**] Amir O Caldeira and Anthony J Leggett. Influence of dissipation on quantum tunneling in macroscopic systems. *Physical Review Letters*, 46(4):211, 1981.

[**21**] L Ferialdi. Dissipation in the Caldeira-Leggett model. *Physical Review A*, 95(5):052109, 2017.

[**22**] Eric Lutz. Fractional Langevin equation. *Phys. Rev. E*, 64:051106, Oct 2001.

[**23**] R. C. Verstraten, R. F. Ozela, and C. Morais Smith. Time glass: A fractional calculus approach. *Phys. Rev. B*, 103:L180301, May 2021.

[**24**] Stanislav Burov and Eli Barkai. Critical exponent of the fractional Langevin equation. *Physical review letters*, 100(7):070601, 2008.

[**25**] R. C. Verstraten. *The fractional Langevin equation*. Master's thesis, Utrecht University, Heidelberglaan 8, 3584 CS Utrecht, 2020.

[**26**] Keith Oldham and Jerome Spanier. *The fractional calculus theory and applications of differentiation and integration to arbitrary order*. Elsevier, 1974.

[**27**] Francesco Mainardi. Fractional calculus: Theory and applications, 2018.

[**28**] Edmundo Capelas de Oliveira and José António Tenreiro Machado. A review of definitions for fractional derivatives and integral. *Mathematical Problems in Engineering*, 2014.

[**29**] Selçuk Ş. Bayın. Definition of the Riesz derivative and its application to space fractional quantum mechanics. *Journal of Mathematical Physics*, 57(12):123501, 2016.

[**30**] Fausto Ferrari. Weyl and Marchaud derivatives: A forgotten history. *Mathematics*, 6(1):6, 2018.

[**31**] Stefan G Samko, Anatoly A Kilbas, Oleg I Marichev, et al. *Fractional integrals and derivatives*, volume 1. Gordon and breach Science publishers, Yverdon Yverdon-les-Bains, Switzerland, 1993.

[**32**] Kenneth S Miller. The Weyl fractional calculus. In *Fractional Calculus and Its Applications: Proceedings of the International Conference Held at the University of New Haven, June 1974*, pages 80–89. Springer, 2006.

[**33**] Stefan K Kehrein and Andreas Mielke. On the spin-boson model with a sub-ohmic bath. *Physics Letters A*, 219(5-6):313–318, 1996.

[**34**] Matthias Vojta, Ning-Hua Tong, and Ralf Bulla. Quantum phase transitions in the sub-ohmic spin-boson model: Failure of the quantum-classical mapping. *Physical review letters*, 94(7):070604, 2005.

[**35**] Frithjof B Anders, Ralf Bulla, and Matthias Vojta. Equilibrium and nonequilibrium dynamics of the sub-ohmic spin-boson model. *Physical review letters*, 98(21):210402, 2007.

[**36**] R. A. Mulder, M. A. Caracanhas, and C. Morais Smith. Quantizing Lévy flights. *Phys. Rev. B*, 103:174301, May 2021.

[**37**] Om.P. Agrawal. Formulation of Euler–Lagrange equations for fractional variational problems. *Journal of Mathematical Analysis and Applications*, 272(1):368–379, 2002.

[**38**] E Barkai. Fractional Fokker-Planck equation, solution, and application. *Physical Review E*, 63(4):046118, 2001.

[**39**] Marcin Magdziarz, Aleksander Weron, Krzysztof Burnecki, and Joseph Klafter. Fractional Brownian motion versus the continuous-time random walk: A simple test for subdiffusive dynamics. *Physical Review Letters*, 103(18):180602, 2009.

[**40**] Kambiz Razminia, Abolhassan Razminia, and JA Tenreiro Machado. Analysis of diffusion process in fractured reservoirs using fractional derivative approach. *Communications in Nonlinear Science and Numerical Simulation*, 19(9):3161–3170, 2014.

[**41**] Wen Chen, Hongguang Sun, Xiaodi Zhang, and Dean Korošak. Anomalous diffusion modeling by fractal and fractional derivatives. *Computers & Mathematics with Applications*, 59(5):1754–1758, 2010.

[**42**] Vasily E Tarasov. Review of some promising fractional physical models. *International Journal of Modern Physics B*, 27(09):1330005, 2013.

[**43**] Robert Brown F.R.S. Hon. M.R.S.E. and R.I. Acad. V.P.L.S. Xxvii. a brief account of microscopical observations made in the months of june, july and august 1827, on the particles contained in the pollen of plants; and on the general existence of active molecules in organic and inorganic bodies. *The Philosophical Magazine*, 4(21):161–173, 1828.

[**44**] Xin Bian, Changho Kim, and George Em Karniadakis. 111 years of Brownian motion. *Soft Matter*, 12(30):6331–6346, 2016.

[**45**] S. N. Kempkes, M. R. Slot, S. E. Freeney, S. J. M. Zevenhuizen, D. Vanmaekelbergh, I. Swart, and C. Morais Smith. Design and characterization of electrons in a fractal geometry. *Nature Physics*, 15(2):127–131, 2019.

[**46**] Sabir Umarov. *Introduction to Fractional and Pseudo-Differential Equations with Singular Symbols*, volume 41. 09 2015.

[**47**] S.C. Lim, Ming Li, and L.P. Teo. Langevin equation with two fractional orders. *Physics Letters A*, 372(42):6309–6320, 2008.

[**48**] Fabio Bagarello. Fourier transforms, fractional derivatives, and a little bit of quantum mechanics. *Rocky Mountain Journal of Mathematics*, 50(2):415 – 428, 2020.

[**49**] Roberta Musina and Alexander I. Nazarov. On fractional Laplacians – 2. *Annales de l'Institut Henri Poincaré C, Analyse non linéaire*, 33(6):1667–1673, 2016.

[**50**] Anna Lischke, Guofei Pang, Mamikon Gulian, Fangying Song, Christian Glusa, Xiaoning Zheng, Zhiping Mao, Wei Cai, Mark M. Meerschaert, Mark Ainsworth, and George Em Karniadakis. What is the fractional Laplacian? a comparative review with new results. *Journal of Computational Physics*, 404:109009, 2020.

[**51**] EC Marino, Leandro O Nascimento, Van Sergio Alves, and C Morais Smith. Interaction induced quantum valley hall effect in graphene. *Physical Review X*, 5(1):011040, 2015.

[**52**] E C Marino, Leandro O Nascimento, Van Sérgio Alves, N Menezes, and C Morais Smith. Quantum-electrodynamical approach to the exciton spectrum in transition-metal dichalcogenides. *2D Materials*, 5(4):041006, sep 2018.

[**53**] EV Kirichenko and VA Stephanovich. The influence of coulomb interaction screening on the excitons in disordered two-dimensional insulators. *Scientific Reports*, 11(1):1–14, 2021.

[**54**] E.C. Marino. Quantum electrodynamics of particles on a plane and the Chern-Simons theory. *Nuclear Physics B*, 408(3):551–564, 1993.

[**55**] E. C. Marino, Leandro O. Nascimento, Van Sérgio Alves, and C. Morais Smith. Unitarity of theories containing fractional powers of the d'Alembertian operator. *Phys. Rev. D*, 90:105003, Nov 2014.

[**56**] W. R. Schneider. Stable distributions: Fox function representation and generalization. In S. Albeverio, G. Casati, and D. Merlini, editors, *Stochastic Processes in Classical and Quantum Systems*, pages 497–511, Berlin, Heidelberg, 1986. Springer Berlin Heidelberg.

[**57**] Jae-Hyung Jeon and Ralf Metzler. Fractional Brownian motion and motion governed by the fractional Langevin equation in confined geometries. *Physical Review E*, 81(2):021103, 2010.

[**58**] V Kobelev and E Romanov. Fractional Langevin equation to describe anomalous diffusion. *Progress of Theoretical Physics Supplement*, 139:470–476, 2000.

[**59**] Alireza Khalili Golmankhaneh, Karmina Ali, Resat Yilmazer, and Mohammed Kaabar. Local fractal Fourier transform and applications. *Computational Methods for Differential Equations*, 10(3):595–607, 2022.

[**60**] Nick Laskin. Fractional quantum mechanics. *Phys. Rev. E*, 62:3135–3145, Sep 2000.

[**61**] Vasily E. Tarasov. Weyl quantization of fractional derivatives. *Journal of Mathematical Physics*, 49(10), 10 2008.

[**62**] Dumitru Baleanu. New applications of fractional variational principles. *Reports on Mathematical Physics*, 61(2):199–206, 2008.

[**63**] Robin C. Verstraten, Tim Ludwig, Rembert A. Duine, and Cristiane Morais Smith. The fractional landau-lifshitz-gilbert equation, 2022.

[**64**] P Nalbach and M Thorwart. Ultraslow quantum dynamics in a sub-ohmic heat bath. *Physical Review B*, 81(5):054308, 2010.

[**65**] T. Koekkoek. *Diffusion in fractals*. Bacherlor's thesis, Utrecht University, Heidelberglaan 8, 3584 CS Utrecht, 2022.

[**66**] Joel Schiff. *The Laplace Transform: Theory and Applications*. 01 1999.

[**67**] Liping Chen, Song Liang, and Ranchao Wu. Laplace transform of fractional order differential equations. 2015.

[**68**] Howard Haber. The complex logarithm, exponential and power functions. Lecture Notes, University of California, 2011.

[**69**] James Ward Brown and Ruel V. Churchill. *Complex Variables and Applications*. McGraw-Hill Education, 2014.

[**70**] Matilde Legua and Luis M. Sánchez-Ruiz. Cauchy principal value contour integral with applications. *Entropy*, 19(5), 2017.

[**71**] R. A. Brewster and J. D. Franson. Generalized delta functions and their use in quantum optics. *Journal of Mathematical Physics*, 59(1):012102, jan 2018.

[**72**] N. N. Lebedev. *Special Functions and Their Applications*. Dover, New York, 1972.

[**73**] Roelof Koekoek. The gamma and the beta function. Lecture Notes, TU Delft, 2021.

[**74**] Jacqueline Bertrand, Pierre Bertrand, and Jean-Philippe Ovarlez. The mellin transform. In *The Transforms and Applications Handbook*. August 1995.

[**75**] Joubert Oosthuizen. The mellin transform. Lecture Notes, University of California, 2011.

[**76**] Harry Bateman. *Tables of Integral Transforms*, volume 1. McGraw-Hill Book Company, New York, 1954.

[**77**] Hans J. Haubold A.M. Mathai, Ram Kishore Saxena. *The H-Function: Theory and Applications*. 2010.

[**78**] Anatoly A. Kilbas and Megumi Saigo. On the H-function. *Integral Transforms and Special Functions*, 12(6):447–462, 2001.

[**79**] B. L. J. Braaksma. Asymptotic expansions and analytic continuations for a class of barnes-integrals. *Compositio Mathematica*, 15:239–341, 1962-1964.

[**80**] Roelof Koekoek. Special functions – hypergeometric functions – barnes' integral representation. Lecture Notes, TU Delft, 2021.

[**81**] Hans J Haubold, Arak M Mathai, Ram K Saxena, et al. Mittag-Leffler functions and their applications. *Journal of applied mathematics*, 2011, 2011.

[**82**] Francesco Mainardi. Why the Mittag-Leffler function can be considered the queen function of the fractional calculus? *Entropy*, 22(12):1359, 2020.

[**83**] Fabio D. A., Reis A., and Riera R. Lacunarity calculation in the true fractal limit. *Journal of Physics A: Mathematical and General Physics*, 27, mar 1994.